PHOTOGRAPH THIS SHEET

AD-A995 337

DTIC ACCESSION NUMBER

LEVEL

INVENTORY

Project 5.3
BLAST EFFECTS ON B-36 TYPE
AIRCRAFT IN FLIGHT

DOCUMENT IDENTIFICATION

DISTRIBUTION STATEMENT A
Approved for public release;
Distribution Unlimited

DISTRIBUTION STATEMENT

ACCESSION FOR		
NTIS	GRA&I	☑
DTIC	TAB	☐
UNANNOUNCED		☐
JUSTIFICATION		
BY		
DISTRIBUTION /		
AVAILABILITY CODES		
DIST	AVAIL AND/OR SPECIAL	
A-1		

DISTRIBUTION STAMP

DTIC
ELECTE
DEC 17 1985
D

DATE ACCESSIONED

QUALITY INSPECTED 3

DATE RETURNED

UNANNOUNCED

85 12 16 013

DATE RECEIVED IN DTIC

REGISTERED OR CERTIFIED NO.

PHOTOGRAPH THIS SHEET AND RETURN TO DTIC-DDAC

DTIC FORM 70A DEC 83

DOCUMENT PROCESSING SHEET

PREVIOUS EDITION MAY BE USED UNTIL STOCK IS EXHAUSTED.

[redacted]

UNCLASSIFIED

WT-750

Copy No. 183 A

AD-A995 337

Operation UPSHOT-KNOTHOLE

EXCLUDED FROM THE G[illegible]

NEVADA PROVING GROUNDS

March - June 1953

Statement A
Approved for public release;
Distribution unlimited

Project [illegible]

BLAST EFFECTS ON B-36 TYPE AIRCRAFT IN FLIGHT

FRD

Classification (Cancelled) (Changed to [illegible])
By Authority of [illegible] Date [illegible]
By [illegible]

CANCELLED

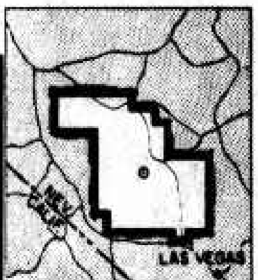

Classification Changed
By Authority of
CN
By DNA [illegible] Date [illegible]
By DOE [illegible] Date [illegible]

HEADQUARTERS FIELD COMMAND, ARMED FORCES SPECIAL WEAPONS PROJECT
SANDIA BASE, ALBUQUERQUE, NEW MEXICO

[redacted]

UNCLASSIFIED

[redacted]

B 9819

[redacted] UNCLASSIFIED

WT-750

This document consists of 102 pages

No. 183 of 220 copies, Series A

OPERATION UPSHOT-KNOTHOLE

Project 5.3

BLAST EFFECTS ON B-36 TYPE AIRCRAFT IN FLIGHT

REPORT TO THE TEST DIRECTOR

Statement A
Approved for public release;
Distribution unlimited

23 Oct 1963

by

Glen F. Purkey

March 1955

Aircraft Laboratory
Wright Air Development Center
Dayton, Ohio

[redacted] UNCLASSIFIED

ABSTRACT

This report is a presentation of the data obtained by Project 5.3 on the blast response of a B-36D aircraft flown in the proximity of the Shot 9 explosion of Operation UPSHOT-KNOTHOLE. The test aircraft was the same B-36D aircraft utilized for similar testing by Project 6.10 during Operation IVY. The instrumentation was modified to include additional measurements on the horizontal tail. Response measurements included: nose, tail, wing tip, and center of gravity accelerations; wing fuselage, and horizontal stabilizer bending moments; and horizontal stabilizer shear. Peak overpressure at the aircraft was also measured.

The purpose of the program was to supplement the blast response data obtained during the IVY tests particularly to investigate more fully the aft fuselage and horizontal stabilizer response characteristics. The purpose was accomplished even though the peak loads obtained were not as high as desired. The peak stabilizer bending moment measured was 34 per cent of limit load. Peak wing bending moments were somewhat higher than those measured during IVY but were still only a fraction of the limit allowable. The data obtained by Project 5.3, combined with previous data, will allow a complete check of the present blast/load theory in the low and medium load ranges. Theoretical extrapolation to loads approaching design limit should be confirmed by additional experimental data.

The position of the aircraft at blast arrival was such that the reflected shock wave arrived 4.44 seconds after the direct shock wave; and, because of fortuitous phasing with low amplitude vibrations initiated by the direct shock, the peak loads produced by the reflected shock were slightly higher. However, with proper phasing and shorter time interval between shocks, the reflected shock could induce peak loads considerably higher than those obtained from the direct shock.

The data obtained by Project 6.10 in IVY are included in this report.

FOREWORD

This report is one of the reports presenting the results of the 78 projects participating in the Military Effects Tests Program of Operation UPSHOT-KNOTHOLE, which included 11 tests detonations. For readers interested in other pertinent test information, reference is made to WT-782, Summary Report of the Technical Director, Military Effects Program. This summary report includes the following information of possible general interest.

a. An over-all description of each detonation, including yield, height of burst, ground zero location, time of detonation, ambient atmospheric conditions at detonation, etc., for the 11 shots.

b. Compilation and correlation of all project results on the basic measurements of blast and shock, thermal radiation, and nuclear radiation.

c. Compilation and correlation of the various project results on weapons effects.

d. A summary of each project, including objectives and results.

e. A complete listing of all reports covering the Military Effects Tests Program.

PREFACE

The primary purpose of this report is the presentation of the response data obtained by Project 5.3 on the exposure of a B-36D aircraft during Shot 9 of Operation UPSHOT-KNOTHOLE. The work was conducted to provide data to supplement similar measurements made during Operation IVY. Because of the direct relation between the work performed on the two operations and the desirability of having the composite data available in a single reference, the results of both IVY and UPSHOT-KNOTHOLE are presented in this report.

All usable response data have been presented as curves of the function versus time. Data relative to method and conditions of exposure are included. Instrumentation details have been omitted, except where nonstandard equipment or procedures were employed. Analysis of the data has been limited to that required to establish the coherence of the data.

The author wishes to take this opportunity to express his appreciation to the many individuals and organizations who have contributed to the successful completion of this project. Specifically acknowledged in the following paragraphs are a few of the individuals and organizations who provided the assiduous effort which is so necessary to the success of any operation.

The untiring efforts of Lt. Francis Williams, Assistant Project Officer of Project 5.3, in accomplishing seemingly impossible assignments in a minimum of time contributed greatly to the success of the B-36D participation.

Much credit is due the flight crews who take the risks involved in atomic testing, while relying for their safety upon the proficiency of the research engineers. Their cooperation and willingness was most gratifying. In particular, the author wishes to express his appreciation for outstanding cooperation and assistance to Lt. Col. Jerry Hunt, Aircraft Commander; Lt. Col. Harold Upton, Radar Operator; and Maj. Samual Baker, Flight Engineer, all of the Strategic Air Command.

The portion of this project using the point load method was supervised by Mr. J. C. Lehmkuhl of the Structures Branch, Aircraft Laboratory, WADC. Mr. Lehmkuhl's interest in the point load method rendered possible the measurement of the B-36D horizontal tail loads by this new and completely independent method.

The assistance of the Cook Research Laboratories and the Consolidated Vultee Aircraft Corporation in conducting the point load calibration was greatly appreciated.

The calculations made to select the aircraft positions were accomplished by the Allied Research Associates, Inc. This information is absolutely necessary in a project of this type.

This writer is grateful to have the opportunity at this time to express his appreciation to the personnel of the Division of Research of the University of Dayton for their valuable assistance in the reduction of the test data and the writing of this report. In particular, the personal interest and individual attention given by Mr. Edward Freeh in the writing of this report was most gratifying.

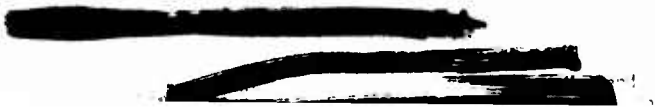

CONTENTS

ABSTRACT 3

FOREWORD 5

PREFACE 7

CONTENTS 9

ILLUSTRATIONS 11

TABLES 14

CHAPTER 1 INTRODUCTION 15

1.1 Background 15
1.2 Objective 15
1.3 Nature and Scope of Investigation 16

CHAPTER 2 PROCEDURE 17

2.1 General 17
2.2 Selection of Aircraft and Input Levels 18
2.3 Instrumentation 19
2.3.1 Inputs and Flight Data 19
2.3.1.1 Overpressure 19
2.3.1.2 Altitude 20
2.3.1.3 Airspeed 20
2.3.1.4 Position 20
2.3.2 Response Measurements 21
2.3.2.1 Bending Moment 22
2.3.2.2 Torsion 22
2.3.2.3 Shear 22
2.3.2.4 Acceleration 25
2.3.3 Response Sign Convention 25
2.3.4 Recording Equipment 25
2.3.4.1 Recording Oscillographs . . . 27
2.3.4.2 High Frequency Pressure Recorder 29
2.3.5 Photography 29

[redacted]

2.3.6 Location in Aircraft 30
2.3.6.1 B-36 Aircraft 30
2.3.6.2 B-47 Aircraft 35
2.3.7 Calibration 39
2.3.7.1 Pressure and Acceleration . . 41
2.3.7.2 Bending, Shear, and Torsion . 42
2.3.7.3 Point Load System 44
2.4 Field Testing Procedure 44
2.4.1 B-36 Aircraft 45
2.4.2 B-47 Aircraft 47

CHAPTER 3 RESULTS, MIKE SHOT 53

3.1 General 53
3.2 Aircraft Position, Inputs, Flight Data 53
3.2.1 B-36 Aircraft 53
3.2.2 B-47 Aircraft 54
3.3 Response Measurements 54
3.3.1 Bending Moment 54
3.3.2 Acceleration 55
3.3.3 Shear and Torsion 55

CHAPTER 4 RESULTS, KING SHOT 61

4.1 General 61
4.2 Aircraft Position, Inputs, Flight Data 61
4.2.1 B-36 Aircraft 61
4.2.2 B-47 Aircraft 63
4.3 Response Measurements 63
4.3.1 B-36 Aircraft 63
4.3.1.1 Bending Moment 63
4.3.1.2 Acceleration 71
4.3.1.3 Shear and Torsion 71
4.3.2 B-47 Aircraft 71

CHAPTER 5 RESULTS, SHOT 9 72

5.1 General 72
5.2 Aircraft Position, Inputs, Flight Data 72
5.3 Response Measurements 73
5.3.1 Bending Moment 73
5.3.2 Acceleration 73
5.3.3 Shear 73

CHAPTER 6 DISCUSSION 90

6.1 General 90
6.2 Wing Bending 91
6.3 Stabilizer Bending 93
6.4 Fuselage Bending 95
6.5 Acceleration 95
6.6 Summary 97

CHAPTER 7 CONCLUSIONS AND RECOMMENDATIONS 100

7.1 Conclusions 100
7.2 Recommendations 100

ILLUSTRATIONS

CHAPTER 2 PROCEDURE

2.1 Typical Bending Gage Installation with Schematic Circuit 23
2.2 Typical Torsion and Shear Gage Installation with Schematic Circuit 24
2.3 Typical Single Spar Shear Gage Installation with Schematic Circuit 26
2.4 Schematic Diagram of Recording Circuit Showing Strain Bridge, Bridge Balancing Unit and Recording Oscillograph 28
2.5 Pylons, Left Wing B-36 Aircraft 30
2.6 Cameras and Camera Housing, B-36 Aircraft . . . 31
2.7 Location of Instrumentation in B-36D Aircraft for IVY 32
2.8 Oscillographs and Bridge Balances, Aft Crew Compartment, B-36 34
2.9 Selector Panel, Aft Crew Compartment, B-36 . . 34
2.10 High Frequency Pressure Recorder, Aft Crew Compartment, B-36 34
2.11 Master Control Panel, B-36 35
2.12 Housing for Blue Box Beneath Aft Fuselage, B-36 35
2.13 Location of Instrumentation in B-36D Empennage for UPSHOT-KNOTHOLE 36
2.14 Location of Instrumentation in B-47B Aircraft for IVY 38
2.15 Oscillograph Installation, B-47B Aircraft . . . 39
2.16 Typical Calibration Curve for Accelerometer . . 42
2.17 Calibration of B-36D Aircraft Empennage in Structures Test Facility of Aircraft Laboratory 43
2.18 Assigned Position and Flight Pattern of B-36D Aircraft for Mike Shot Showing Flight Times from Leaving Orbit to Blast Arrival 46
2.19 Assigned Position and Flight Pattern of B-36D Aircraft for King Shot 48

[redacted]

2.20 Assigned Position and Flight Pattern of B-36D Aircraft for Shot 9 51
2.21 Assigned Position and Flight Pattern of B-47B Aircraft for Mike Shot 52
2.22 Assigned Position and Flight Pattern of B-47B Aircraft for King Shot 54

CHAPTER 3 RESULTS, MIKE SHOT

3.1 Position of B-36D and B-47B Aircraft for Mike Shot 57
3.2 Wing Bending versus Time after Shock Arrival, Left Wing Station 390, B-36D, Mike Shot 59
3.3 Wing Bending versus Time after Shock Arrival, Right Wing Station 390, B-36D, Mike Shot . . . 59
3.4 Wing Bending versus Time after Shock Arrival, Left Wing Station 110, B-36D, Mike Shot 60
3.5 Wing Bending versus Time after Shock Arrival, Left Wing Station 604, B-36D, Mike Shot 60
3.6 Wing Bending versus Time after Shock Arrival, Left Wing Station 1062, B-36D, Mike Shot . . . 61
3.7 Fuselage Bending versus Time after Shock Arrival, Fuselage Station 1040, B-36D, Mike Shot 61
3.8 Stabilizer Bending versus Time after Shock Arrival, Left Horizontal Stabilizer Station 62, B-36D, Mike Shot 62
3.9 Vertical Acceleration versus Time after Shock Arrival, B-36D Tail, Fuselage Station 1770, Mike Shot 62
3.10 Vertical Acceleration versus Time after Shock Arrival, B-36D Nose, Fuselage Station 212, Mike Shot 63
3.11 Vertical Acceleration versus Time after Shock Arrival, B-36D Center of Gravity, Fuselage Station 907, Mike Shot 63

CHAPTER 4 RESULTS, KING SHOT

4.1 Position of B-36D and B-47B Aircraft for King Shot 65
4.2 Wing Bending versus Time after Shock Arrival, Left Wing Station 390, B-36D, King Shot 67
4.3 Wing Bending versus Time after Shock Arrival, Right Wing Station 390, B-36D, King Shot . . . 67
4.4 Wing Bending versus Time after Shock Arrival, Left Wing Station 604, B-36D, King Shot 68
4.5 Wing Bending versus Time after Shock Arrival, Left Wing Station 1062, B-36D, King Shot . . . 68
4.6 Fuselage Bending versus Time after Shock Arrival, Fuselage Station 1040, B-36D, King Shot 69

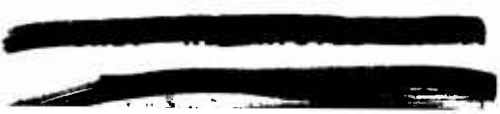

4.7 Stabilizer Bending versus Time after Shock Arrival, Left Horizontal Stabilizer Station 62, B-36D, King Shot 66
4.8 Vertical Acceleration versus Time after Shock Arrival, B-36D Tail, Fuselage Station 1770, King Shot 67
4.9 Vertical Acceleration versus Time after Shock Arrival, B-36D Nose, Fuselage Station 212, King Shot 67
4.10 Vertical Acceleration versus Time after Shock Arrival, B-36D Center of Gravity, Fuselage Station 907 (Left Side), King Shot 68
4.11 Vertical Acceleration versus Time after Shock Arrival, B-36D Center of Gravity, Fuselage Station 907 (Right Side), King Shot 68
4.12 Wing Bending versus Time after Shock Arrival, Left Wing Station 186, B-47B, King Shot . . . 69
4.13 Wing Bending versus Time after Shock Arrival, Right Wing Station 186, B-47B, King Shot . . . 69
4.14 Vertical Acceleration versus Time after Shock Arrival, B-47B Tail, Fuselage Station 1121.5, King Shot 70
4.15 Vertical Acceleration versus Time after Shock Arrival, B-47B Center of Gravity, Fuselage Station 587.8, King Shot 70

CHAPTER 5 RESULTS, SHOT 9

5.1 Wing Bending versus Time after Shock Arrival, Left Wing Station 390, B-36D, Shot 9 74
5.2 Wing Bending versus Time after Shock Arrival, Right Wing Station 390, B-36D, Shot 9 75
5.3 Wing Bending versus Time after Shock Arrival, Left Wing Station 604, B-36D, Shot 9 76
5.4 Wing Bending versus Time after Shock Arrival, Left Wing Station 1062, B-36D, Shot 9 77
5.5 Fuselage Bending versus Time after Shock Arrival, Fuselage Station 1040, B-36D, Shot 9 78
5.6 Stabilizer Bending versus Time after Shock Arrival, Left Horizontal Stabilizer Station 62, B-36D, Shot 9 79
5.7 Stabilizer Bending versus Time after Shock Arrival, Right Horizontal Stabilizer Station 62, B-36D, Shot 9 80
5.8 Stabilizer Bending (Point Load Measurement) versus Time after Shock Arrival, Left Horizontal Stabilizer Station 62, B-36D, Shot 9 81
5.9 Stabilizer Bending (Point Load Measurement) versus Time after Shock Arrival, Right Horizontal Stabilizer Station 62, B-36D,

Shot 9 82
5.10 Stabilizer Bending (Point Load Measurement) versus Time after Shock Arrival, Right Horizontal Stabilizer Station 144, B-36D, Shot 9 83
5.11 Vertical Acceleration versus Time after Shock Arrival, B-36D Tail, Fuselage Station 1770, Shot 9 84
5.12 Vertical Acceleration versus Time after Shock Arrival, B-36D Nose, Fuselage Station 212, Shot 9 85
5.13 Vertical Acceleration versus Time after Shock Arrival, B-36D Center of Gravity, Fuselage Station 907, Shot 9 86
5.14 Stabilizer Shear (Point Load Measurement) versus Time after Shock Arrival, Left Horizontal Stabilizer Station 62, B-36D, Shot 9 87
5.15 Stabilizer Shear (Point Load Measurement) versus Time after Shock Arrival, Right Horizontal Stabilizer Station 62, B-36D, Shot 9 88
5.16 Stabilizer Shear (Point Load Measurement) versus Time after Shock Arrival, Right Horizontal Stabilizer Station 144, B-36D, Shot 9 89

CHAPTER 6 DISCUSSION

6.1 Peak Positive Wing Bending Moments Measure in Mike, King, and Shot 9 Plotted versus Wing Station (Expressed as Distance in Inches from Aircraft Center Line) 92
6.2 Comparison of Bending Measurements made at Station 62 of the Left Horizontal Stabilizer, B-36D during Mike and Shot 9 94
6.3 Comparison of Fuselage Bending Measurements made at Station 1040 on the B-36D during Mike, King and Shot 9 96
6.4 Comparison of Center of Gravity Acceleration versus Time with Wing Bending (Station 110) versus Time, B-36D, Mike Shot 98

TABLES

CHAPTER 2 PROCEDURE

2.1 Instrumentation, B-36D Aircraft, IVY 33
2.2 Instrumentation, B-36D Empennage UPSHOT-KNOTHOLE 37
2.3 Instrumentation, B-47B Aircraft, IVY 40

[redacted]

CHAPTER 1

INTRODUCTION

1.1 BACKGROUND

With the recent advances in the development of high yield nuclear weapons, it has become increasingly important to consider the effects of the weapon upon the delivery aircraft. Capabilities of present operational bombardment aircraft, as now known, will not permit the delivery of weapons above certain sizes; the limit yield is generally based upon allowable thermal or blast damage to the delivery aircraft, although in specific instances other weapon effects could be controlling. The maximum size that can be safely delivered by a particular aircraft depends to a great extent upon the delivery technique employed. Because of the major role assigned to B-36 aircraft in the over-all war plan, a knowledge of the maximum delivery capabilities of this type aircraft is of primary interest. Accordingly, in Operation IVY where there occurred the first test of a nuclear device of megaton yield, an instrumented B-36 aircraft was exposed to obtain thermal and blast response data that could be used for the verification or modification of existing analytical techniques employed to correlate aircraft response with thermal and blast forcing functions. The blast induced loads obtained during the two IVY shots were too low to provide adequate verification of the blast load theory at loads approaching the maximum capabilities of the aircraft. In addition, the response data from IVY showed that the aft fuselage and empennage of the B-36 aircraft were more vulnerable than had previously been recognized. In view of the above, it was deemed advisable to instrument further the empennage of the B-36 aircraft and to re-expose it in Operation UPSHOT-KNOTHOLE at a higher input level.

1.2 OBJECTIVE

The objective of this investigation was to supplement data obtained in IVY on the blast response of a B-36 aircraft flying in the vicinity of a nuclear detonation. The data will be utilized to substantiate the blast/load theory employed to correlate aircraft response with blast input. The ultimate objective is the determination of the maximum delivery capabilities of the B-36 aircraft.

[redacted]

1.3 NATURE AND SCOPE OF INVESTIGATION

In essence, the work consisted of positioning an instrumented aircraft at some point in space relative to the burst point of a nuclear device and then of measuring certain of the aircraft responses for comparison with values obtained analytically. Since the purpose of the work was to determine delivery capabilities, the aircraft was manned during the test, and the flight pattern was one that could be used for a bombing mission.

The same B-36 aircraft employed in IVY blast effects tests was further instrumented for exposure in Shot 9 (8 May) of UPSHOT-KNOTHOLE. Instrumentation included the measurement of: overpressure; wing, fuselage, and horizontal stabilizer bending moments; horizontal stabilizer shear; and nose, tail, wing tip and center of gravity accelerations. In addition, photographic instrumentation was employed to measure and record the deflection of certain components.

NOTE: The remainder of this report is written as a composite presentation of results obtained by Project 5.3, UPSHOT-KNOTHOLE, and by Project 6.10, IVY, as mentioned in the Preface.

[redacted]

CHAPTER 2

PROCEDURE

2.1 GENERAL

This chapter is divided into three main sections presented in approximate chronological order covering the following subjects: selection of aircraft and criteria for exposure, instrumentation and calibration of aircraft, and field testing procedure. A brief history of the operation is given below.

Both the B-36D aircraft and the B-47B aircraft were SAC (Strategic Air Command) aircraft assigned to WADC (Wright Air Development Center). The B-36D aircraft was manned by a crew from SAC; the B-47B aircraft by a WADC crew. The B-36D aircraft was instrumented by personnel from WADC Aircraft Laboratory during the period 9 May 1952 to 15 June 1952, while the aircraft was located at Wright Field. Calibration of the aircraft by the Structures Test facility of Aircraft Laboratory was completed 15 August 1952. Following maintenance work performed at Carswell AFB, the B-36D aircraft was flown to the forward area arriving at Kwajalein on 21 September 1952. The B-47B aircraft was instrumented by AIRL (Aeronautical Ice Research Laboratory) and readied for overseas flight at Wright-Patterson AFB. Insufficient time was available for calibration prior to overseas movement primarily because of maintenance difficulties. It arrived at Kwajalein on 2 October 1952. Both Aircraft participated in the Mike (1 November 1952) and King (16 November 1952) shots of IVY. The B-36D and B-47B aircraft returned to the USA on 21 November 1952 and 23 November 1952, respectively. Following the return, Structures Test facility performed a check calibration on the B-36D aircraft and a complete calibration on the B-47B aircraft.

Prior to participation in Shot 9 of UPSHOT-KNOTHOLE, the empennage of the B-36D aircraft was more completely instrumented. Insufficient time was available for calibration prior to the test; however, an instrumentation sensitivity check was performed at CVAC (Consolidated Vultee Aircraft Corporation) to determine attenuation settings. For participation in the shot the aircraft was based at Kirtland AFB in Albuquerque, arriving there approximately 2 weeks before Shot 9. After the test the aircraft was flown to Fort Worth, Texas, where Convair calibrated the empennage instrumentation by the point-load system, as well as by the

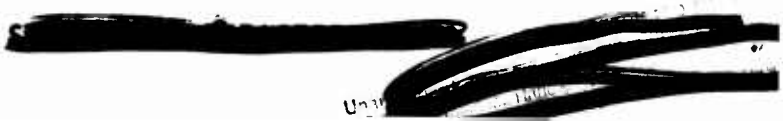

distributed-load or conventional calibration procedure. Technical assistance was provided by personnel from the Cook Research Laboratories, Inc., who were also responsible for reduction of the calibration data.

2.2 SELECTION OF AIRCRAFT AND INPUT LEVELS

This work was conducted as a part of the over-all problem of determining delivery capabilities of bombardment aircraft. In particular, it was concerned with feasibility studies relative to the delivery of high yield nuclear weapons. The actual weapons had not as yet been developed for air delivery purposes at the time the test aircraft were being selected. Aircraft considered were limited to those which, from preliminary estimates of probable over-all bomb size, could accommodate the megaton yield weapons being developed. In the planning stages of this experiment available information indicated the present B-36 aircraft would be capable of carrying bombs of the megaton yield range, although its ability to deliver this weapon safely was not known. The ability of a B-47 aircraft or a B-50 aircraft to accommodate a weapon of this size appeared doubtful. Consideration of the operational capabilities of B-50 aircraft suggested it was unlikely this type aircraft would be utilized for delivery of high yield weapons. In view of the above, plus the fact that structural response data had been obtained on B-50 aircraft during GREENHOUSE and was to be supplemented during UPSHOT-KNOTHOLE, it was decided to exclude the B-50 aircraft.

Because of the major role assigned B-36 aircraft in the over-all war plan and because of the probability B-36 aircraft can carry and deliver high yield bombs, highest priority was given to determining the maximum delivery capabilities of B-36 aircraft. It was considered desirable to include also a B-47 aircraft in the program even though budget and manpower considerations would not allow as complete an instrumentation program as was designed for the B-36 aircraft.

The primary consideration in the selection of input levels was personnel safety. During IVY the Weapons Effects Element was responsible for positioning the aircraft at the optimum location for the accomplishment of the mission with due regard for crew safety. In determining the danger regions for manned aircraft, five weapon effects must be considered. These may be summarized as follows:

1. Direct gamma radiation
2. Thermal radiation from the fireball
3. Gamma radiation and turbulence within the cloud
4. Overpressure of the shock wave
5. Material velocity (gust) of the shock wave

Aircraft maneuvers were designed so that thermal and blast inputs received would be similar to those that would be experienced on a straight and level flight bombing run. Based upon the above flight configuration, calculations were made as to the minimum safe distance for each of the two aircraft at detonation time and shock arrival. Preliminary analysis showed that the limiting criterion was either the temperature rise of the skin or the gust-induced structural loads. Maximum allowable skin temperature rises, set by the University of California, at Los Angeles

(UCLA), were 400°F for the 0.020 in. magnesium skin of the B-36 aircraft and 350°F for the 0.025 in. aluminum skin of the B-47 aircraft. Gust loads were not to exceed 100 per cent limit load for any component. Calculation of blast-induced loads was primarily the responsibility of Allied Research Associates, Inc. (ARA). Calculations relative to thermal radiation were performed by UCLA.

Utilizing the most conservative realistic values for all variables not firmly established, it was determined that the positioning of both aircraft for IVY would be based upon the maximum allowable skin temperature rise. For the lower yield weapon employed in Shot 9, UPSHOT-KNOTHOLE, gust-loading was limiting. The exact position assigned each aircraft for the three shots is given in paragraph 2.4, Field Testing.

2.3 INSTRUMENTATION

Since both instrumented aircraft were manned, many of the problems related to data-recording were minimized. Remote control (external to the aircraft) of equipment and telemetering of the data were not necessary. The equipment was located in a heated, pressurized compartment so that temperature and pressure extremes were not encountered. Aircraft vibration and shock acceleration in the air and also humidity, fungi, and salt spray on the ground were the main considerations governing recording equipment selection.

The sensing elements, being located for the most part in regions that were neither heated nor pressurized, were subjected during each flight to wide temperature and pressure fluctuations, as well as to the above mentioned adverse environmental conditions. In addition, certain sensing devices were subjected to thermal radiation, either directly or indirectly. The above factors were considered in the selection of instrumentation.

The major portion of the instrumentation was devoted to measuring and recording aircraft responses including bending, shear, torsion, and acceleration measurements. To facilitate correlation of input and response, overpressure measurements were also made. General flight data, such as airspeed, altitude, and orientation with respect to the burst point, were determined and recorded. Photographic instrumentation was employed for visual response determinations.

2.3.1 Inputs and Flight Data

The measurement of overpressure-inputs and the obtaining of general flight data, such as airspeed and altitude, are discussed in the sub-paragraphs following. Standard aircraft equipment was used to determine the desired flight variables. Existing equipment was modified in some instances to provide additional indicators for use by project personnel operating the instrumentation equipment.

2.3.1.1 Overpressure

Two types of instrumentation were employed for measuring overpressure inputs. One type, the High Frequency Pressure Recorder manufactured by Cook Research Laboratories, used a piezoelectric crystal as

the pressure sensitive element. Because the output of the crystal was quite low, significant amplification of the signal was required prior to recording. At the oscilloscope-camera recording unit the signal was fed into two amplifiers, one set to produce full-scale deflection for 2 psi input and the other set for a full-scale deflection with a 6 psi input. The equipment was designed with a frequency response of 50 to 250,000 cps.

The other method for measuring overpressure inputs employed a Model 3PAD10W Wiancko pressure transducer capable of measuring pressure differentials to 10 psi. The pressure pick-up consisted of a torsional, straight line Bourdon pressure element. To this was attached a variable reluctance armature which was caused to rotate in accordance with pressure variations on the sensing element. Consolidated Engineering Corporation 3 kc carrier equipment was used to amplify the gage output and supply a proportional DC signal to a recording oscillograph. The response to pressure was linear within a ±3 per cent up to 500 cps with a maximum rise time of 0.7 msec to 90 per cent of the full-scale output.

2.3.1.2 Altitude

The altitude of the aircraft above MSL was determined by several pieces of non-recording equipment, namely: Radio Altimeter SCR-718, Radar Bombing System ("K" system), and the standard aneroid altimeter used by the navigator. The aneroid altimeter was the least accurate of the three; however, it was the only instrument that could be used during zero time. The procedure followed was to check the radio altimeter and "K" system radar against each other. If agreement was obtained the aneroid altimeter was made to correspond with the more accurate electronic equipment. The aneroid altimeter was continually checked against the radio altimeter until shortly before zero time when the radio altimeter was shut off. Periodic altitude readings were recorded by the navigator in the flight log.

2.3.1.3 Airspeed

Airspeed measurements were made by means of the navigator's airspeed indicator installed in the aircraft. In both aircraft the instrument was calibrated using the "K" system radar. The radar equipment was used to determine wind velocity and aircraft velocity relative to the ground. With this information the correct indicated airspeed could be calculated. Airspeed indicator readings were recorded in the flight log periodically by the navigator.

2.3.1.4 Position

In this paragraph are described the equipment used to determine the location of the aircraft as projected on and measured with respect to some point on the earth's surface; i.e., position without regard to aircraft altitude (in some instances altitude was also determined as a secondary result). Methods and equipment are given below:

a. Radar Navigation

b. Bombing Equipment, Optical Sight
c. Aerial Mapping Camera
d. Radar Tracking from Ground
e. Station Keeping, Radar
f. Optical Ground Tracking

In the radar navigation method, the aircraft radar is used to determine the slant range distance to various targets placed at known locations in the test area. Knowing aircraft altitude, it is possible to calculate position using the above slant range data. Data recording was accomplished by means of radar scope photos.

With the optical bomb sight, visual sightings are made on landmarks or targets indicated on a chart and the aircraft position calculated.

The aerial mapping camera is activated shortly before time zero and operates through detonation time until the film is exhausted. The exact time of each photographic exposure was recorded by the oscillograph. If the aircraft flies over terrain having some recognizable features, it would be possible from scrutiny of the aerial photographs to chart the course of the aircraft as a function of time and determine its location at zero time.

The slant range and azimuth data from ground based radar tracking equipment can be used to determine aircraft location. This equipment also gives an approximate altitude figure and was used primarily for monitoring purposes to determine that aircraft would not be in a danger region at burst time or shock arrival.

"Station keeping" is the method whereby an aircraft is positioned by maintaining a fixed position with respect to another airborne aircraft, in this instance the "drop" aircraft. The two aircraft fly at constant, though possibly different, altitudes. If the difference in altitude is known, then the position of the test aircraft can be expressed in terms of a bearing and slant range to the "drop" aircraft. The correct bearing and slant range is maintained by use of radar.

Two-station optical ground tracking can be used to determine aircraft position if altitude is known. Operation depends upon measuring the azimuth and elevation angles from the two ground stations to the aircraft as a function of time. Exact location of ground stations must be known.

2.3.2 Response Measurements

Aircraft reaction to blast loading was measured in terms of acceleration, shear, torsion, and bending response at various points on the structure. The sensing elements or devices used for these measurements in all instances employed the strain gage principle, which makes use of the fact that the resistance of a wire varies in direct proportion to its elongation within the elastic limits of the wire. Strain gages are made of especially compounded wire that can be either bonded to a part of a structure or stretched between two objects that move relative to each other. The former application is generally used when measuring the strain in a structural member. The latter application, the unbonded strain gage, is generally employed in specific sensing devices such as

pressure transducers and accelerometers. Because bending, shear, and torsion in a structure can be determined by proper measurement and interpretation of strains developed, bonded strain gages may be used as the primary sensing element for the measurement of these response functions. Consideration of the factors mentioned in paragraph 2.3 led to the choice of Baldwin EBDF-13D strain gages for all bonded strain gage use. These strain gages had a nominal resistance of 350 ohms and were temperature compensated.

From previous experience it was known that the major problem regarding strain gage use would be the obtaining and maintaining of a good, atmosphere-tight bond between the gage and the metal. Several methods were tried but because of time limitations field testing was precluded. The method finally adopted for strain gage application was the conventional procedure employing Armstrong cement as the bonding agent.

2.3.2.1 Bending Moment

Bending moment measurements were made on the wings of both aircraft and the fuselage and horizontal stabilizers of the B-36 aircraft. The bending moment gage comprised four strain gages bonded to the primary structure and connected electrically so as to produce an output proportional to the bending induced. A typical bending gage installation employed for two-spar structures and a schematic diagram of the electrical circuit are shown in Fig. 2.1. The resulting strain bridge, a four-active-arm Wheatstone bridge circuit, is relatively unresponsive to loads other than those producing vertical bending. In some instances the bending of individual spars was measured and the bridge outputs combined, in a manner determined by special calibration, to give total bending moment. The installation was essentially the same as that shown in Fig. 2.1 for the two-spar structure, except that all four strain gages were placed on the one spar, two at the top and two at the bottom, using the same electrical interconnection. In the B-36D aircraft, fuselage bending is absorbed by the four main longerons. To determine fuselage bending, one gage was located on the inside of the outer flange of each longeron for a total of four gages. The standard bending gage bridge circuit was employed to combine strain gage outputs.

2.3.2.2 Torsion

The torsion bridge, an installation for direct measurement of torsion, was located in the left outer wing panel of the B-36 aircraft. Sixteen strain gages were located on the inside and outside surfaces of the skin between the front and rear spar; eight gages on the upper skin, four inside and four outside, and eight gages on the lower skin. A sketch of the installation and schematic circuit diagram is shown in Fig. 2.2. The resulting circuit is essentially a four-active-arm Wheatstone bridge circuit somewhat analogous to the bending gage except that there are four strain gages per arm.

2.3.2.3 Shear

Two types of shear measurements were made: the direct measure-

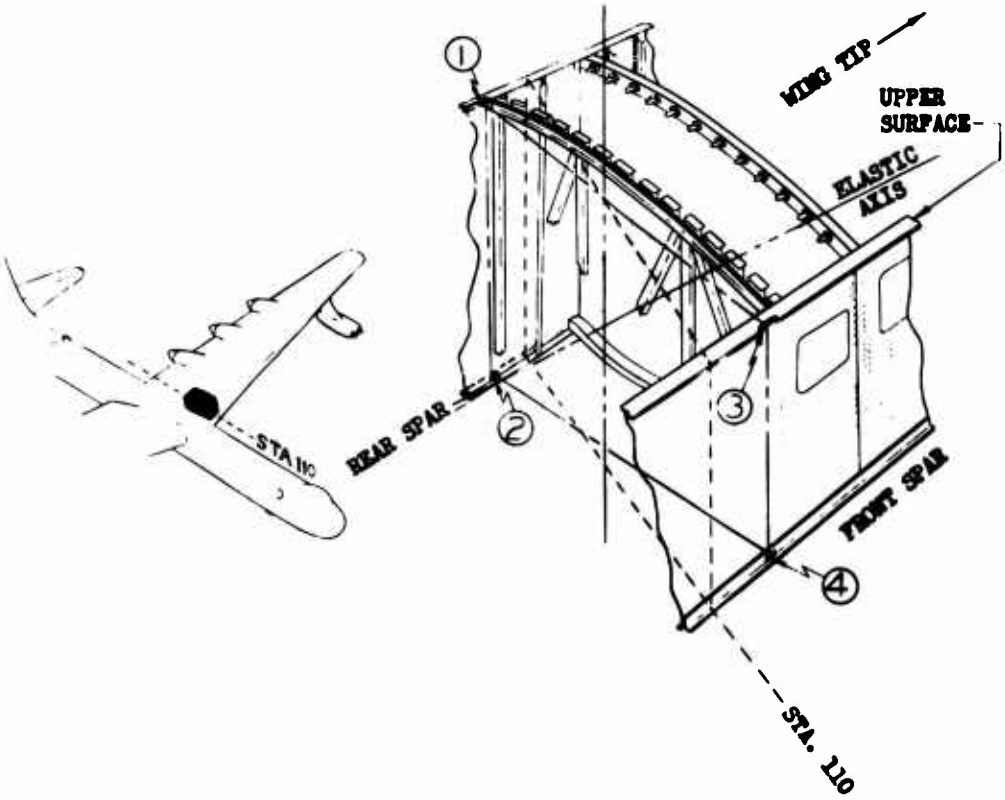

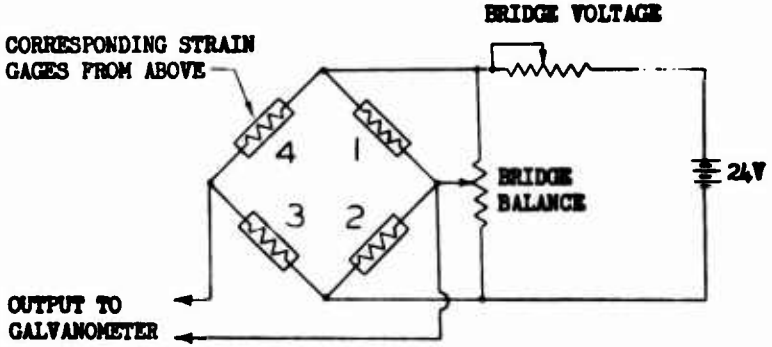

Fig. 2.1 Typical Bending Gage Installation with Schematic Circuit

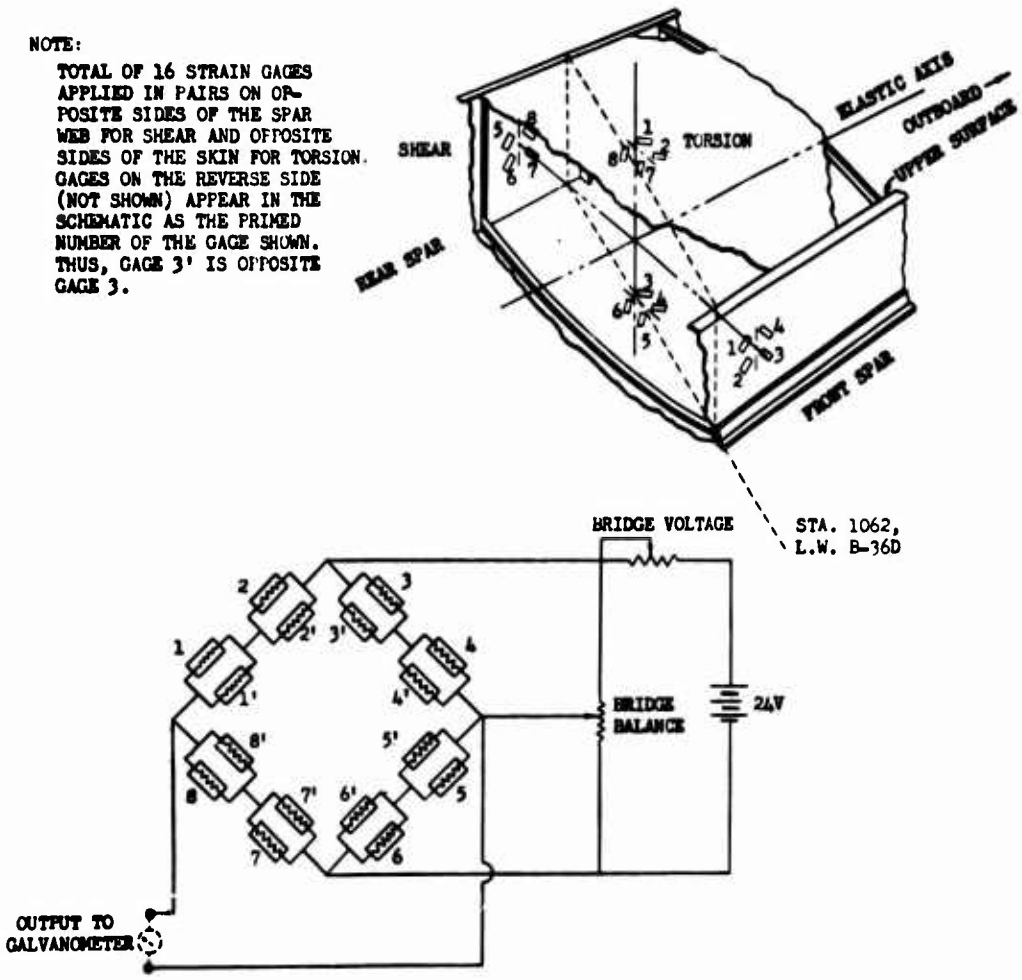

Fig. 2.2 Typical Torsion and Shear Gage Installation with Schematic Circuit

ment which employed a shear gage designed to cancel the effects of torsion and measure total shear on the component directly, and the indirect method, wherein the shear in individual structural members was measured. The output of the latter gage was not used directly but was combined with the output of other gages in accordance with an empirically determined formula to yield a value for total shear.

As with the torsion gage, the shear gage employed 16 strain gages and was likewise located in the left outer wing panel of the B-36 aircraft. Placement of the strain gages on the webs of the front and rear spars and the electrical interconnection thereof are shown in Fig. 2.2. The resulting circuit is a four-active-arm Wheatstone bridge very similar to that employed for the torsion gage. The installation used for measuring shear in a single spar is shown in Fig. 2.3.

2.3.2.4 Acceleration

The Statham, Type A-18, accelerometer was used for all acceleration measurements. Accelerometers covering the range of ± 6 g and ± 12 g and having a nominal bridge resistance of 350 ohms were selected. These transducers are accurate to 1 per cent of full scale with a response to transverse acceleration of not more than 2 per cent. Damping, 0.6 to 0.7 of critical, was provided by a special silicone fluid. Temperature of the unit was maintained constant by means of an internal, thermostatically controlled, heater unit.

2.3.3 Response Sign Convention

For convenience in indicating the direction of response, an arbitrary sign convention had been adopted for use in this report. In the definitions below, a normal flight configuration is assumed. The positive direction for the various responses is defined as follows:

a. Acceleration, Normal - an increase in the upward velocity or decrease in the downward velocity of the aircraft or any component thereof.
b. Bending (Aft Fuselage) - tail deflection upward, compression in upper surface.
c. Bending (Wings and Stabilizers) - tip deflection upward, compression in the upper surface.
d. Overpressure - the differential pressure above ambient pressure.
e. Shear (Wing and Stabilizers) - tip deflection upward; same sign as positive bending.
f. Torsion (Wing) - leading edge of wing deflected upward with respect to remainder of wing.

2.3.4 Recording Equipment

The major portion of the data was recorded by means of a standard recording oscillograph. Where very fast response was required, a modified oscilloscope with a recording camera was employed. The principle of operation and salient features of the recorders and associate equipment are

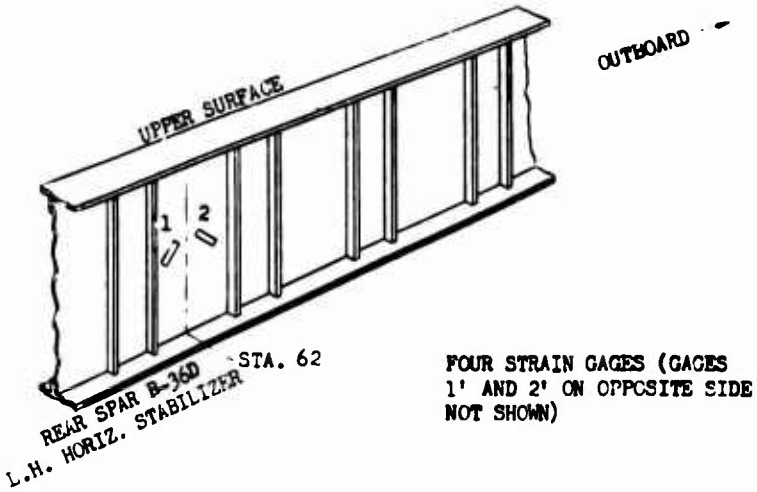

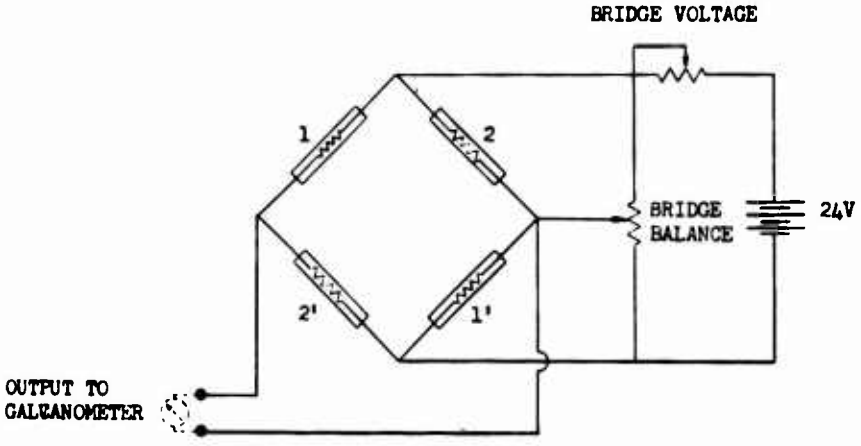

Fig. 2.3 Typical Single Spar Shear Gage Installation with Schematic Circuit

discussed in the sub-paragraphs below.

2.3.4.1 Recording Oscillographs

Consolidated Engineering Corporation, Type 5-114-P-3, 18-channel recording oscillographs were used to record all response measurements. Selection was based upon previous experience which indicated this equipment, if properly installed, would adequately record the desired data under the anticipated test conditions. Further, the equipment was immediately available. The oscillograph was made insensitive to aircraft vibrations and blast-induced shock accelerations by simple shock mounting. No special modifications, other than provisions for increasing paper speed by overriding the governor, were deemed necessary. Pertinent information relative to the oscillograph and operation thereof is summarized below:

a.	Active data channels . .	18, plus one dynamic reference
b.	Power	24-28 volts DC
c.	Paper width	7 in.
d.	Paper length	125 ft
e.	Record speed used . . .	6 in./sec
f.	Approximate maximum recording time	250 sec
g.	Timing marks	0.01 sec intervals

Outputs from the sensing elements are in the form of fluctuating DC voltages. Operation of the oscillograph depends upon converting the electrical output of the various gages into a proportional galvanometer deflection that can be recorded as a function of time. To accomplish this, oscillographs are equipped with galvanometers of the D'Arsonval type having a mirror attached to the upper tension support. Thus mounted, the mirror follows the movement of the galvanometer coil. To record the galvanometer movements, a beam of light is reflected by the mirror onto a moving sheet of photosensitive paper. The resulting trace on the photographic paper is a permanent, time-history record of the variation of the response function being measured. Galvanometers are chosen on the bases of sensitivity and frequency response required for the type of measurement being made. A separate galvanometer is used for each channel.

A Consolidated Engineering Corporation Type 8-104A Bridge Balancing Unit was used to couple the sensing devices to the oscillograph and provide the proper bridge voltage and bridge balancing resistance. In addition to the above functions, the bridge unit also provides a known bridge unbalance for calibration purposes, adjusts the input circuit resistance so that the galvanometer is properly damped, and provides for signal attenuation. A schematic of a typical four-active-arm bridge including the bridge balancing unit and oscillograph is shown in Fig. 2.4. Bridge voltage, supplied from a 24 volt aircraft battery, is adjusted by means of the rheostat shown. The bridge is then balanced by means of the bridge balance potentiometer so that there is no deflection of the galvanometer. If the sensing element were now subjected to a measurable input, the Wheatstone bridge would become unbalanced producing

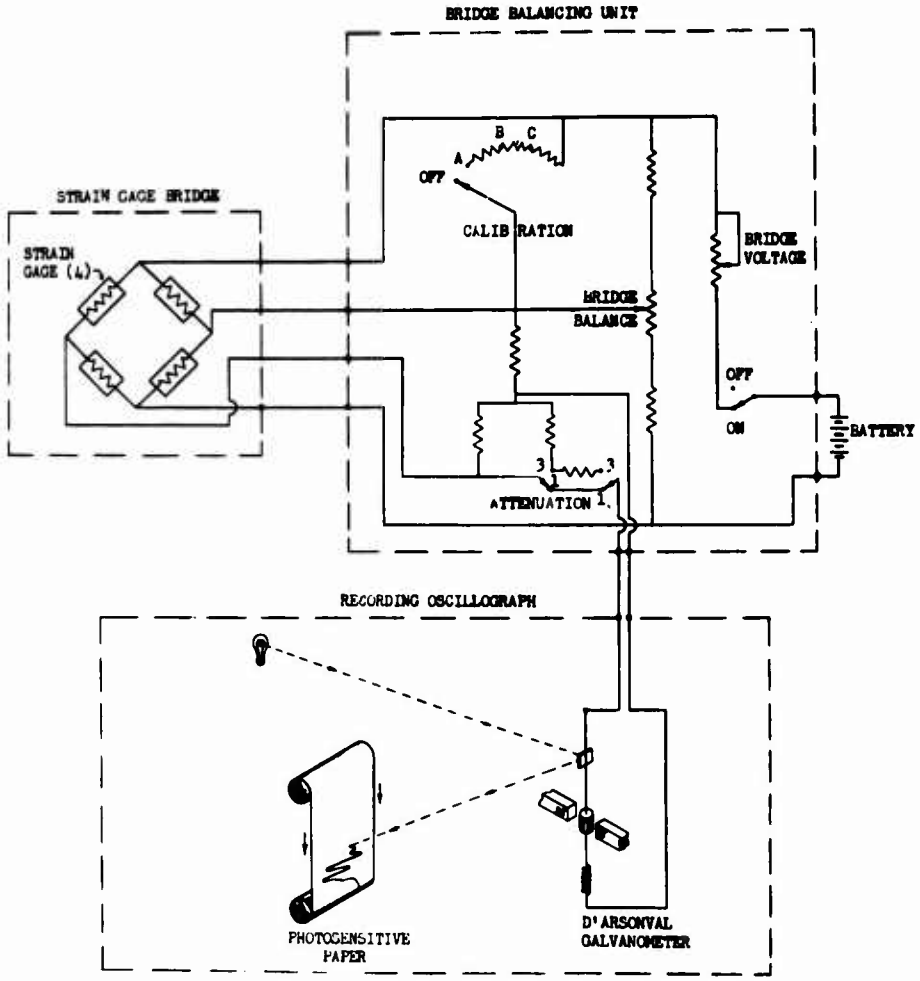

Fig. 2.4 Schematic Diagram of Recording Circuit Showing Strain Bridge, Bridge Balancing Unit and Recording Oscillograph

a signal that would be transmitted through the bridge balancing unit to the galvanometer in the oscillograph which in turn would cause a beam of light to be deflected from a zero position on the moving sheet of photographic paper. If the signal is too strong, it may be attenuated by changing the attenuation switch from position 1 to position 3. The calibration device is used as a rapid check on the sensitivity of the system. It does not aid in determining the relationship between gage output and the measured function. The calibration device provides a known bridge unbalance by putting a resistance in parallel with one of the arms of the bridge which in turn produces a certain galvanometer deflection which is a measure of the over-all sensitivity. This operation is generally referred to as a "calibrate step." If the unbalance is such that the galvanometer deflection is in the direction designated as positive, it is known as "cal plus"; if the deflection is in the opposite direction, it is known as "cal minus."

A photosensitive device manufactured by Edgerton, Germeshausen & Grier, Inc., and known as a "blue box" was employed to provide a time reference on the oscillograph record. The device is actuated by bomb lighting and, hence, can be used to indicate burst time. The unit was located in the bottom of the fuselage aft of the rear crew compartment.

2.3.4.2 High Frequency Pressure Recorder

The High Frequency Pressure Recorder, Type PR-3, was manufactured by Cook Research Laboratories. In conjuction with the crystal microphone pressure transducer explained in paragraph 2.3.1.1, the system was capable of measuring recording pressure transients as a function of time. Basically, the system consisted of a pressure transducer that supplied an electrical signal to the horizontal deflection plates of an oscilloscope causing a beam deflection recorded by a continuous strip camera. The oscilloscope, a modified Type 279 Du Mont Dual-Beam Oscilloscope, had an amplifier for each of two beams. The gain of these amplifiers was so adjusted that for one amplifier a 2 psi input would cause full-scale deflection while the other amplifier required 6 psi on the crystal to produce full-scale deflection. The system was calibrated in the air by introducing a 400 cycle square wave signal of the proper magnitude to simulate the transducer output corresponding to a 2 psi pressure differential.

2.3.5 Photography

Motion picture photography was employed to measure the deflection of various components as a result of blast loading. Displacements were to be measured with respect to the part of the aircraft upon which the camera was mounted. The cameras, a total of five, were mounted as a unit atop the fuselage between the wings at fuselage station number 785. The wing tips, nose, and empennage could be viewed from this location. Pylons were placed on the wings and aft fuselage as reference markers (Fig. 2.5).

The cameras comprised three 16 mm GSAP cameras and two, Model H, 35 mm Camera-Flex cameras. The GSAP cameras and Camera-Flex cameras were operated at speeds of 64 frames per second and 128 frames per second,

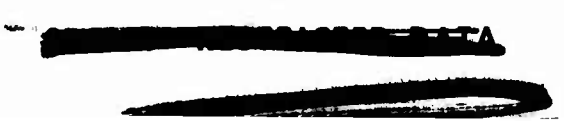

respectively. The cameras were disposed as follows: one GSAP and one Camera-Flex camera viewing the left wing, one GSAP and one Camera-Flex camera viewing the tail, and one GSAP camera sighting forward along the top of the fuselage. Figure 2.6 shows the camera installation with the cover off and cover in place. Operation of the cameras was controlled manually by a switch in the aft crew compartment.

Fig. 2.5 Pylons, Left Wing
B-36 Aircraft

2.3.6 Location in Aircraft

Location of the sensing devices and instrumentation equipment installed in the two aircraft is described for each aircraft in the sub-paragraphs below. The instrumentation of the individual aircraft was not changed between Mike and King Shots. For Shot 9, additional instrumentation was added to the B-36 empennage.

2.3.6.1 B-36 Aircraft

The location of sensing elements and recording equipment utilized on the B-36 aircraft for IVY is shown schematically in Fig. 2.7. The code numbers are used to cross-reference Fig. 2.7 and Table 2.1 which supply additional detail on the various installations. The aircraft was instrumented for 14 response and two input measurements. The pressure transducers were mounted in the boom on the left wing, shown in Fig. 2.7, to minimize the influence of the aircraft on the free air overpressure measurement. Instrumentation was located either in the fuselage or the left side of the aircraft, except for one bending gage installed in the right wing to check loading symmetry. The method of installing and electrically connecting the various gages has been discussed earlier in paragraph 2.3.2, which also includes sketches of typical installations.

The oscillographs and associate equipment were located in the aft crew compartment shown in Fig. 2.8. The view shows the left side of the compartment looking forward. The table occupies the space normally used by the lower bunk. Two of the four oscillographs mounted on the table are shown. The oscillograph in the foreground was used to record blast data; the remaining three were used to record thermal data.

To facilitate switching from main to spare gages and to permit recording any of the gage outputs on any of the 16 channels, a selector panel, shown in Fig. 2.9, was installed. The bridge balances employed are also shown. The high frequency pressure recorder used in the measure-

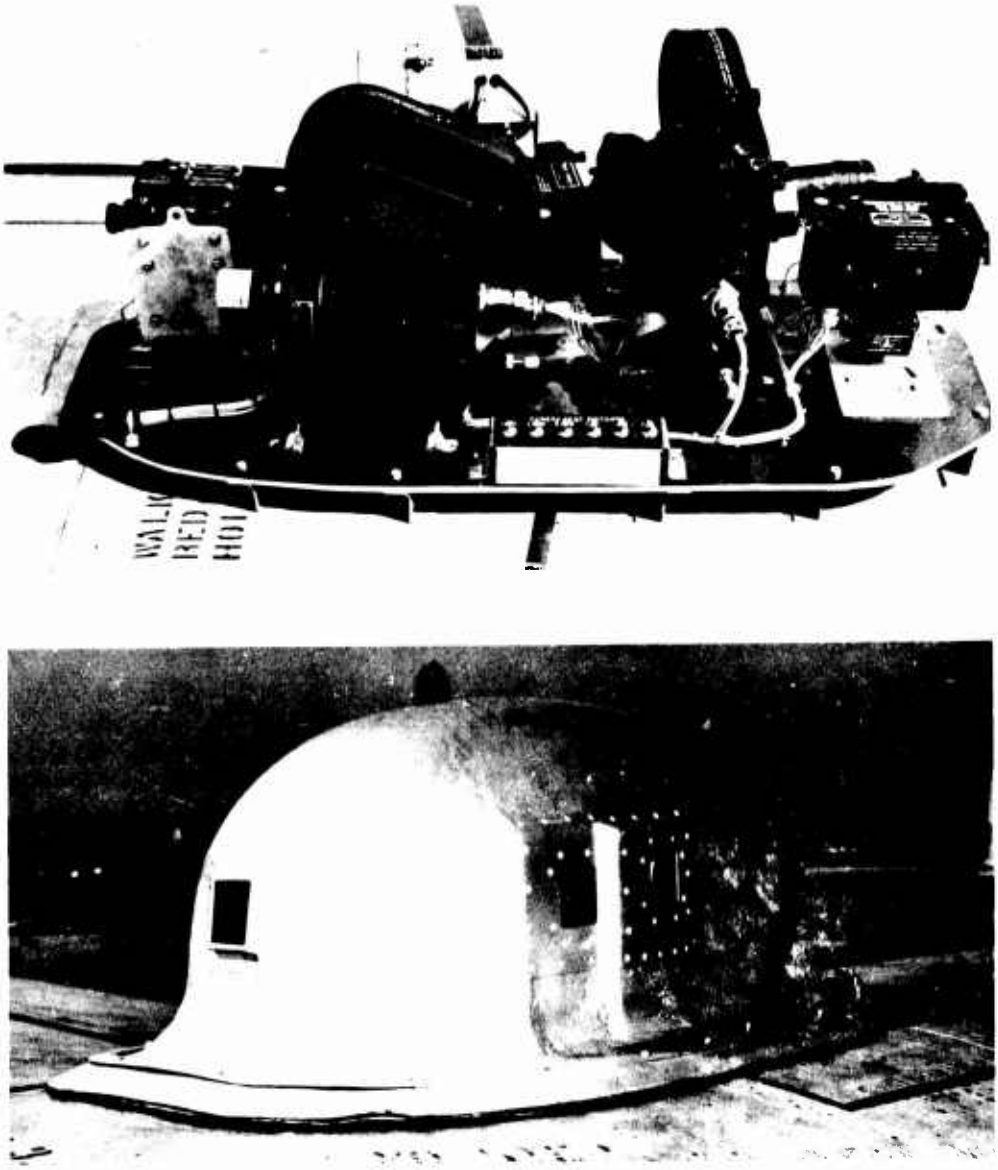

Fig. 2.6 Cameras and Camera Housing, B-36 Aircraft

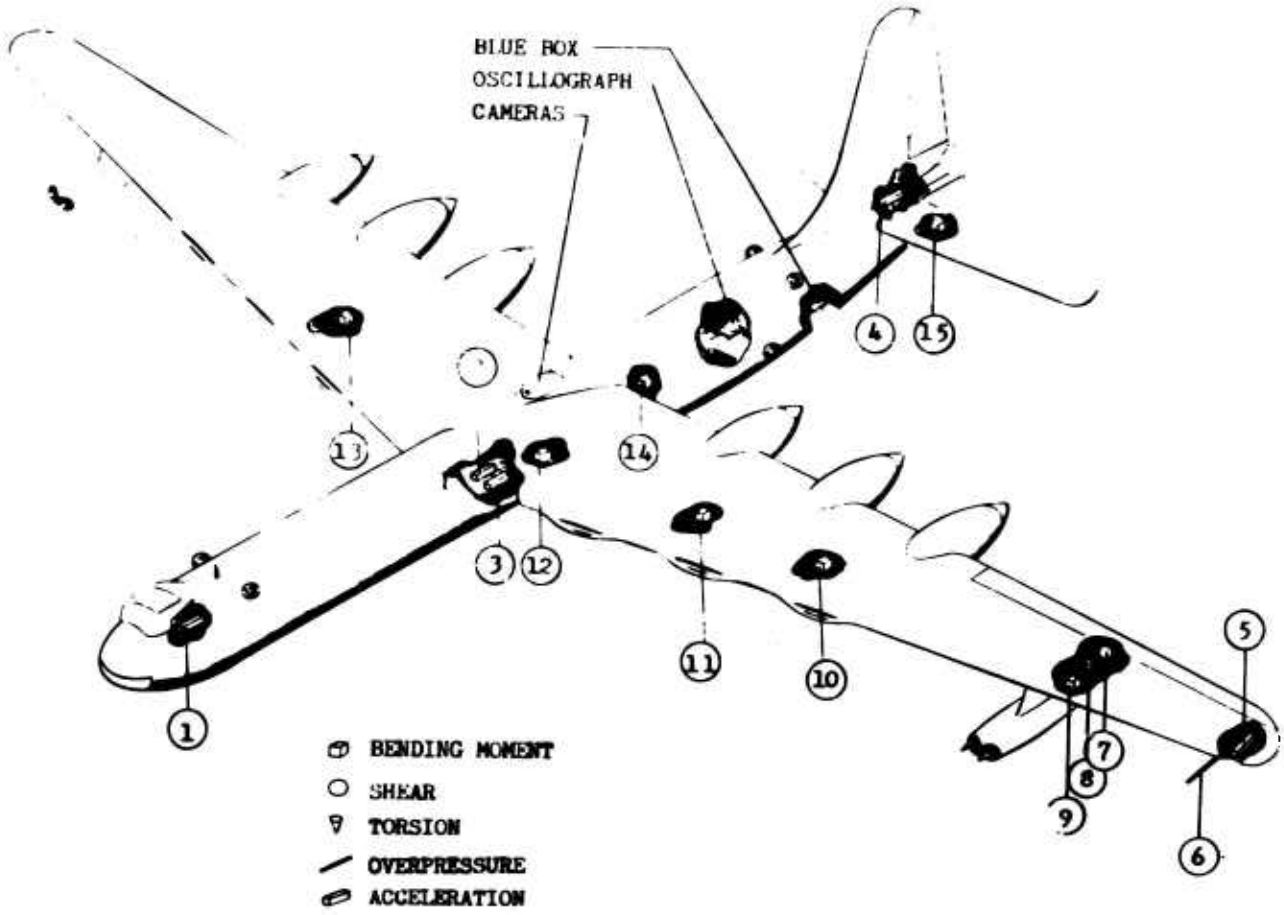

Fig. 2.7 Location of Instrumentation in B-36D Aircraft for IVY

TABLE 2.1 - Instrumentation, B-36D Aircraft, IVY

Reference Number	Measurement	Galvanometer Type (CEC No.)	Location Component
1	Acceleration	7-215	Nose Wheelwell, Fus. Sta. 212
2	Acceleration	7-225	Lower Right Main Longeron, Fus. Sta. 907, (Bomb Bay)
3	Acceleration	7-225	Lower Left Main Longeron, Fus. Sta. 907, (Bomb Bay)
4	Acceleration	7-239	Rear Spar, Horizontal Stabilizer, Fus. Sta. 1770
5	Acceleration	7-239	Wing Tip, Left Wing, Sta. 1340
6	Pressure	7-223	Boom on Left Wing, Sta. 1301
7	Shear	7-215	Front & Rear Spar Web, Left Wing, Sta. 1062
8	Torsion	7-239	Upper & Lower Skin, Left Wing, Sta. 1062
9	Bending Moment	7-215	Caps, Front & Rear Spar, Left Wing, Sta. 1062
10	Bending Moment	7-215	Caps, Front & Rear Spar, Left Wing, Sta. 604
11	Bending Moment	7-215	Caps, Front & Rear Spar, Left Wing, Sta. 390
12	Bending Moment	7-215	Caps, Front & Rear Spar, Left Wing, Sta. 110
13	Bending Moment	7-215	Caps, Front & Rear Spar, Right Wing, Sta. 390
14	Bending Moment	7-215	Upper & Lower Main Longerons of Bomb Bay, Fus. Sta. 1040
15	Bending Moment	7-215	Caps, Front & Rear Spar, Left Stabilizer Sta. 62

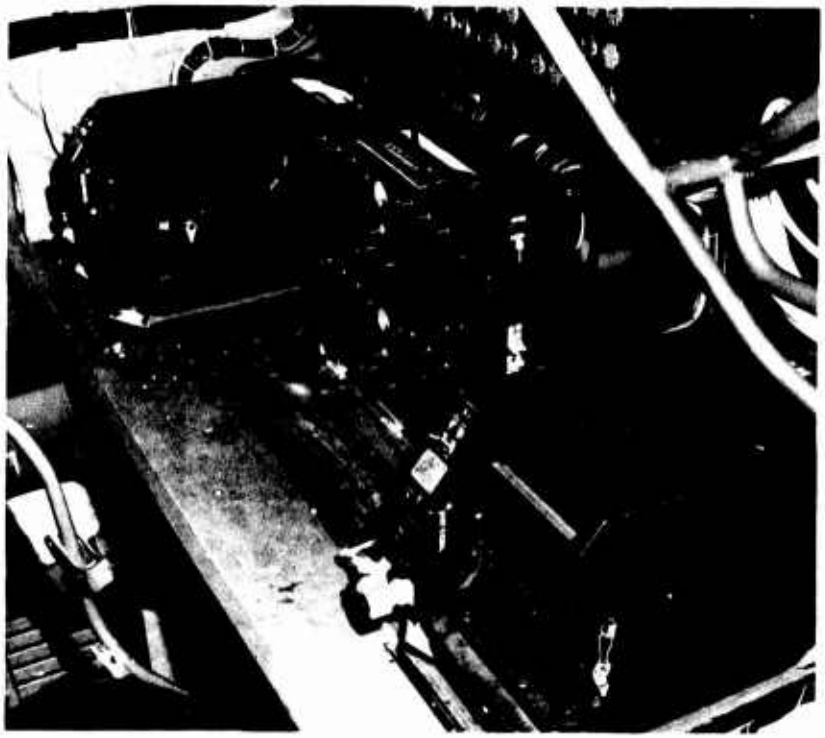

Fig. 2.8 Oscillographs and Bridge Balances, Aft Crew Compartment, B-36

Fig. 2.9 Selector Panel, Aft Crew Compartment, B-36

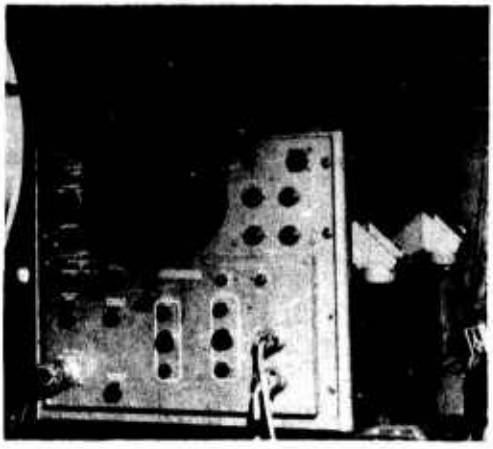

Fig. 2.10 High Frequency Pressure Recorder, Aft Crew Compartment, B-36

ment of the peak overpressure of the blast wave is shown in Fig. 2.10. The Fairchild continuous strip camera is shown in position. Operation of all recording equipment, including the cameras measuring component deflection, was controlled from one panel shown in Fig. 2.11. The blue box fiducial was mounted in a specially constructed housing in the bottom of the fuselage aft of the rear crew compartment. The housing had a window facing to the rear to admit bomb light to the instrument. An external view of the installation is shown in Fig. 2.12.

Fig. 2.11 Master Control Panel, B-36

Instrumentation for UPSHOT-KNOTHOLE was the same as that for IVY except for the additional measurements made on the horizontal tail. Figure 2.13 in conjunction with Table 2.2 shows the instrumentation employed. A total of 14 strain channels were recorded: two were a direct measurement of total bending; six measured the shear of individual spars; and the remaining six measured the bending of individual spars. Outputs from the 12 single spar shear and bending strain bridges were combined to obtain total bending, total shear, and torsion at the three instrumented stations.

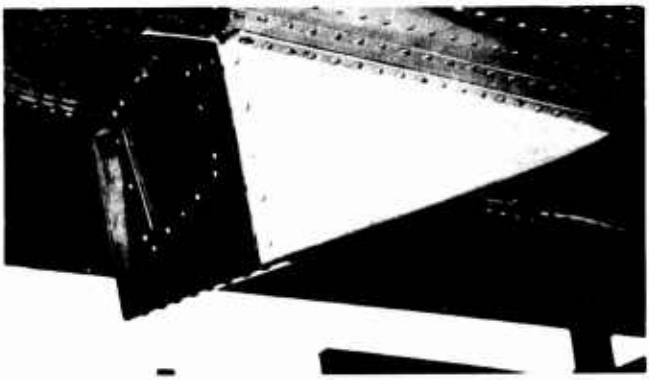

Fig. 2.12 Housing for Blue Box Beneath Aft Fuselage, B-36

2.3.6.2 B-47 Aircraft

Blast response instrumentation of the B-47 aircraft was limited to four measurements: two wing bending moments and two accelerations.

[redacted]

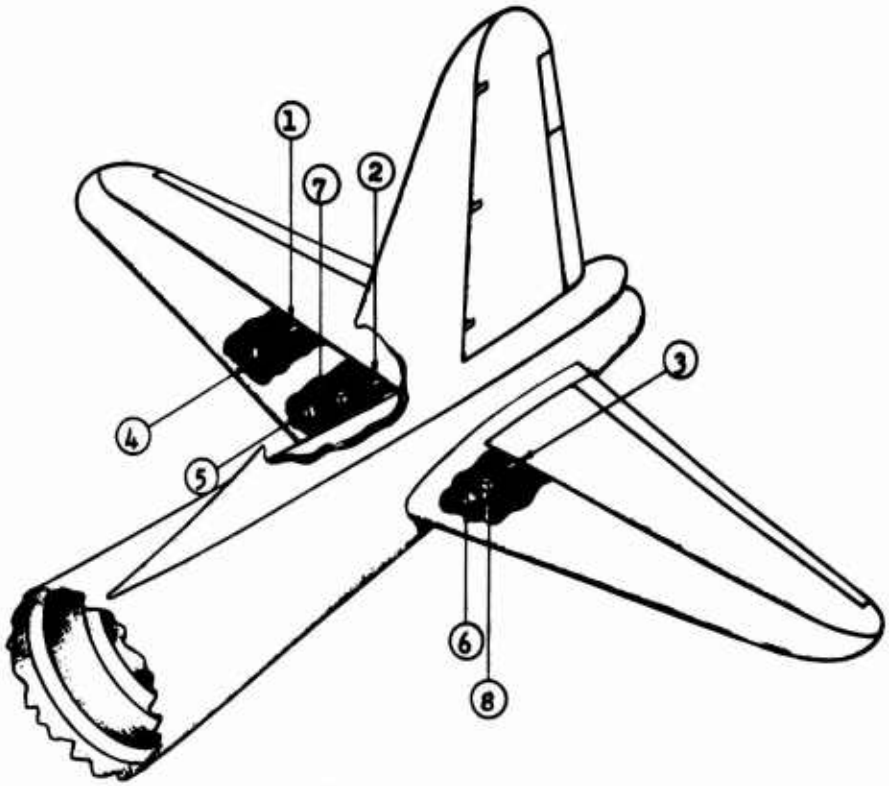

Fig. 2.13 Location of Instrumentation in B-36D Empennage for UPSHOT-KNOTHOLE

TABLE 2.2 - Instrumentation, B-36D Empennage UPSHOT-KNOTHOLE

Reference Number	Measurement	Galvanometer Type (CEC No.)	Location Component
1	Spar Shear, (One Bridge/Spar)	7-215	Front & Rear Spar, Right Horizontal Stabilizer Station 144
2	Spar Shear, (One Bridge/Spar)	7-215	Front & Rear Spar, Right Horizontal Stabilizer Station 62
3	Spar Shear, (One Bridge/Spar)	7-215	Front & Rear Spar, Left Horizontal Stabilizer Station 62
4	Spar Bending, (One Bridge/Spar)	7-212	Front & Rear Spar, Right Horizontal Stabilizer Station 144
5	Spar Bending, (One Bridge/Spar)	7-212	Front & Rear Spar, Right Horizontal Stabilizer Station 62
6	Spar Bending, (One Bridge/Spar)	7-212	Front & Rear Spar, Left Horizontal Stabilizer Station 62
7	Total Bending, (One Bridge Total)	7-212	Front & Rear Spar, Right Horizontal Stabilizer Station 62
8	Total Bending, (One Bridge Total)	7-212	Front & Rear Spar, Left Horizontal Stabilizer Station 62

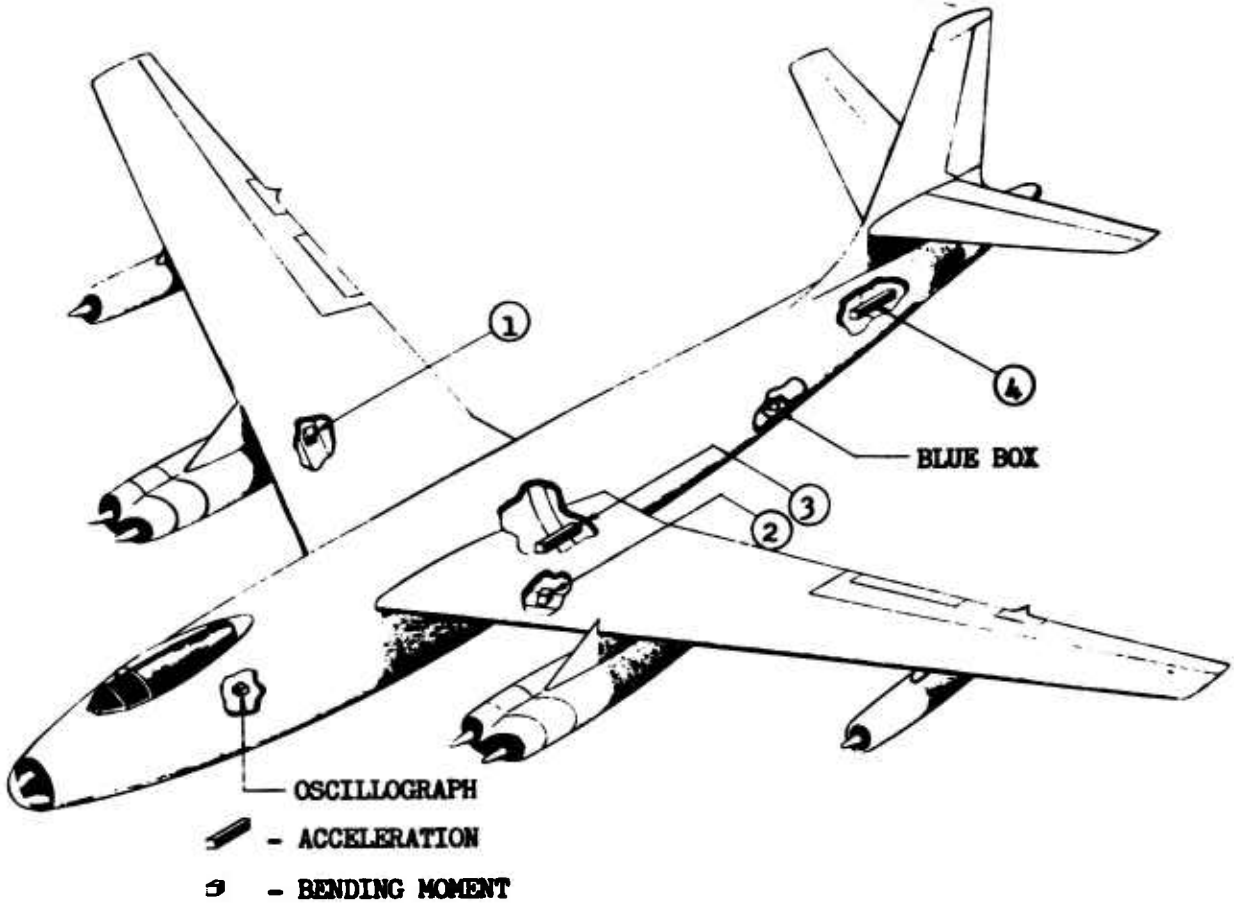

Fig. 2.14 Location of Instrumentation in B-47B Aircraft for IVY

Figure 2.14 is a schematic of the aircraft showing instrumentation location; Table 2.3 provides additional details. The bending gages measured total bending moment and were similar to those used on the wing of the B-36 aircraft. The oscillograph was installed in the aft portion of the cabin and operated remotely by the co-pilot. A view of the installation is shown in Fig. 2.15.

Fig. 2.15 Oscillograph Installation, B-47B Aircraft

2.3.7 Calibration

Because of the difficulty involved in predicting the precise response of a particular part of a complicated structure for a given load condition, and because of the individuality of each recording channel, it is generally necessary to calibrate built-up strain gage instrumentation experimentally, by applying known incremental values of the related function and correlating gage output with the applied loads, rather than by theoretical calculation. The above experimental procedure was followed for the calibration of all bending, shear, and torsion gages installed on both aircraft with the exception of the additional instrumentation installed on the B-36D empennage for UPSHOT-KNOTHOLE. The additional gages installed on the empennage were calibrated by a system known as the "point load" system. With this system a given response function is determined by properly combining the outputs of several bridges instead of using the output of a single bridge as in the standard procedure. As explained in the NACA Report TN2993, the point load system is capable of

TABLE 2.3 - Instrumentation, B-47B Aircraft, IVY

Reference Number	Measurement	Galvanometer Type (CEC No.)	Location Component
1	Bending Moment	7-215	Caps, Front and Rear Spars, Right Wing Station 186
2	Bending Moment	7-215	Caps, Front and Rear Spars, Left Wing Station 186
3	Acceleration	7-212	Center of Gravity, Bomb Bay Fuselage Station 587.8
4	Acceleration	7-212	Aft Fuselage, Battery Compartment, Fuselage Station 1121.5

greater accuracy than the conventional method, particularly where variable and irregular loading is involved, e.g., the center of pressure on the wing displaced toward the trailing edge.

The purpose of any calibration is the establishment of a relationship between instrumentation output and the magnitude of the function being measured. Experimental calibration is sometimes approximate because of the difficulty in simulating actual inputs of a known, controllable value, as for example in the calibration of a pressure transducer. Reliability of many experimental calibrations, therefore, must be determined, in part, from theoretical considerations. The procedures used in calibrating the instrumentation installed in the B-36 and B-47 aircraft were primilary the same as those used in past operations. These procedures are described in detail in Chapters 2 and 3 of Greenhouse Report WT-31.

2.3.7.1 Pressure and Acceleration

As mentioned previously in paragraph 2.3.1.1, both the Wiancko pressure gage and the Cook High Frequency Pressure Recorder were used for overpressure measurements. The former gage utilized a torsional diaphragm-variable reluctance transducer, whereas the latter gage employed a crystal microphone as the pressure sensing element. The output of both gages was amplified prior to recording; however, the amplifier for the crystal microphone did not respond to frequencies below 20 cps. Thus, the Cook system could not measure static pressure levels as could the Wiancko gage.

For calibration, the Wianko gage was hooked-up as it was for actual operation and the circuit balanced for zero galvanometer deflection. Using the calibrate steps provided in the bridge amplifier, a positive and negative calibration step was introduced into the circuit and the resulting galvanometer deflections measured. The gage was then subjected to various positive and negative pressures of known value to determine galvanometer deflection as a function of pressure. The deflections were read as percentages of the deflection obtained for the calibrate step and were recorded as percentages of cal-plus (positive calibration step) or cal-minus (negative calibration step). The galvanometer deflection obtained in the calibration step is defined as 100 per cent cal. The resulting calibration curve for the gage is a plot of pressure versus per cent of a known calibrating signal (per cent cal). The calibration curve was drawn as a straight line. If the data points were found to deviate significantly from a straight line after repeated calibrations, the gage was not used. Theoretically, a linear response should be obtained. After the static pressure calibration, the gage was rechecked in a shock tube.

The Cook High Frequency Pressure Recorder contains a calibration circuit that produces a 0.62V 400 cycle square wave output which is equivalent in voltage level to the output of the crystal when subjected to a blast pressure of 2 psi. This signal is introduced into the system at the pressure transducer and follows the same path as the transducer signal to produce ultimately a trace on the photographic record. The maximum displacement of the trace represents the displacement that will be obtained for a 2 psi input if the system is operating properly. Over-all

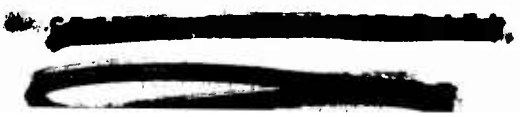

operation of the pressure measuring device was checked by measuring blast pressures produced in a shock tube. Accuracy of the instrument was found to be within the accuracy of the calibration.

Accelerometers were calibrated by subjecting the instrument to known accelerations while connected to an oscillograph through a bridge balance unit in the manner employed for field measurements. Desired accelerations were obtained by using a device known as a "shake table." As for the pressure gage, positive and negative calibrate steps were obtained, and the final calibration expressed as acceleration versus per cent cal. A typical calibration curve is shown in Fig. 2.16.

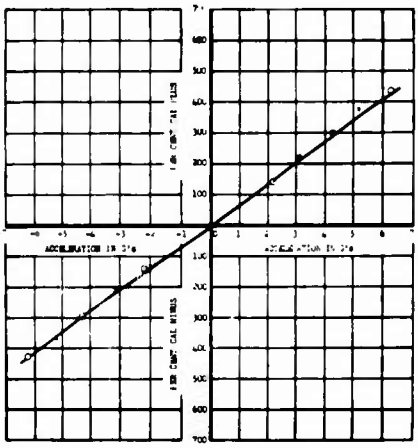

Fig. 2.16 Typical Calibration Curve for Accelerometer

2.3.7.2 Bending, Shear, and Torsion

The calibration procedures described in this section apply only to instrumentation designed such that the output of a single bridge, consisting of from 4 to 16 strain gages, is used to determine the value of the response function. Calibration of the bending, shear, and torsion gages, as defined above, will be termed standard or conventional calibration and is basically the same for the three gage types. In essence, the calibration consists of subjecting various portions of the aircraft to certain known loads, such that the exact value of a particular function, for example, bending moment, can be calculated at a given gage location. Gage outputs are then related to the calculated values of their related function over the desired range.

To calibrate for wing bending moment, it was necessary to support the aircraft at points along the fuselage so that no load was carried by landing gear attached to the wings. A dead weight relieving load was then applied at various points along the wing and the gages balanced for zero output. Incremental distributed loads were then applied in gradually increasing amounts up to a maximum allowable value and then removed again in a similar step-wise manner until the zero stress condition was again attained. The gage output was recorded each time the applied load was changed for both the loading and unloading phases. The gages were calibrated for both up-bending and down-bending. Calibration steps were employed as before and the final calibration expressed as in-lb of bending moment versus per cent cal. Calibration of the bending gages on the fuselage and horizontal stabilizers was accomplished by the same method used for wing bending calibration. Wing mounted landing gear was allowed to take load while calibrating the fuselage and empennage. Framework and apparatus used to apply the calibrating loads are shown in Fig. 2.17.

Shear gages were calibrated coincidentally with the bending gages. Calibration consisted of summing applied loads outboard of the

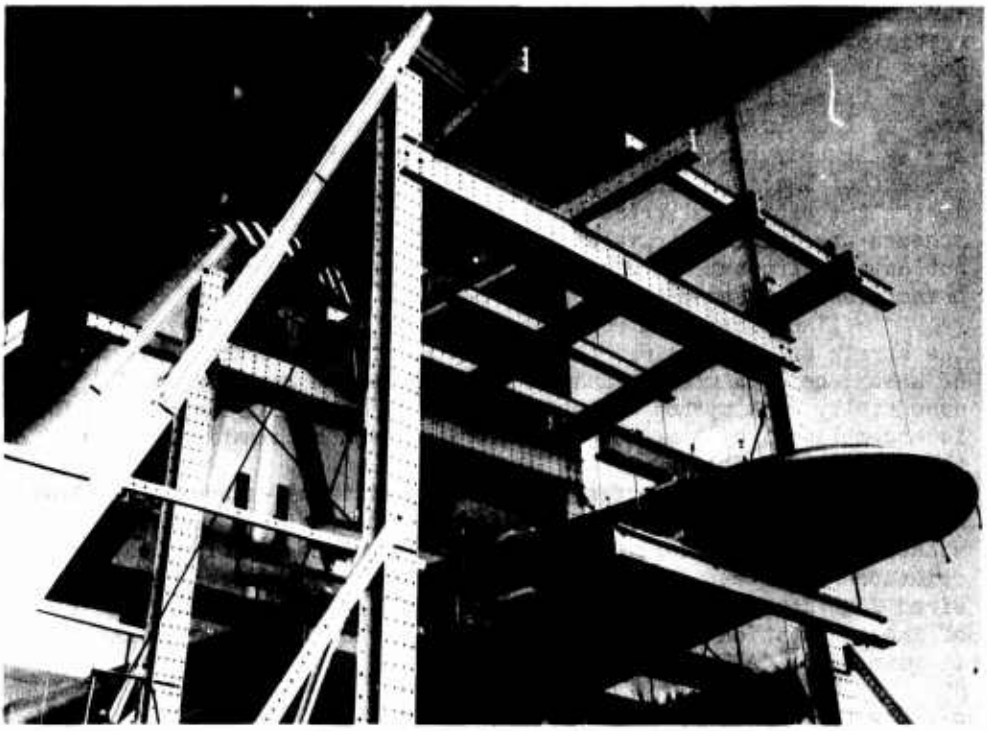

Fig. 2.17 Calibration of B-36D Aircraft Empennage in Structures Test Facility of Aircraft Laboratory

gage location and plotting these loads as a function of the galvanometer deflection expressed as a percentage of cal. The only torsion gage was installed in the left outer wing panel of the B-36D aircraft. For calibration, a dead weight relieving load was applied so that bending and shear stresses, as well as torsional stresses, were reduced to zero at the gage location. As before, the gage was balanced out and calibration steps taken, after which a vertical force couple was applied outboard of the gage, such that the leading edge was deflected upward and the trailing edge downward and vice versa for the negative torsion calibration. Because torsion was applied by a couple action, the total bending and shear induced was zero. The torsion applied was determined by the magnitude of the force couple and the distance of the points of application from the elastic axis. The in-lb of torque applied for each load increment was calculated, and gage output, expressed as a percentage of cal, was plotted versus torsional response in in-lb.

2.3.7.3 Point Load System

The National Advisory Committee for Aeronautics (NACA) has developed and presented in NACA Report TN 2993, a method for measuring shear, bending moment, and torsion in the principal lifting or control surfaces of an airborne aircraft. This method, as utilized in this investigation, is hereafter referred to as the Point Load Method. The point load method differs from other methods of strain gage instrumentation primarily in the manner in which the three principal terms pertinent to load investigations, i.e., shear, bending moment, and torque, are separated. In the past, strain bridge installations for the measurement of loads on aircraft have been made using many schemes for reducing the effects of cross coupling and interaction. Most of these schemes are still quite valuable in the field of less complex structures, but as the structures become more complex, errors increase and the principles of these methods become more and more difficult to apply.

The point load method is based on the premise that, in general, the strain along all lines through any point in a structure is a function of shear, bending moment, and torque. The point load system consists essentially of a method of separating these principal functions. This is accomplished by a method of calibration and mathematical analysis of the calibration data.

Point loads were applied on 13 points of each semi-span of the horizontal tail surface for four different conditions. Combined gage equations were then derived from these data. The equations express the relationship between the response of the selected bridges and the desired function. A detailed presentation of how the point load method of instrumentation was calibrated and employed to measure blast loading is given in NACA Report TN 2993.

2.4 FIELD TESTING PROCEDURE

After the aircraft were instrumented, as described in paragraph 2.3, they were flown to check out the instrumentation and then readied for overseas flight for participation in IVY. The IVY tests, conducted at the Pacific Proving Grounds in the Fall of 1952, comprised two shots, Mike and King. Both the B-36D and the B-47 aircraft were flown in the two IVY shots. In the Spring of 1953, the B-36 aircraft was exposed during Shot 9 of UPSHOT-KNOTHOLE tests held at the Nevada Proving Grounds.

The field testing procedure consisted of two essential parts: positioning the aircraft for the desired inputs and operation of the instrumentation equipment for measurement and recording of the response data. The position selected was a point in space where, from predicted data, the maximum allowable input would be realized if the weapon yield reached its upper limit. To position the aircraft at the point selected with a maximum of accuracy and a minimum of danger required precision timing and flawless navigation. The procedures employed for exposing the two aircraft are given below.

2.4.1 B-36 Aircraft

On Mike Shot, the B-36 aircraft was to be flying straight and level at an altitude of 40,000 ft and heading away from ground zero at burst time and shock arrival. Since allowable temperature rise was the controlling factor, aircraft position was based on slant range at time zero and not at shock arrival. The minimum safe distance at burst time, based on a 20 MT yield, was calculated to be 91,200 ft; the expected slant range at shock arrival thus became 140,000 ft. Figure 2.18 shows the flight pattern designed to position the B-36 aircraft for Mike Shot. Intended positions at time zero and shock arrival are shown.

The B-36 aircraft left Kwajelein Air Base at 0300 hours on the morning of shot day and flew to the assigned orbiting area over the Eniwetok Atoll, arriving approximately 3 hours before scheduled shot time. The prescribed orbit was maintained by means of radar navigation using an I.P. (initial point) on Runit Island. During the orbiting, flight instruments such as altimeters and airspeed indicators were cross-checked and wind velocity determined. Knowing wind velocity and the prescribed maneuver after leaving the orbit, it was possible to calculate the exact time, based upon time zero, the aircraft must leave the I.P. in order to be in proper position at the time of detonation. With this information, and knowing the time required to complete one revolution of the orbit, it was possible to determine the exact time the aircraft must pass over the I.P. each pass up to shot time. Slight corrections were made each revolution to keep crossing the I.P. at the calculated time. On the last pass the aircraft flew straight over the I.P., continued in straight and level flight for the proper time interval, then made a 90° turn to the left and flew straight away from the vertical line through ground zero as shown in the sketch referred to above. Test altitude was maintained for a short period after shock arrival to permit an instrumentation check.

Beginning in the afternoon of shot day minus one, a complete inspection and functional check-out of the instrumentation was conducted. All cameras were checked, loaded after sunset, and set for remote control operation. Approximately two and one-half hours before take-off time on shot day, another complete instrumentation check-out was begun. After take-off, the instrumentation equipment was turned on and all channels checked while climbing to the test altitude of 40,000 ft.

All strain channels were balanced while the aircraft was in a leg of the orbit, that is, in straight and level flight. Thus, loads measured would be those in excess of the normal (one g) flight loads. Balancing of strain gages continued until 15 minutes before time zero, at which time a new magazine was installed in the oscillograph. At this point all instrumentation equipment was operating but the recording equipment was not turned on. Five minutes before time zero protective coverings were placed over all windows. Ten seconds before scheduled shot time all recording equipment was activated. The equipment was allowed to run until at least one minute after shock arrival. A clearing run was made about 10 minutes after shock arrival while the aircraft was still at the test altitude.

On King Shot, the second shot of IVY, the B-36 aircraft was re-exposed in a manner similar to that employed for Mike Shot. The predicted

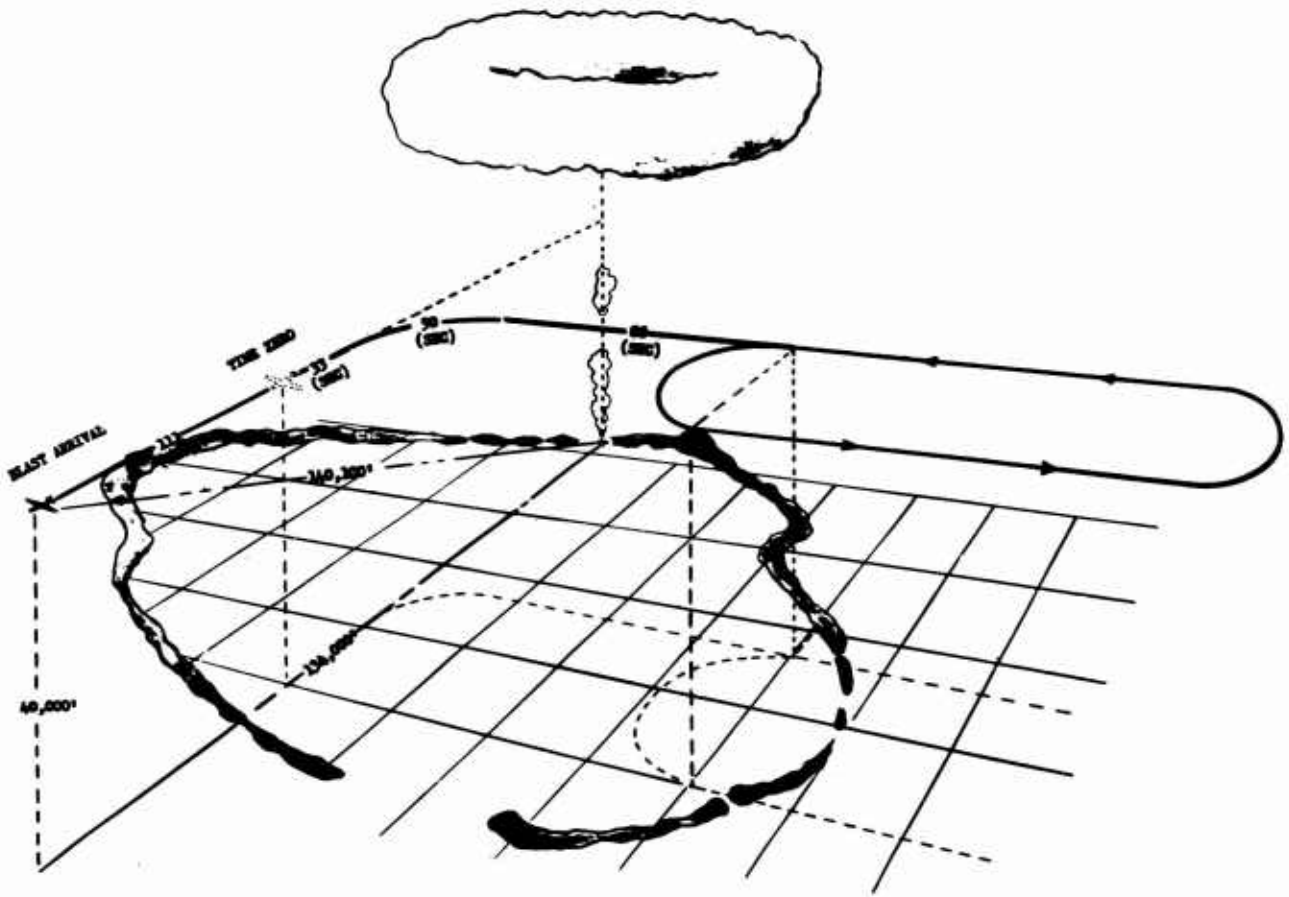

Fig. 2.18 Assigned Position and Flight Pattern of B-36D Aircraft for Mike Shot Showing Flight Times from Leaving Orbit to Blast Arrival

yield being considerably smaller for King Shot, the intended slant range at zero time and shock arrival was reduced to 34,000 ft and 62,500 ft, respectively. King Shot was an air drop and, therefore, it was necessary to synchronize all maneuvers, time-wise, with the drop aircraft. Figure 2.19 shows diagrammatically the planned flight pattern of the B-36D aircraft for King Shot. Operation of the instrumentation equipment was essentially the same as that employed for Mike Shot.

For Shot 9 of UPSHOT-KNOTHOLE, the B-36 aircraft was based at Kirtland AFB. The position assigned for participation in Shot 9 was determined by the allowable load on the horizontal tail. To permit positioning at a higher blast input, the weight configuration of the aircraft was adjusted so as to obtain a download on the horizontal tail. This was accomplished by loading 25,000 lb of bombs in the forward bomb bay to produce a forward shift in the center of gravity. Accounting for the initial download on the tail, the minimum safe slant range at shock arrival, assuming a 34 KT weapon yield, was computed to be 26,500 ft. The flight pattern designed to achieve this slant range is shown in Fig. 2.20. The test aircraft flew an orbit identical to that flown by the drop aircraft except that the orbit was displaced upward 3000 ft and forward 4880 ft. The test aircraft maintained the proper orbit by using a form of radar navigation known as "station keeping." The "K" system radar was used to maintain the desired slant range between the drop aircraft and the test aircraft, and an altimeter was utilized to keep the aircraft at the correct altitude. The procedure for data recording was approximately that employed for IVY.

2.4.2 B-47 Aircraft

The different structural configuration and performance characteristics of the B-47 aircraft allowed it to be positioned closer to the burst point at time zero than was the B-36 aircraft. At burst time and shock arrival on Mike Shot, the B-47 aircraft was to be flying straight and level at an altitude of 35,000 ft and heading directly away from ground zero. If the weapon yield reached the predicted upper limit, the maximum allowable temperature would be induced in the 0.025 in. aluminum skin if the aircraft were at a slant range of 75,600 ft at burst time. Positioning on this basis, the resulting slant range at shock arrival becomes 181,948 ft. The flight pattern set-up to position the aircraft for the shot is shown in Fig. 2.21. The aircraft left Kwajelein Air Base at 0810 hours on shot day and proceeded to the orbiting area east of Eniwetok Atoll to begin the prescribed flight maneuvers. As with the B-36 aircraft, the flight plan called for orbiting until a specified interval before time zero, then leaving the orbit and executing a 90° turn to the left at the proper time so as to orient the aircraft with the tail toward the explosion prior to burst time. Before the maneuver was completed, the radar equipment failed causing the aircraft to be out of position.

The three man crew of the aircraft comprised the pilot, co-pilot, and navigator, thus allowing no instrumentation engineer aboard during the flight. The final instrumentation check and balancing of strain channels, therefore, was completed prior to take-off. A comprehensive instrumentation check-out was scheduled for the day before the test and

[redacted]

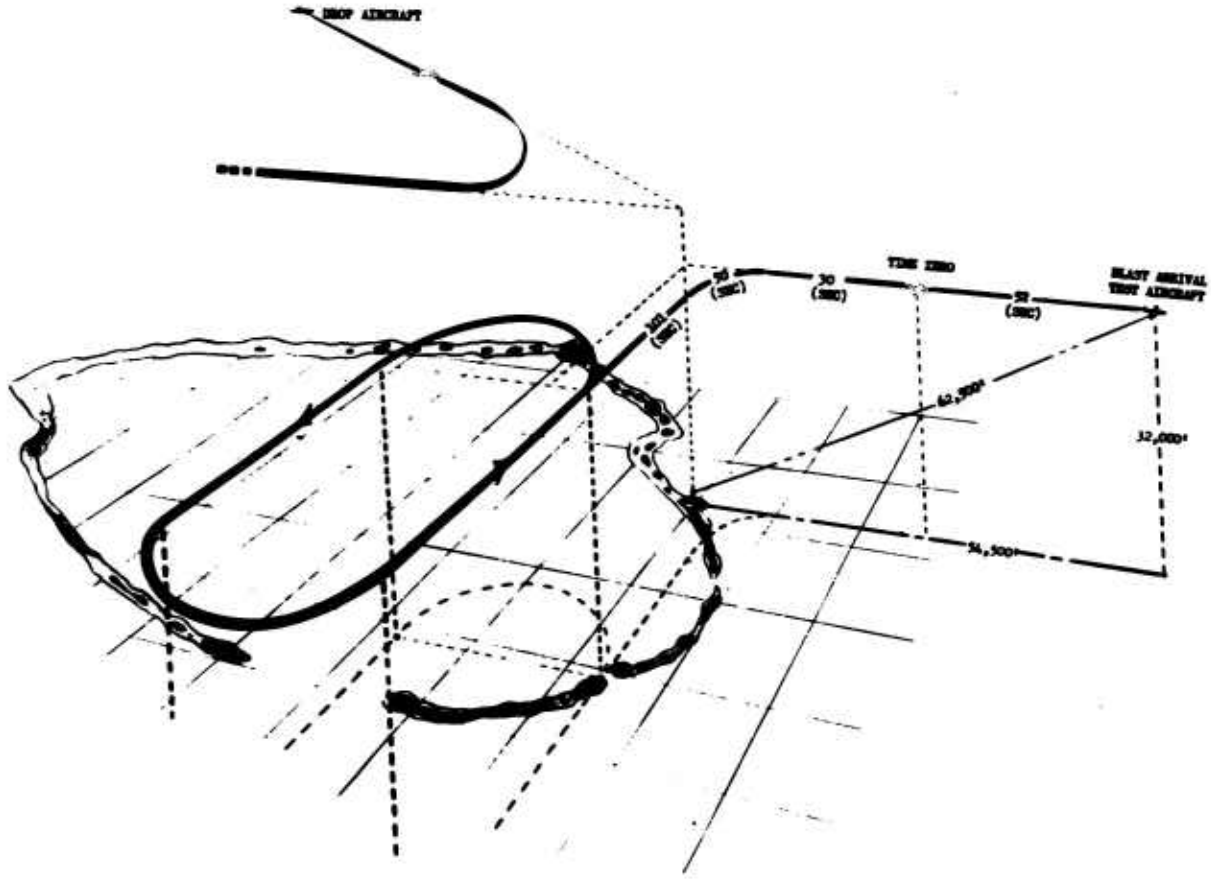

Fig. 2.19 Assigned Position and Flight Pattern of B-36D Aircraft for King Shot

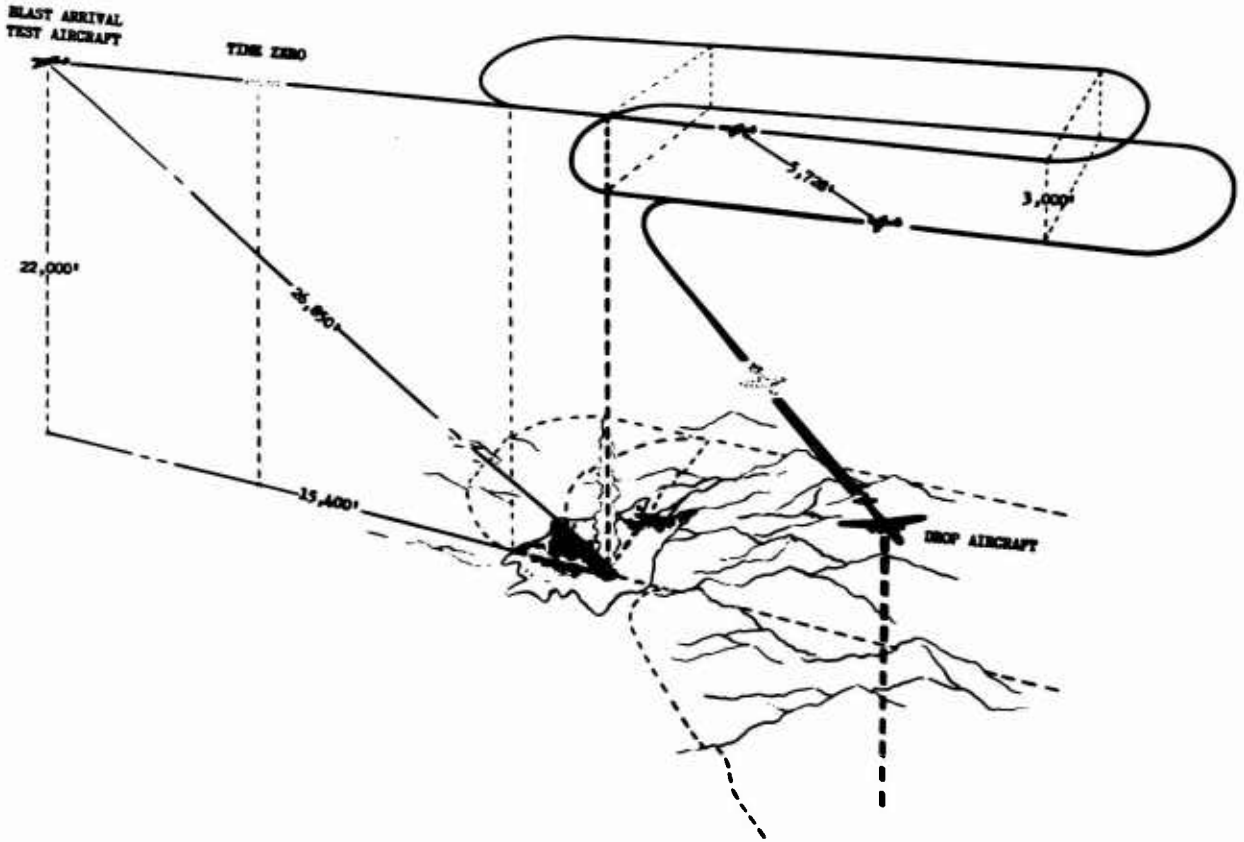

Fig. 2.20 Assigned Position and Flight Pattern of B-36D Aircraft for Shot 9

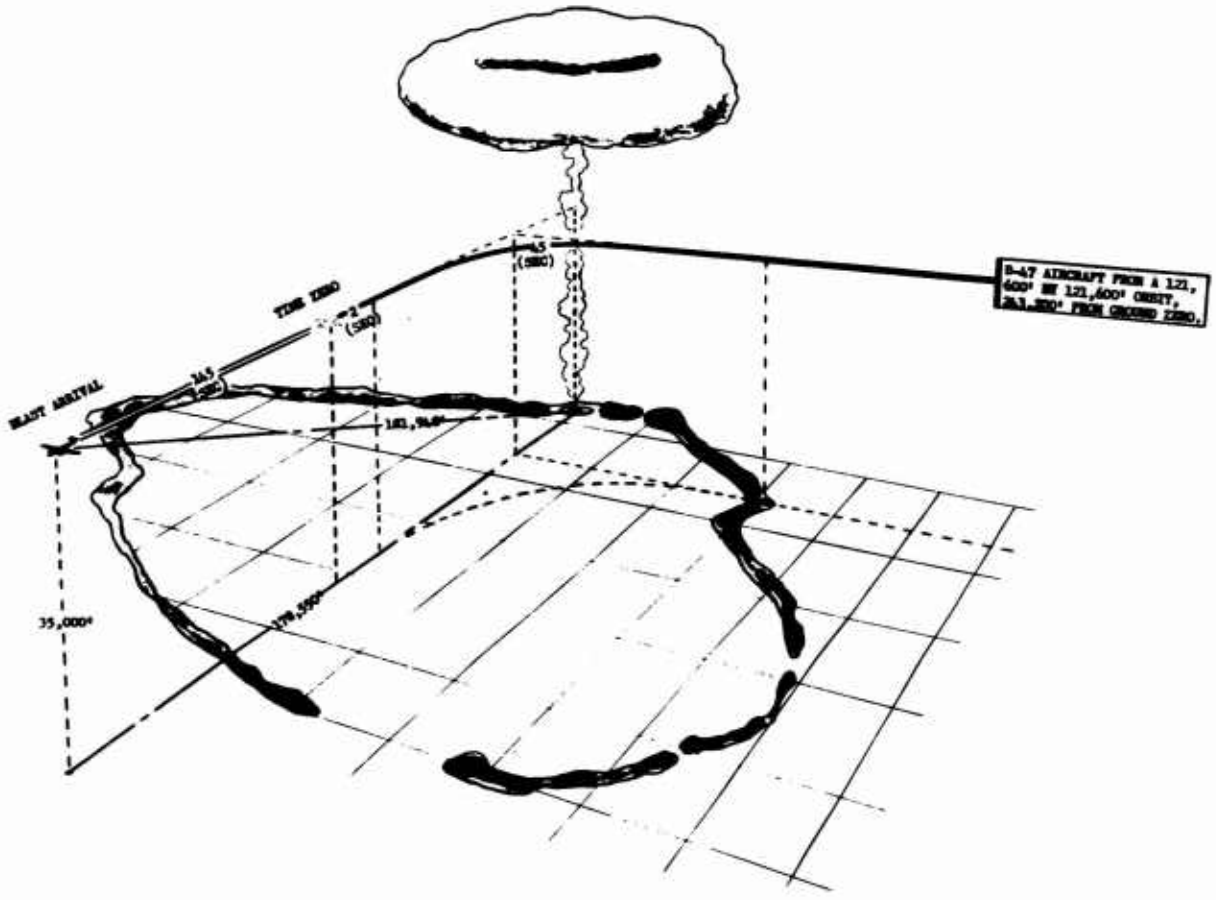

Fig. 2.21 Assigned Position and Flight Pattern of B-47B Aircraft for Mike Shot

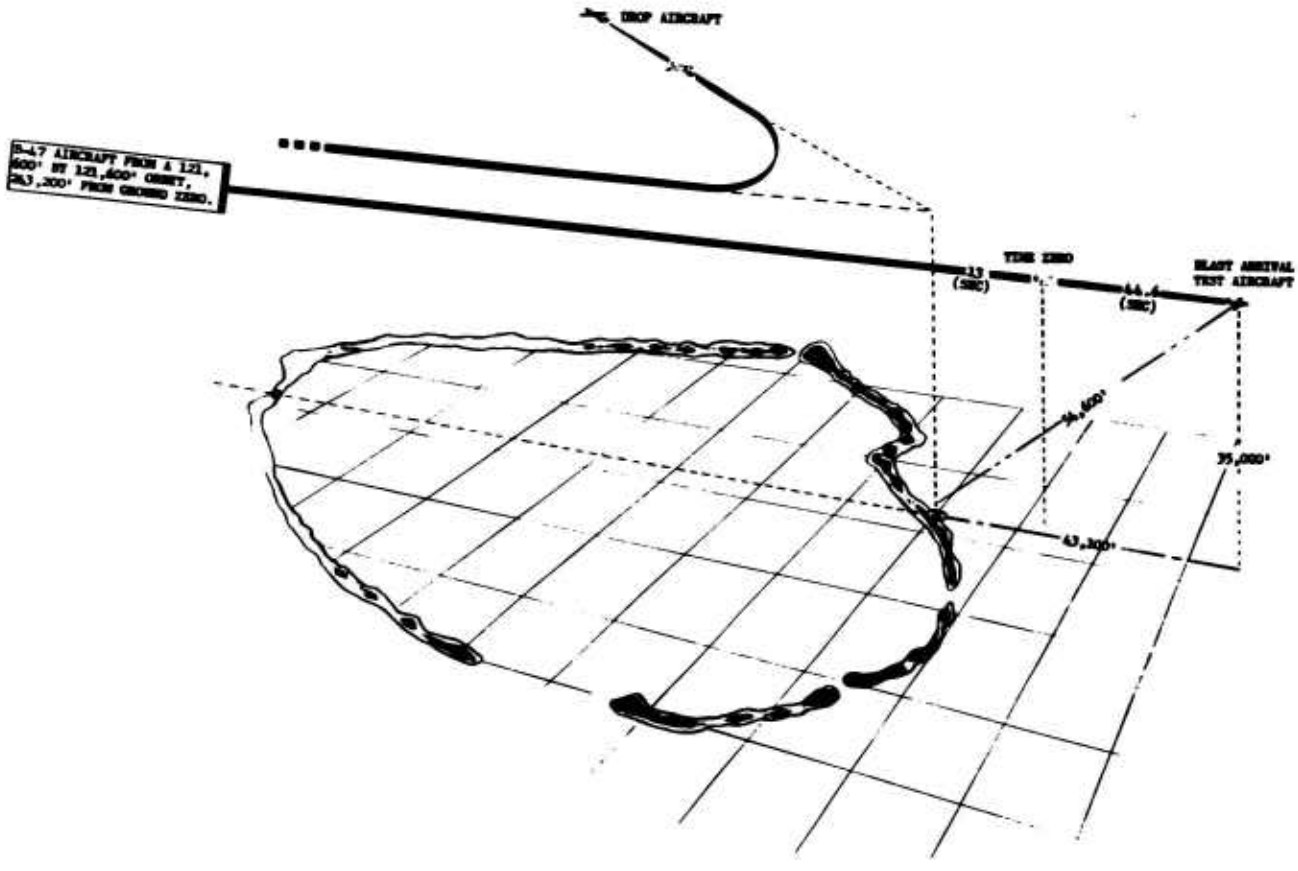

Fig. 2.22 Assigned Position and Flight Pattern of B-47B Aircraft for King Shot

repeated on the morning of shot day. After the final check, all switches were left in operating position except the oscillograph drive switch. At time zero minus 5 seconds, the co-pilot turned on the oscillograph drive switch, then turned it off again after a 5 minute interval. After landing, the balance was checked before shutting off power. Since the strain channels were balanced while the aircraft was on the ground, the loads measured included the normal flight loads, as well as loads induced by the blast. The data presented in the results section are given in terms of loads above normal (one g) flight loads. These loads were obtained by using the flight loads just prior to shock arrival as a zero reading for the wing bending moment. These values were checked by determining total load using the ground balance and subtracting out the (one g) flight load. Results from both methods were in good agreement.

The position selected for exposure of the B-47 aircraft in King Shot was an altitude of 35,000 ft and a slant range of 54,600 ft at shock arrival. The flight pattern is shown in Fig. 2.22. An orbit was again employed for synchronization with the drop ship; however, after leaving the orbit, a straight and level flight configuration was maintained. Operation of the instrumentation was as explained for Mike Shot.

CHAPTER 3

RESULTS, MIKE SHOT

3.1 GENERAL

The experimental device for Mike Shot was housed in a structure located on Elugelab Island in the Eniwetok Atoll. It was detonated at 0800 on the morning of 1 November 1952. The hydrodynamic yield was reported as 10.4 MT. This yield was considerably higher than the predicted most probable yield used as the basis for adjusting instrument sensitivity, and as a consequence certain channels of information were unintelligible for a short period after shock arrival because of the wide fluctuations caused by the higher-than-anticipated inputs. After burst time and before shock arrival, the B-36 aircraft was allowed to lose approximately 1500 ft of altitude in order to increase flying speed. The aircraft was leveled off at an altitude of approximately 38,500 ft prior to shock arrival. Position at shock arrival, except for the lower altitude, was approximately as planned. Acceptable blast response measurements were made; overpressure measurements did not evince a high degree of reliability. No blast response instrumentation data were obtained from the B-47 aircraft because of its excessive range at shock arrival.

3.2 AIRCRAFT POSITION, INPUTS, FLIGHT DATA

Data relative to the conditions of exposure for each aircraft are given in the sub-paragraphs below. Where several measurements were made, the best average value is reported. Meteorological data such as the magnitude and direction of the wind at the test altitude were not recorded.

3.2.1 B-36 Aircraft

Data pertinent to the exposure of the B-36D aircraft in Mike Shot are summarized below:

a. Altitude, MSL, 38,500 ft
b. Horizontal range at shock arrival, 127,100 ft

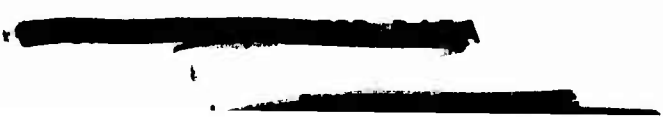

c. Slant range at shock arrival, 132,800 ft
d. True airspeed, 278 knots
e. True ground speed, 254 knots
f. True heading, 187°
g. Aircraft attitude, 4° nose high
h. Angle of incidence of shock front, 16.8°
i. Shock arrival time, 102.8 sec
j. Peak overpressure (WADC), 0.33 psi
k. Peak overpressure (AFCRC), 0.224 psi
l. Gross weight at shock arrival, 232,000 lb
m. Center of gravity location at shock arrival, 36.4% MAC

The actual position of the B-36 aircraft relative to ground zero and assigned position is shown in Fig. 3.1. The position is based upon data from the aircraft "K" system radar, the U.S.S. Estes radar track, IBDA photos, and calculations using time of shock arrival. The peak overpressure measured by instrumentation aboard the test aircraft was 0.33 psi; however, the ratio of signal level to noise level was discouragingly low and the reading thus obtained of doubtful accuracy. The Air Force Cambridge Research Center (AFCRC) calculated the overpressure at the B-36 aircraft position from canister data and arrived at a figure of 0.22 psi. In view of the supposed accuracy of this calculation and the lack of confidence in the directly measured value, it is recommended that the figure of 0.22 psi be regarded as the more representative overpressure input.

3.2.2 B-47 Aircraft

Because of a radar failure, the B-47 aircraft at shock arrival was at a slant range 25 per cent greater than that intended. From available data, it has been estimated that the aircraft was at a slant range of approximately 224,000 ft at shock arrival. The assigned altitude of 35,000 ft was maintained. No blast response data were obtained; as a result of the increased range, the oscillograph recording paper was exhausted before shock arrival, approximately 189 sec after burst time. The AFCRC calculated that the peak overpressure input realized by the test aircraft was 0.14 psi. Thus, even if the response data had been recorded, the loads would have been so small as to render the data of little value.

3.3 RESPONSE MEASUREMENTS

Blast response measurements presented below are from the B-36 aircraft only, since malposition resulted in no data for the B-47 aircraft. Only those data deemed reliable have been presented. In a few instances where positive trace indentification could not be made, the curves are presented in dashed form. The data are presented as time-histories; zero time was taken as the time the shock struck the tail.

3.3.1 Bending Moment

Curves of bending moment above normal flight loads vs time are

presented for the wings, fuselage, and horizontal stabilizers in Fig. 3.2 through Fig. 3.8. The first 0.15 sec after shock arrival are shown as a dashed line for the bending moment of the left horizontal stabilizer, Fig. 3.8, because the trace could not be followed continuously through this interval. All bending gages yielded acceptable results.

3.3.2 Acceleration

Tail, nose, and center of gravity acceleration records are presented in Fig. 3.9, Fig. 3.10, and Fig. 3.11, respectively. The wing tip accelerometer provided no usable data. Because of the wide, rapid fluctuations of the acceleration traces at shock arrival, the traces could not be read with any degree of accuracy until 0.4 sec had elapsed. These curves have not been faired, although some fairing is indicated for certain analyses.

3.3.3 Shear and Torsion

No shear or torsion data were obtained. The shear gage was inoperative prior to the test. The torsion gage output was recorded, but the data obtained were not reliable.

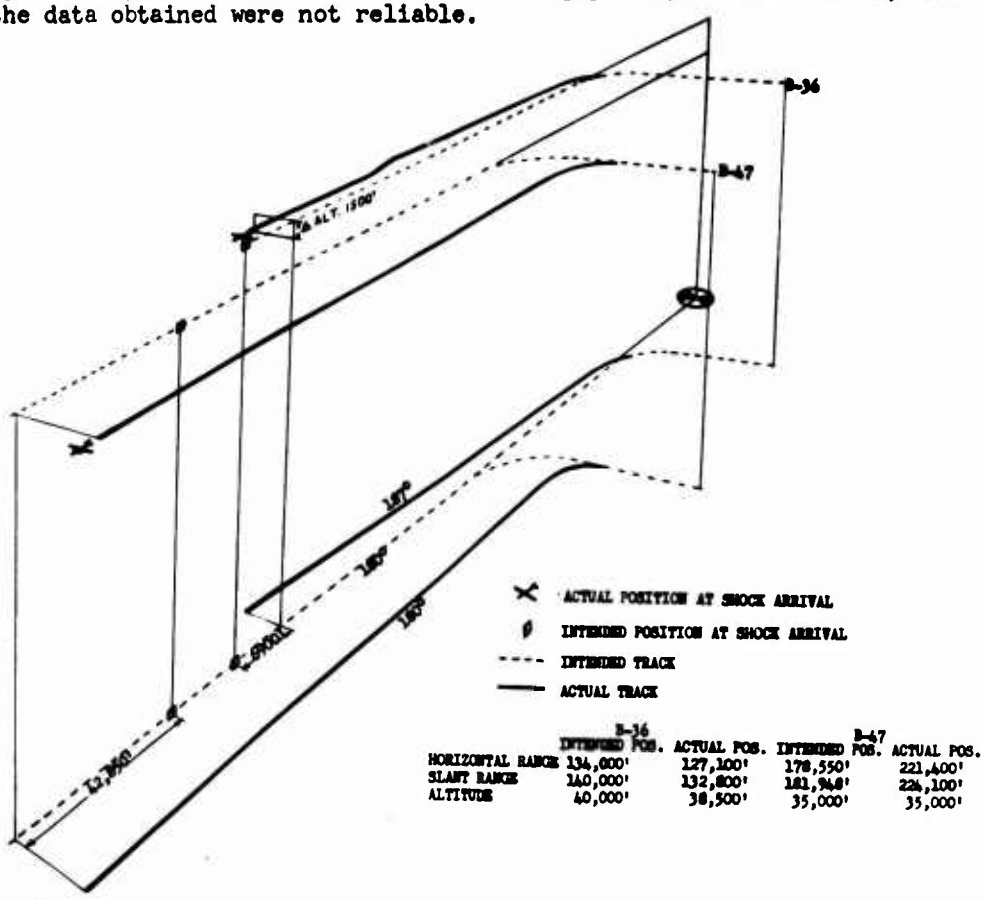

Fig. 3.1 Position of B-36D and B-47B Aircraft for Mike Shot

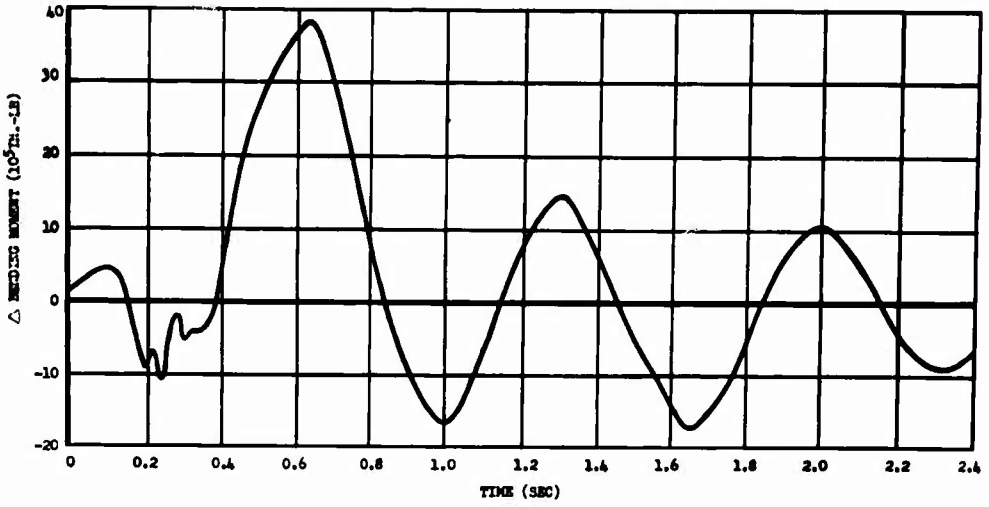

Fig. 3.2 Wing Bending versus Time after Shock Arrival, Left Wing Station 390, B-36D, Mike Shot

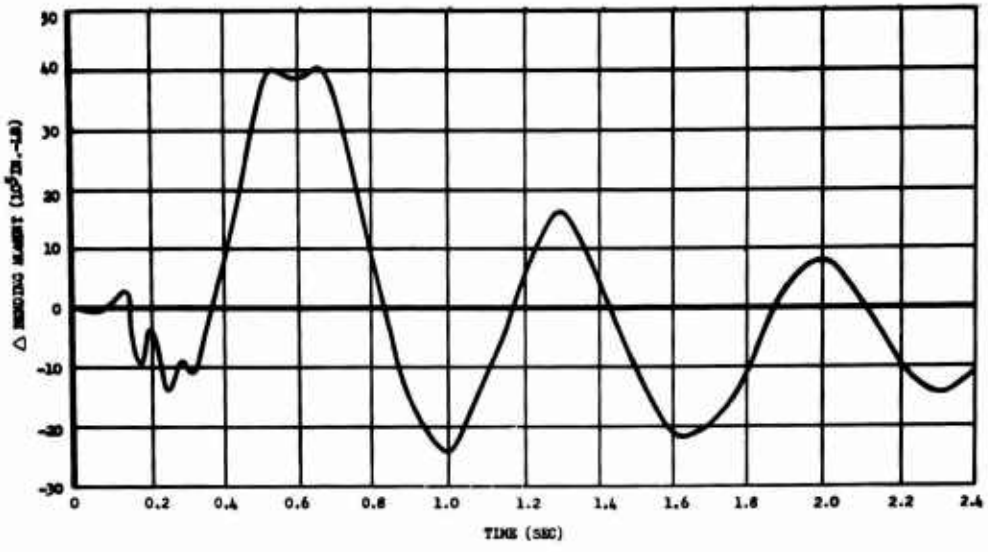

Fig. 3.3 Wing Bending versus Time after Shock Arrival, Right Wing Station 390, B-36D, Mike Shot

S[redacted]

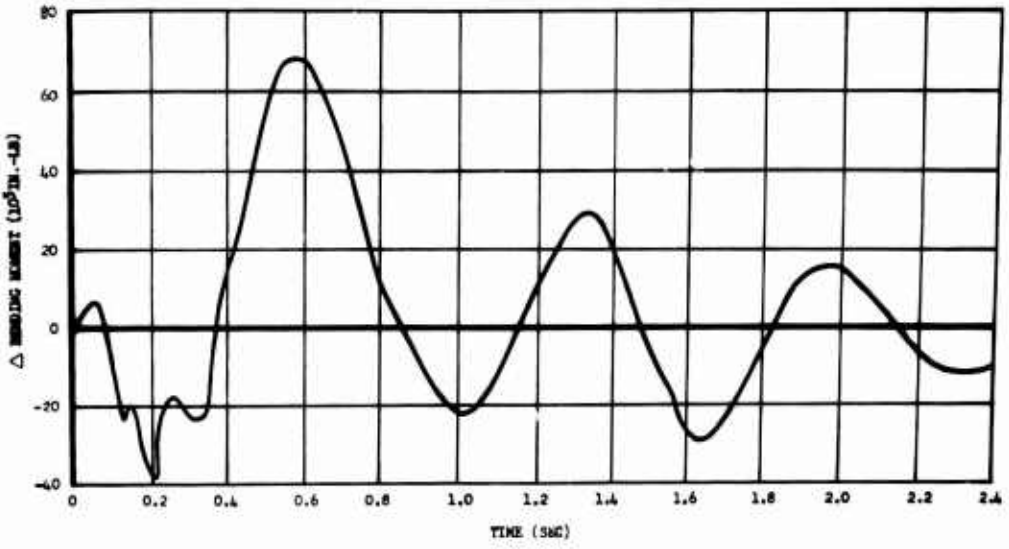

Fig. 3.4 Wing Bending versus Time after Shock Arrival, Left Wing Station 110, B-36D, Mike Shot

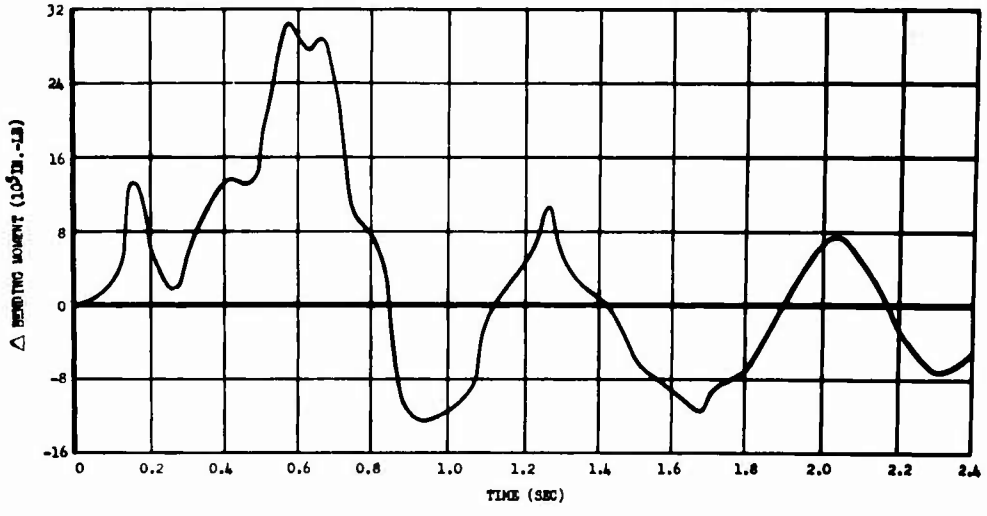

Fig. 3.5 Wing Bending versus Time after Shock Arrival, Left Wing Station 604, B-36D, Mike Shot

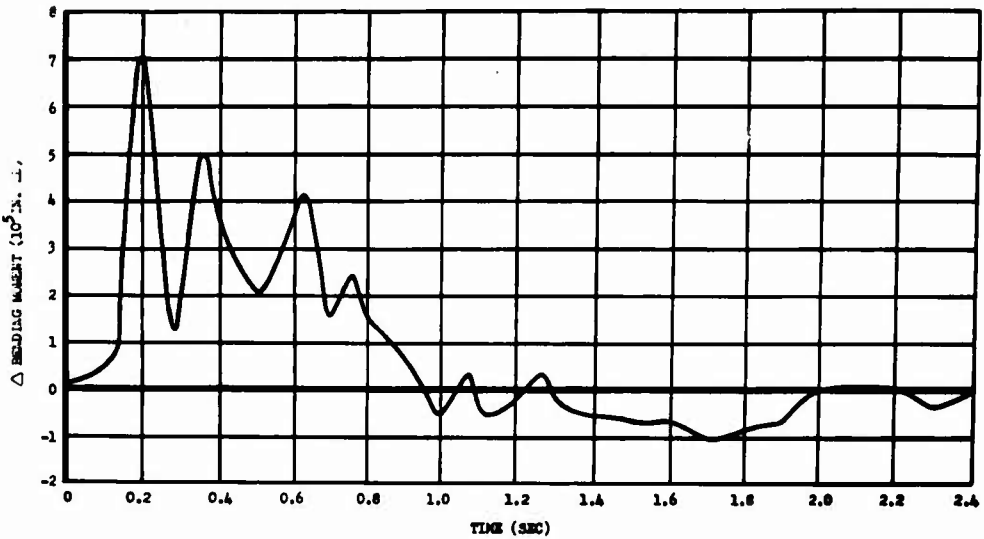

Fig. 3.6 Wing Bending versus Time after Shock Arrival, Left Wing Station 1062, B-36D, Mike Shot

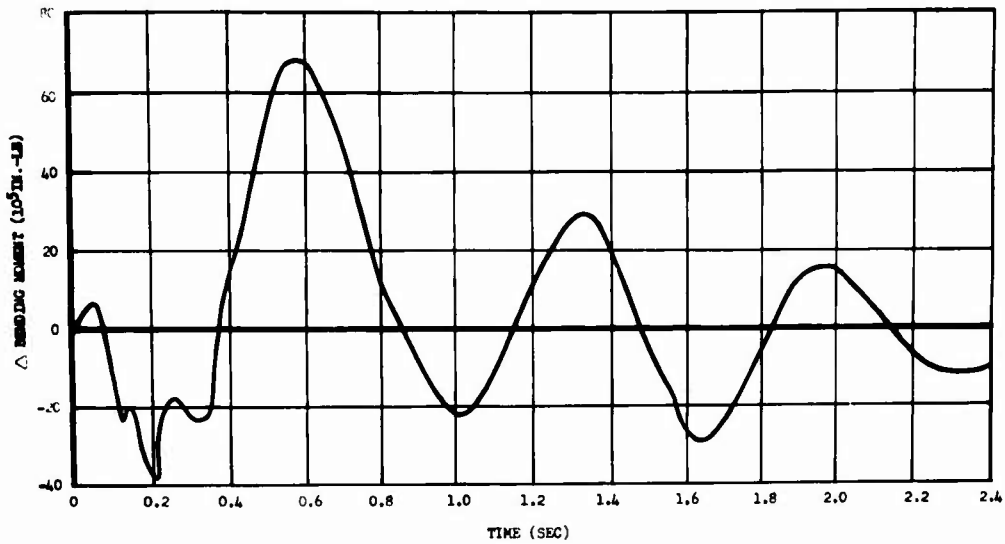

Fig. 3.7 Fuselage Bending versus Time after Shock Arrival, Fuselage Station 1040, B-36D, Mike Shot

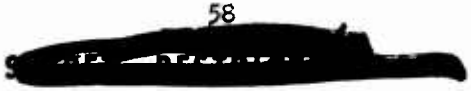

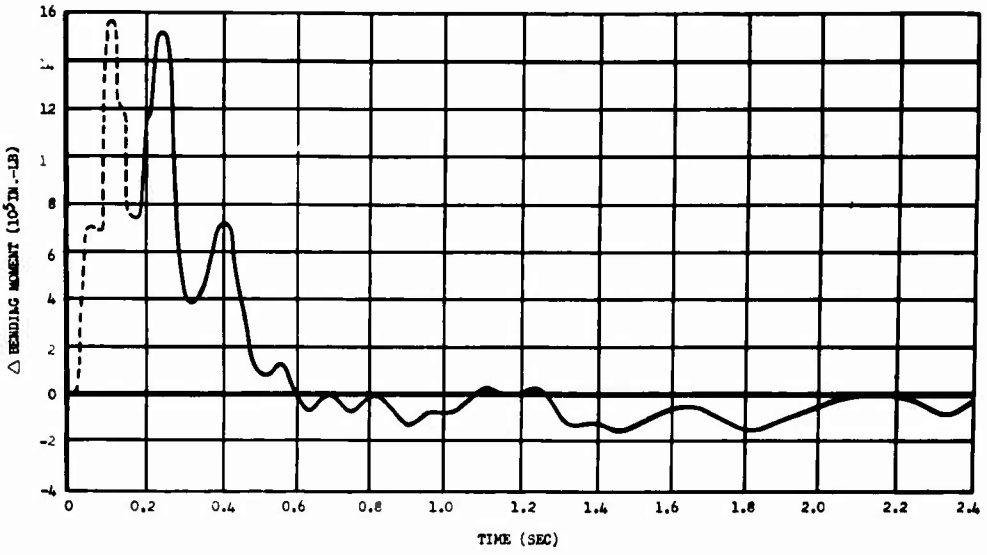

Fig. 3.8 Stabilizer Bending versus Time after Shock Arrival, Left Horizontal Stabilizer Station 62, B-36D, Mike Shot

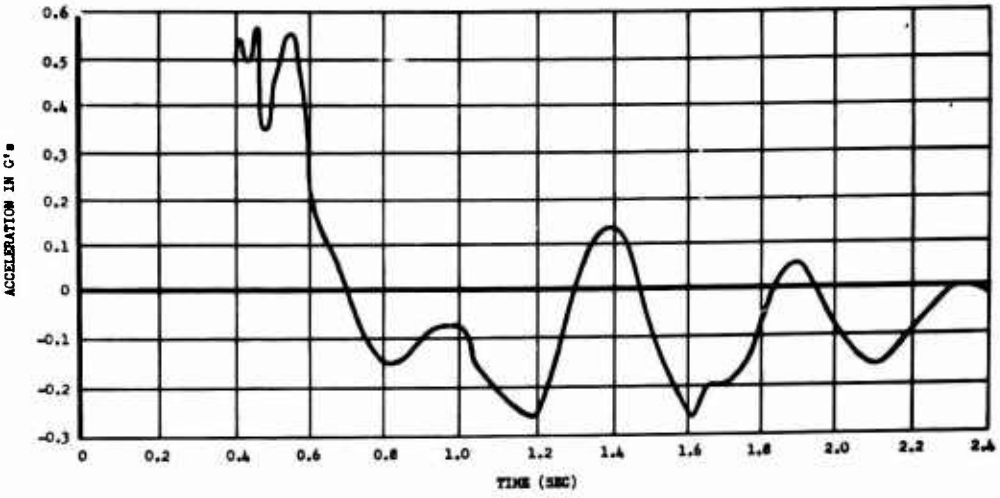

Fig. 3.9 Vertical Acceleration versus Time after Shock Arrival, B-36D Tail, Fuselage Station 1770, Mike Shot

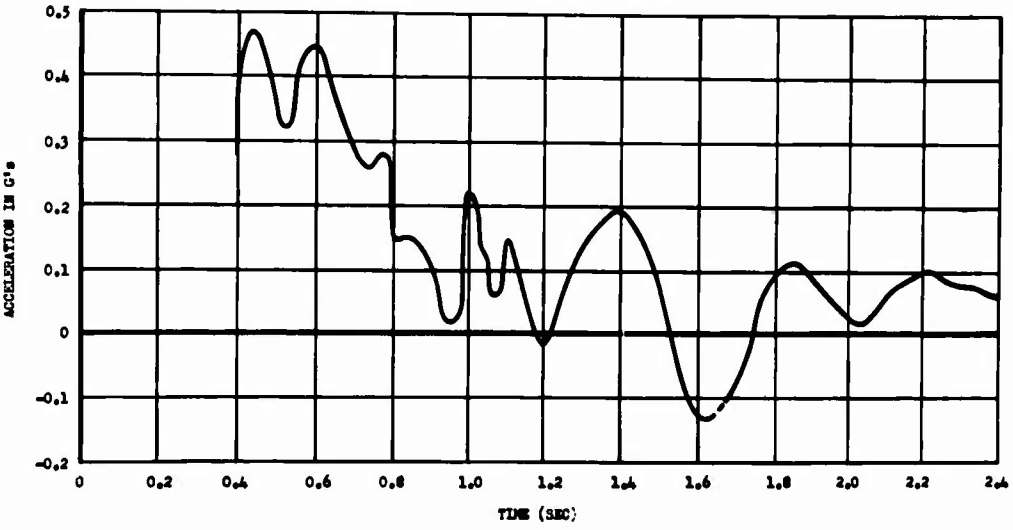

Fig. 3.10 Vertical Acceleration versus Time after Shock Arrival, B-36D Nose, Fuselage Station 212, Mike Shot

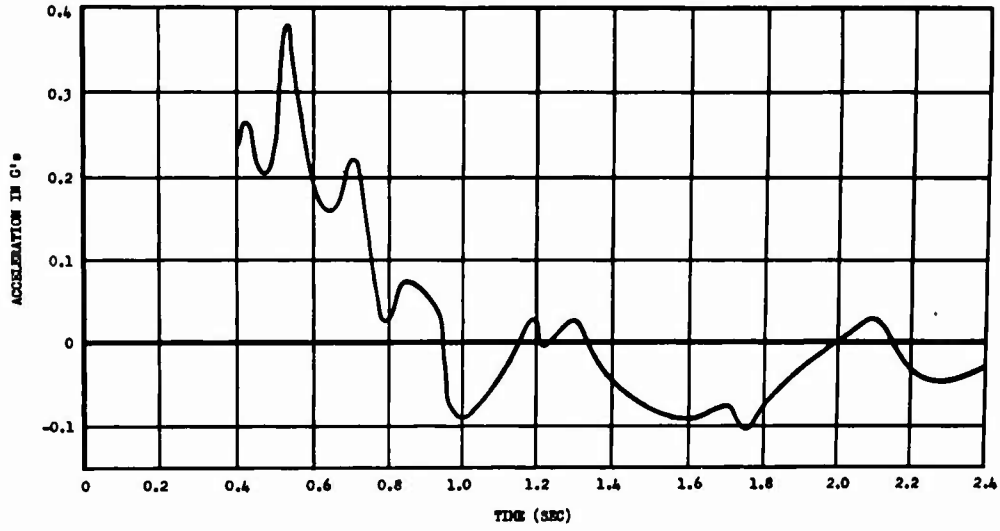

Fig. 3.11 Vertical Acceleration versus Time after Shock Arrival, B-36D Center of Gravity, Fuselage Station 907, Mike Shot

CHAPTER 4

RESULTS, KING SHOT

4.1 GENERAL

The King Shot weapon was dropped on the Runit Island target by a B-36H aircraft at 1000 hours on 16 November 1952. The burst height was approximately 1500 ft and the radiochemical yield was 540 KT. Both test aircraft were exposed to the weapon outputs. The B-36 aircraft was at a greater range than intended; however, usable response data were obtained.

4.2 AIRCRAFT POSITION, INPUTS, FLIGHT DATA

Supplemental data relative to the exposure of the B-36 and B-47 aircraft in King Shot are summarized in the sub-paragraphs below. A diagram showing the location of each aircraft for King Shot is shown in Fig. 4.1.

4.2.1 B-36 Aircraft

Data required for analysis of the response measurements made on the B-36 aircraft during King Shot are summarized below:

a. Altitude, MSL, 32,000 ft
b. Height of Burst, 1500 ft
c. Horizontal range at shock arrival, 85,200 ft
d. Slant range at shock arrival, 90,500 ft
e. True airspeed, 237 knots
f. True ground speed, 252 knots
g. True heading, 90°
h. Aircraft attitude, 4° nose high
i. Angle of incidence of shock front, 19.7°
j. Shock arrival time, 77.2 sec
k. Peak overpressure (WADC), no reliable data
l. Peak overpressure (AFCRC), 0.16 psi
m. Gross weight at shock arrival, 260,000 lb
n. Center of gravity location at shock arrival, 35.9% MAC

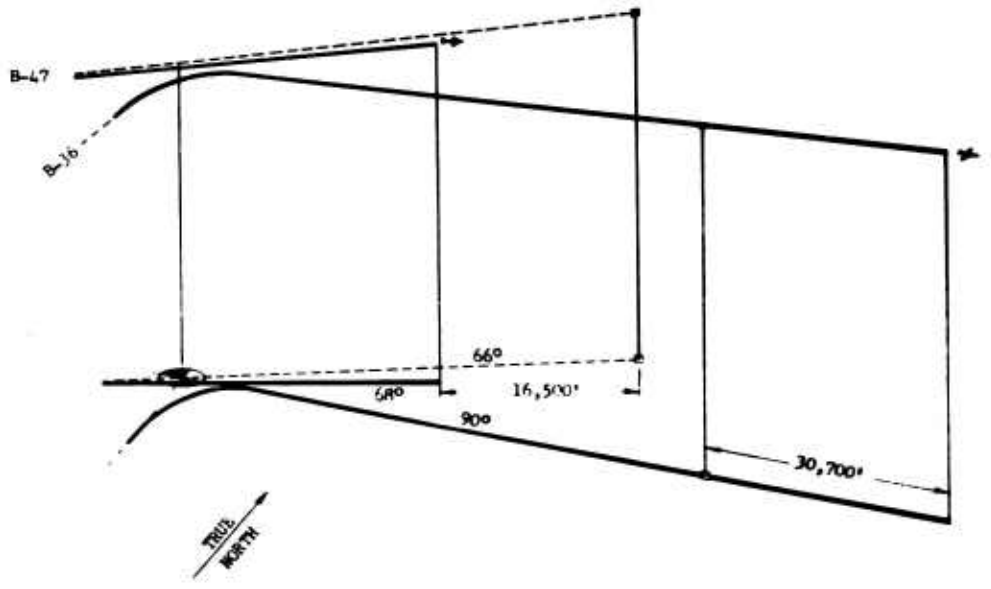

→ ACTUAL POSITION AT SHOCK ARRIVAL

φ INTENDED POSITION AT SHOCK ARRIVAL

--- INTENDED TRACK

—— ACTUAL TRACK

	B-36		B-47	
	INTENDED POS.	ACTUAL POS.	INTENDED POS.	ACTUAL POS.
HORIZONTAL RANGE	54,500	85,200	43,100	26,600
SLANT RANGE	62,500	90,500	54,600	42,760
ALTITUDE	32,000	32,000	35,000	35,000

Fig. 4.1 Position of B-36D and B-47B Aircraft for King Shot

The aircraft position at shock arrival was 28,000 ft farther from ground zero than originally planned. The wide discrepancy is attributed to the failure of the "K" system radar. The position quoted is based upon calculations using time of shock arrival and upon crew estimate. At shock arrival the aircraft was out of range for the radar aboard the U.S.S. Estes; hence no radar track data were obtained. No reliable overpressure data were obtained from instrumentation aboard the aircraft, primarily because of the low input level.

4.2.2 B-47 Aircraft

Data, other than response measurements, pertinent to the exposure of the B-47 aircraft in King Shot are summarized below:

a. Altitude, MSL, 35,000 ft
b. Height of Burst, 1500 ft
c. Horizontal range at shock arrival, 26,600 ft
d. Slant range at shock arrival, 42,760 ft
e. True airspeed, 440 knots
f. True ground speed, 412 knots
g. True heading, 68°
h. Aircraft attitude, 1° nose high
i. Angle of incidence of shock front, 51.4°
j. Shock arrival time, 32.2 sec
k. Peak overpressure (AFCRC), 0.336 psi
l. Gross weight at shock arrival, 120,000 lb

4.3 RESPONSE MEASUREMENTS

Measurements made on the blast response of the B-36 and B-47 aircraft in King Shot are presented in the sub-paragraphs below. All data are presented as time-histories with only the obvious, small amplitude oscillations faired out. The time axis is based upon time of shock arrival at the tail. To obtain time relative to burst time; for the B-36 aircraft add 77.2 sec; for the B-47 aircraft add 32.2 sec.

4.3.1 B-36 Aircraft

Because the B-36 aircraft was too far from air zero on this shot, the forcing functions, and therefore the measured loads, were lower than anticipated. The data are of value; however, their utility in checking the blast-load theory would have been greatly enhanced had the responses been several-fold higher. The peak measured bending moment of the horizontal stabilizer was only 12 per cent of limit load.

4.3.1.1 Bending Moment

Bending moment measurements are presented in terms of bending moment above, or below, normal (one g) flight loads. Wing, fuselage, and horizontal stabilizer bending measurements are presented in Figs. 4.2 through 4.7. Acceptable results were obtained from all bending gages, except the root bending gage on the left wing. This gage was found in-

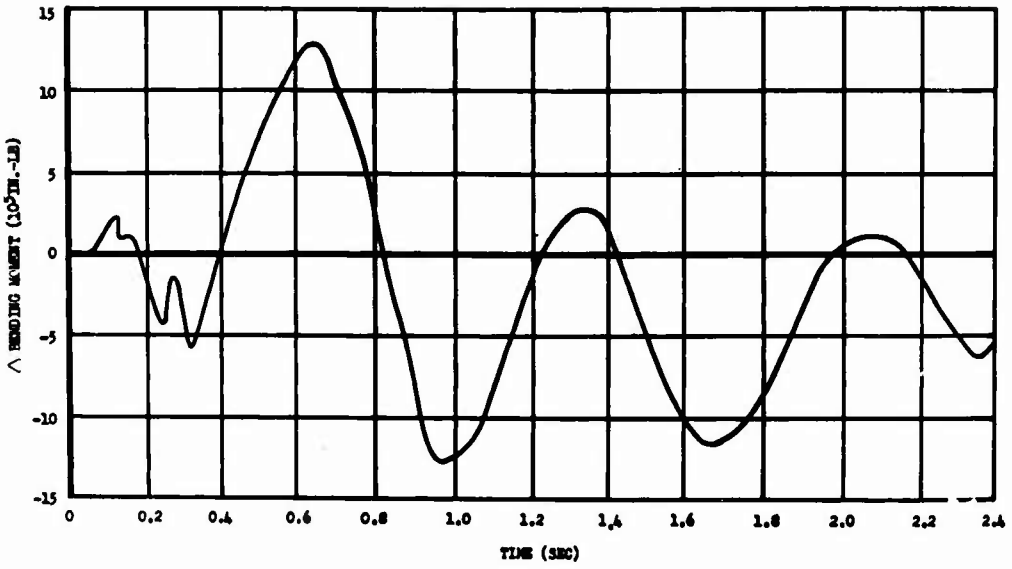

Fig. 4.2 Wing Bending versus Time after Shock Arrival, Left Wing Station 390, B-36D, King Shot

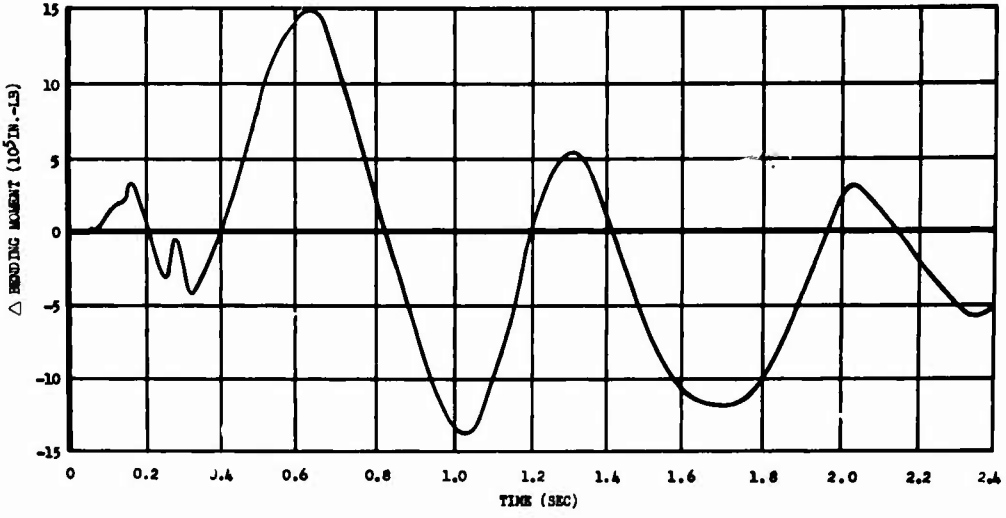

Fig. 4.3 Wing Bending versus Time after Shock Arrival, Right Wing Station 390, B-36D, King Shot

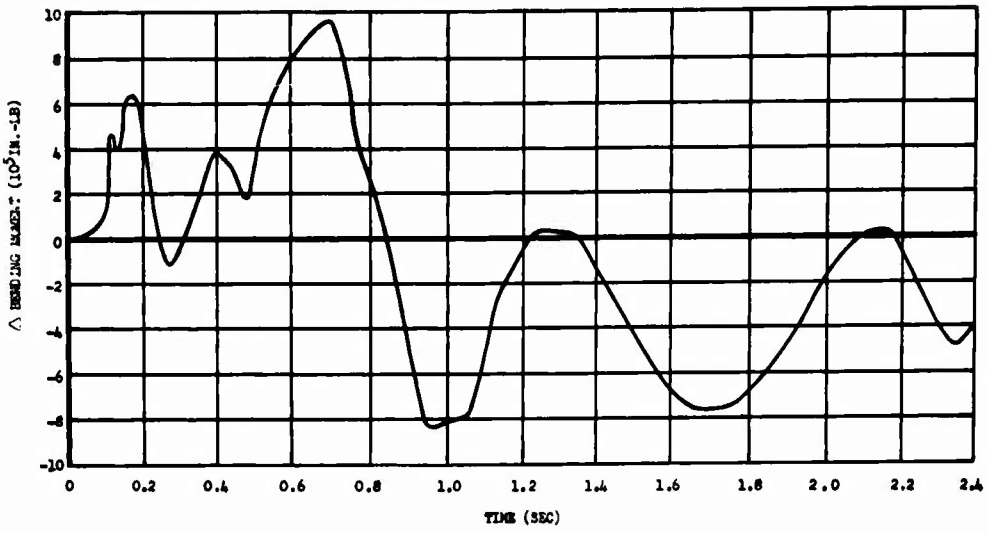

Fig. 4.4 Wing Bending versus Time after Shock Arrival, Left Wing Station 604, B-36D, King Shot

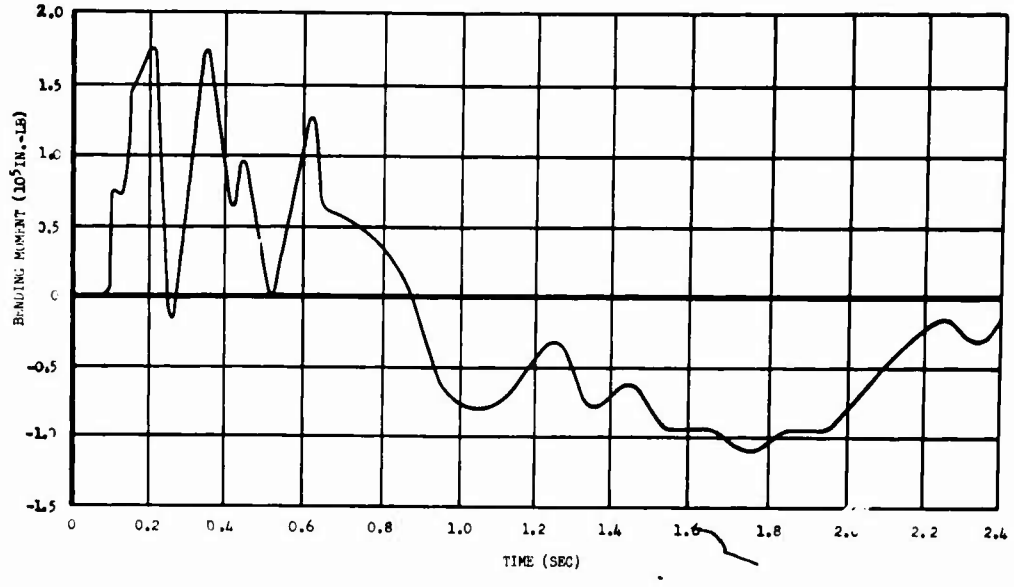

Fig. 4.5 Wing Bending versus Time after Shock Arrival, Left Wing Station 1062, B-36D, King Shot

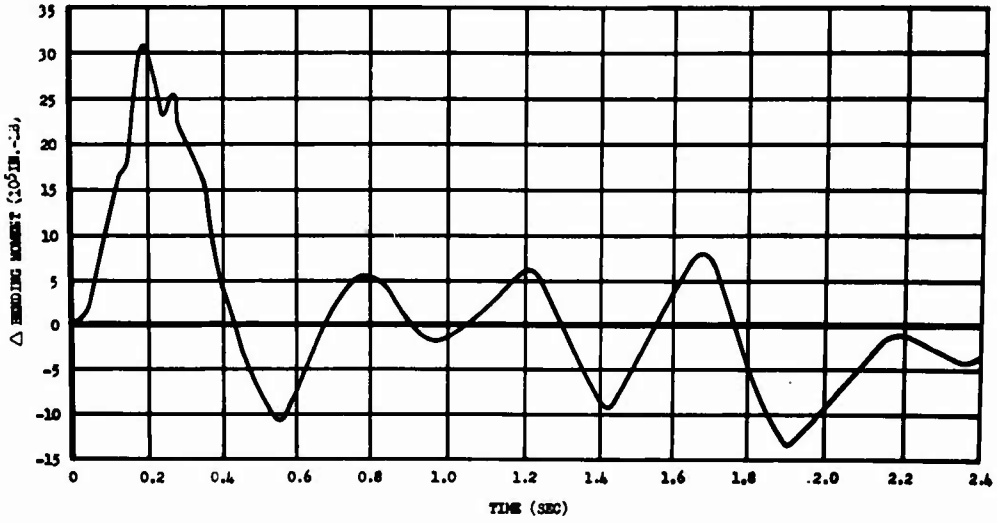

Fig. 4.6 Fuselage Bending versus Time after Shock Arrival, Fuselage Station 1040, B-36D, King Shot

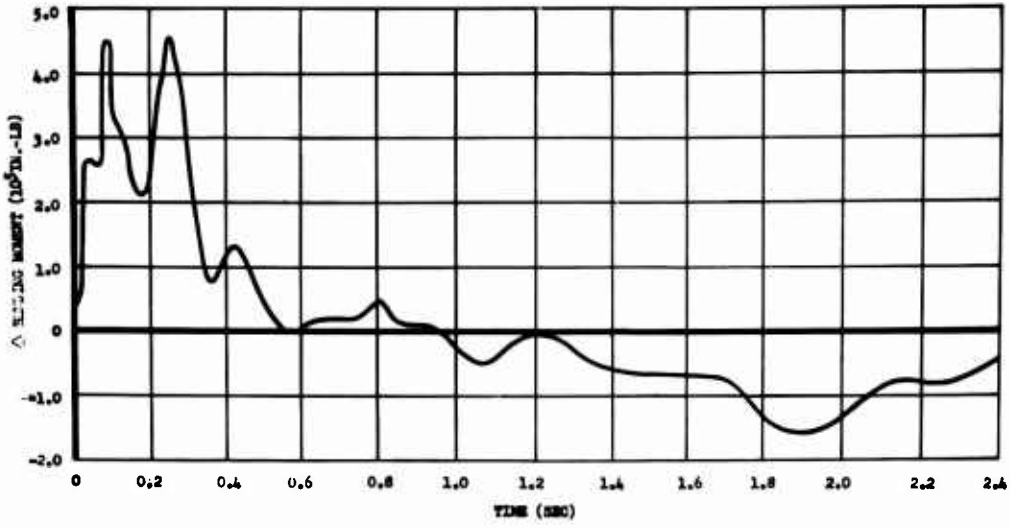

Fig. 4.7 Stabilizer Bending versus Time after Shock Arrival, Left Horizontal Stabilizer Station 62, B-36D, King Shot

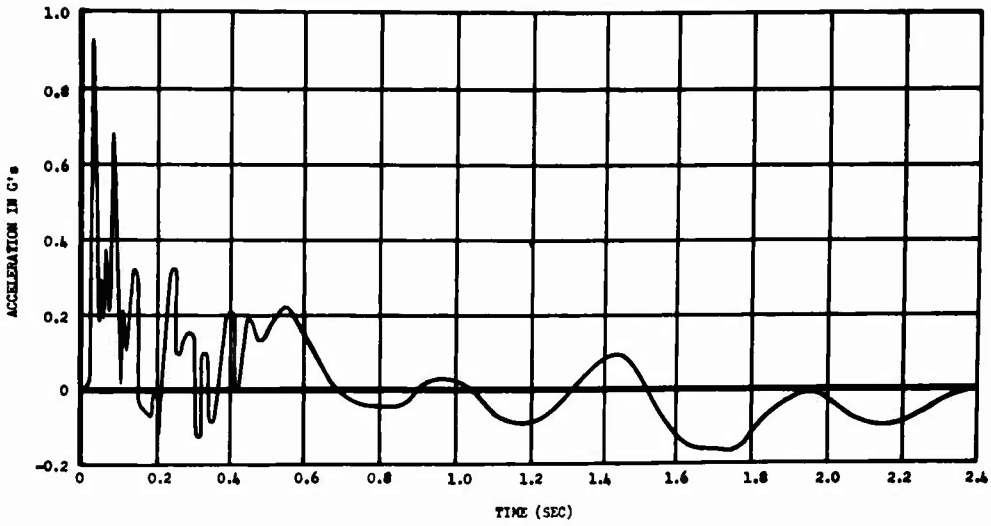

Fig. 4.8 Vertical Acceleration versus Time after Shock Arrival, B-36D Tail, Fuselage Station 1770, King Shot

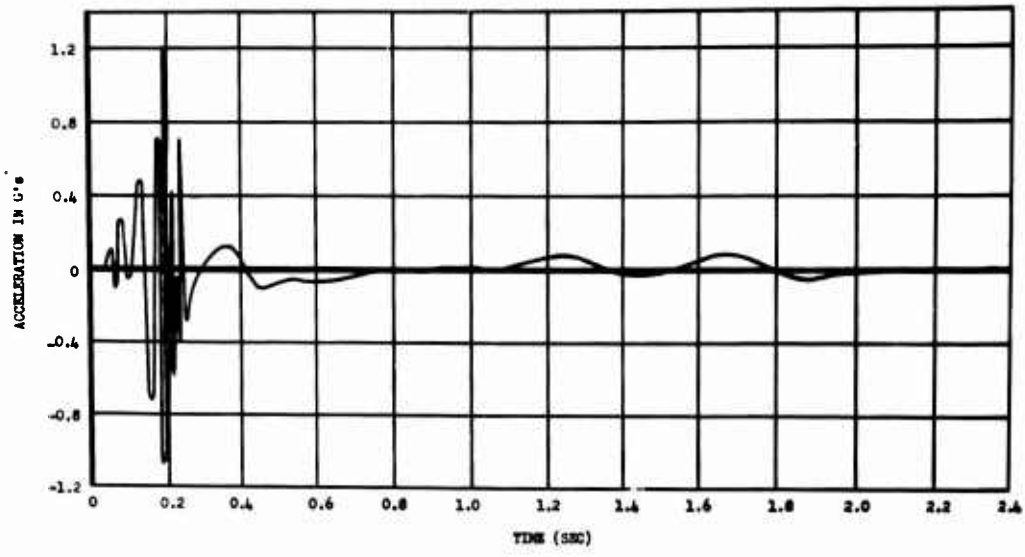

Fig. 4.9 Vertical Acceleration versus Time after Shock Arrival, B-36D Nose, Fuselage Station 212, King Shot

[redacted]

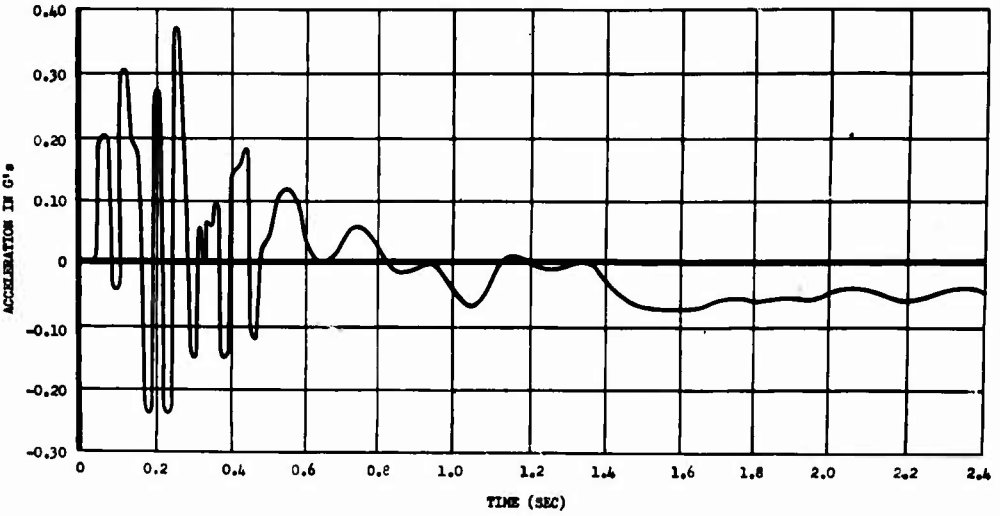

Fig. 4.10 Vertical Acceleration versus Time after Shock Arrival, B-36D Center of Gravity, Fuselage Station 907 (Left Side), King Shot

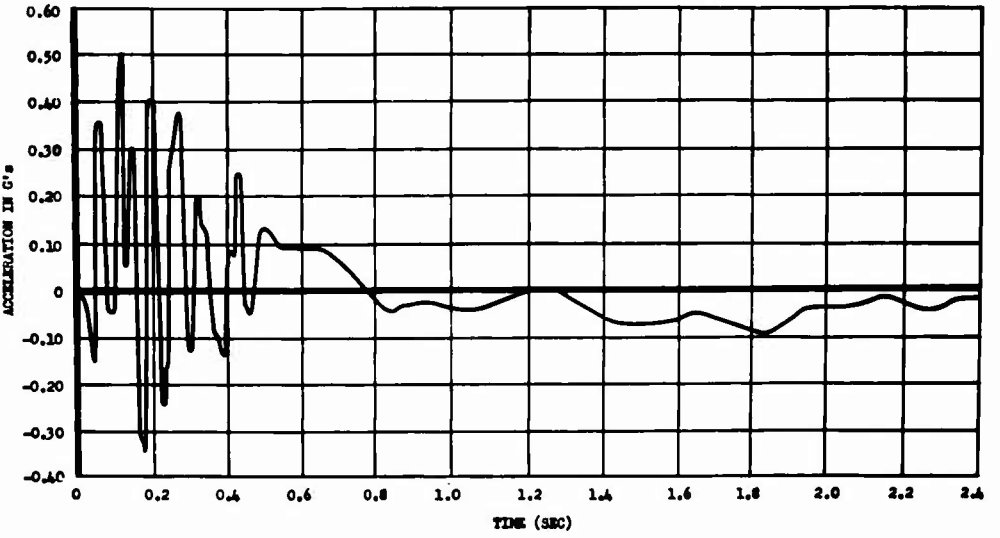

Fig. 4.11 Vertical Acceleration versus Time after Shock Arrival, B-36D Center of Gravity, Fuselage Station 907 (Right Side), King Shot

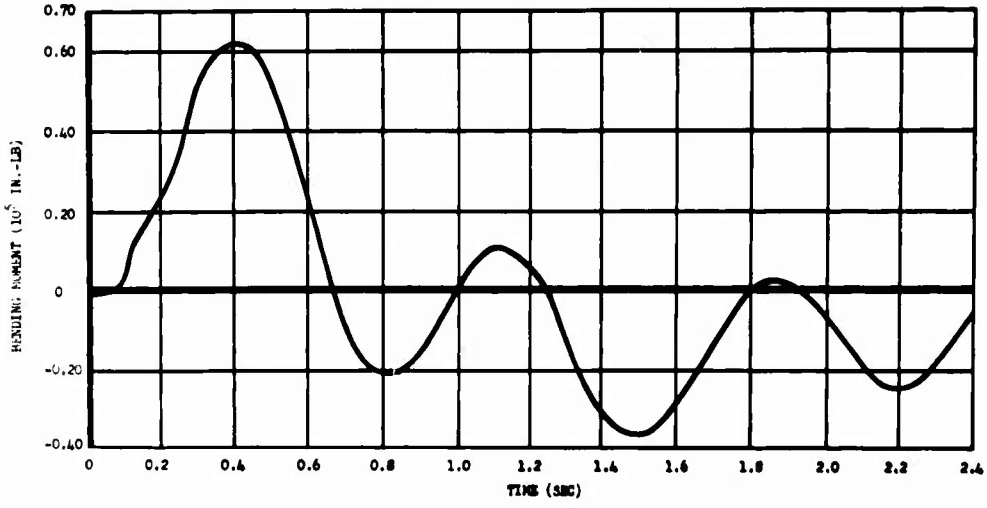

Fig. 4.12 Wing Bending versus Time after Shock Arrival, Left Wing Station 186, B-47B, King Shot

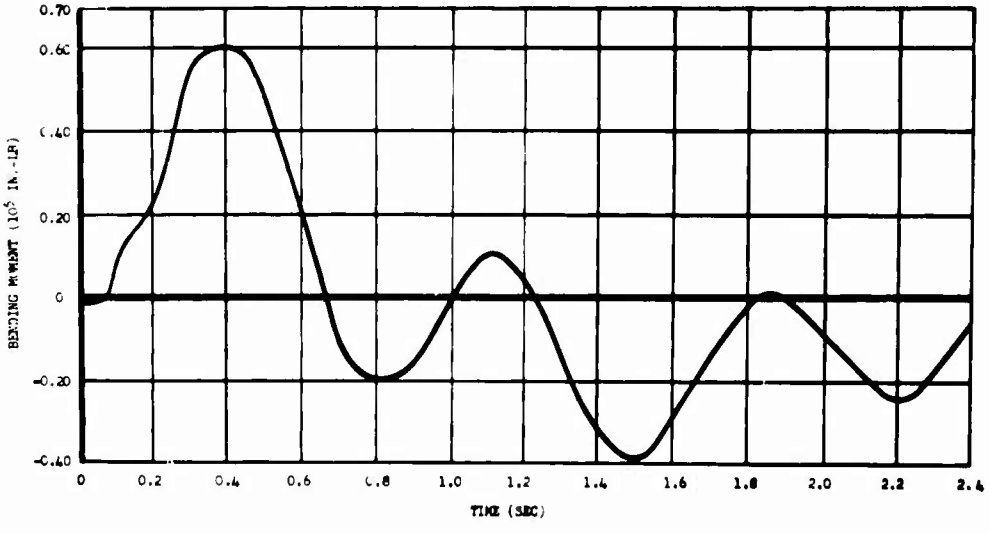

Fig. 4.13 Wing Bending versus Time after Shock Arrival, Right Wing Station 186, B-47B, King Shot

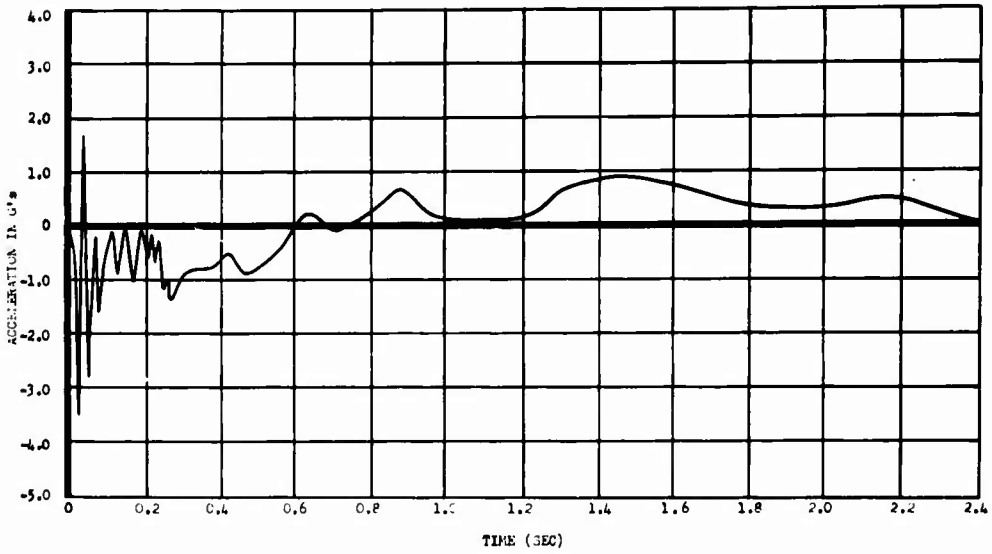

Fig. 4.14 Vertical Acceleration versus Time after Shock Arrival, B-47B Tail, Fuselage Station 1121.5, King Shot

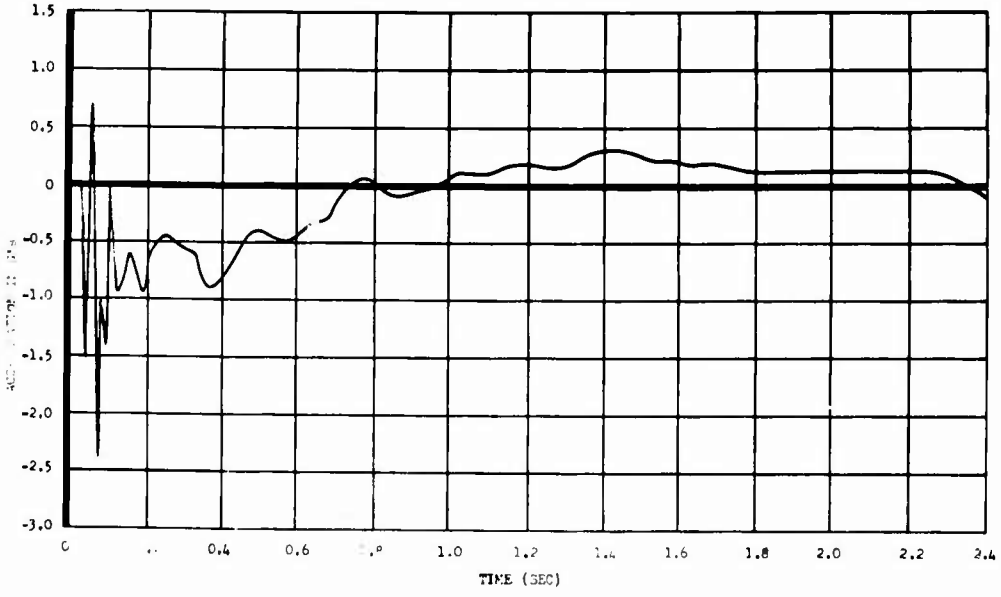

Fig. 4.15 Vertical Acceleration versus Time after Shock Arrival, B-47B Center of Gravity, Fuselage Station 587.8, King Shot

[redacted]

operative prior to take-off and no recording was attempted.

4.3.1.2 Acceleration

Normal acceleration data for the tail, nose, and center of gravity are presented in Figs. 4.8 through 4.11. No usable data were obtained from the accelerometer in the left wing tip. The sharp spikes, characteristic of acceleration measurements of this type, have not been faired out.

4.3.1.3 Shear and Torsion

Both the shear gage and the torsion gage in the left outer wing panel were inoperative prior to the test; hence, no data for these response functions were obtained.

4.3.2 B-47 Aircraft

The B-47 aircraft was essentially at intended position at blast arrival. The four response channels all produced usable data. The wing bending moment measurements are presented in Figs. 4.12 and 4.13; the vertical acceleration measurements are presented in Figs. 4.14 and 4.15.

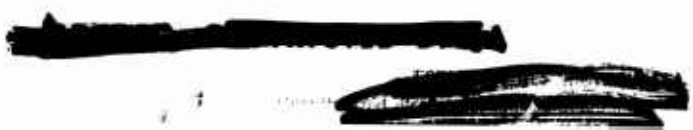

CHAPTER 5

RESULTS, SHOT 9

5.1 GENERAL

The Shot 9 weapon was dropped on the Frenchman Flat testing area by a B-50 aircraft at 0729 hours (PST) on 8 May 1953. The burst height was 3423 ft above ground level or 5558 ft MSL. The yield by radiochemical determination was found to be 26 KT. The B-36 aircraft took part in this test; the B-47 aircraft did not. Because of the lower yield, the test aircraft was positioned closer and more nearly over the burst point for Shot 9 than was possible with the larger yield weapons in the IVY tests. In the position chosen, the aircraft received both the incident and reflected shocks. The response to the two shocks was remarkably similar. Good blast response data were obtained.

5.2 AIRCRAFT POSITION, INPUTS, FLIGHT DATA

Information pertinent to the exposure of the B-36 aircraft in Shot 9 is summarized below:

a. Altitude, MSL, 25,135 ft
b. Weapon burst height, 2423 ft above ground level, 5558 ft MSL
c. Horizontal range at shock arrival, 14,500 ft
d. Slant range at first shock arrival, 24,700 ft
e. True airspeed, 262 knots
f. True ground speed, 185 knots
g. True heading, 250°
h. Aircraft attitude, 2.5° nose high
i. Angle of incidence of shock front, 54.8°
j. Shock arrival time, first shock, 21.03 sec; second shock 25.47 sec
k. Peak overpressure (WADC), 0.15 psi (first shock)
l. Peak overpressure (AFCRC), 0.165 psi (first shock)
m. Calculated gross weight at shock arrival, 242,563 lb
n. Center of gravity location at shock arrival, 22.2% MAC

The aircraft position given above is based upon data from the "K"

system radar, aerial mapping camera photographs, calculations using time of shock arrival, and from optical ground tracking data. The actual position was essentially that intended. The measured overpressure of 0.15 psi agrees reasonably well with the calculated value of 0.165 psi.

5.3 RESPONSE MEASUREMENTS

The blast response measurements made on the B-36 aircraft during Shot 9 are presented in the sub-paragraphs following. Measurements on the tail were made according to two instrumentation procedures arbitrarily defined as the point load method and the conventional or distributed load method. The response data obtained by the two methods were in good agreement. In the plotting of the data as time-histories, the time axis has been broken such that the first and second shock appear one above the other for ease of comparison. Zero time was taken as time of shock arrival as in the Mike and King presentations.

5.3.1 Bending Moment

Curves of incremental bending moment above "one g" flight loads as measured by the conventional method are reported in Figs. 5.1 through 5.7. The stabilizer bending moments measured by the point load method are presented in Figs. 5.8, 5.9, and 5.10. The left wing bending moment at Station 390 has been reported, Fig. 5.1, although it is believed this value is in error. The reasons for suspecting this measurement are set forth in the Discussion. Except for the above, all bending gages yielded data considered valid. Point load bending data were in general agreement with conventionally measured values.

5.3.2 Acceleration

Tail, nose, and center of gravity normal acceleration data are presented in Figs. 5.11, 5.12, and 5.13, respectively. Wing tip accelerations measurements were not made. Sharp spikes were not averaged, but reported as read from the records.

5.3.3 Shear

Shear was measured on the horizontal stabilizer by the point load method. From a cursory comparison, the shear data are in agreement with what would be expected on the basis of bending measurements. The shear data are presented in Figs. 5.14 through 5.16.

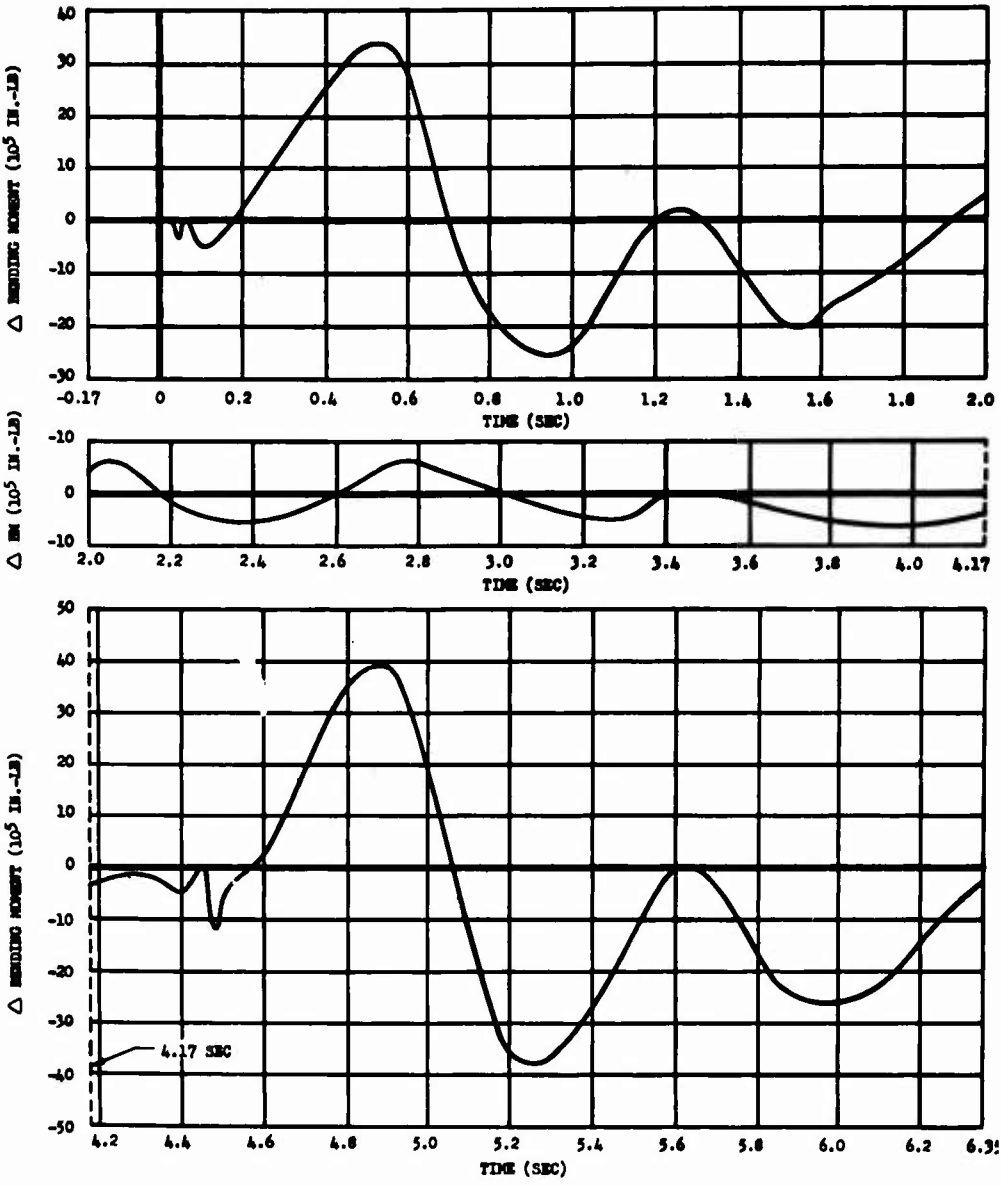

Fig. 5.1 Wing Bending versus Time after Shock Arrival, Left Wing Station 390, B-36D, Shot 9

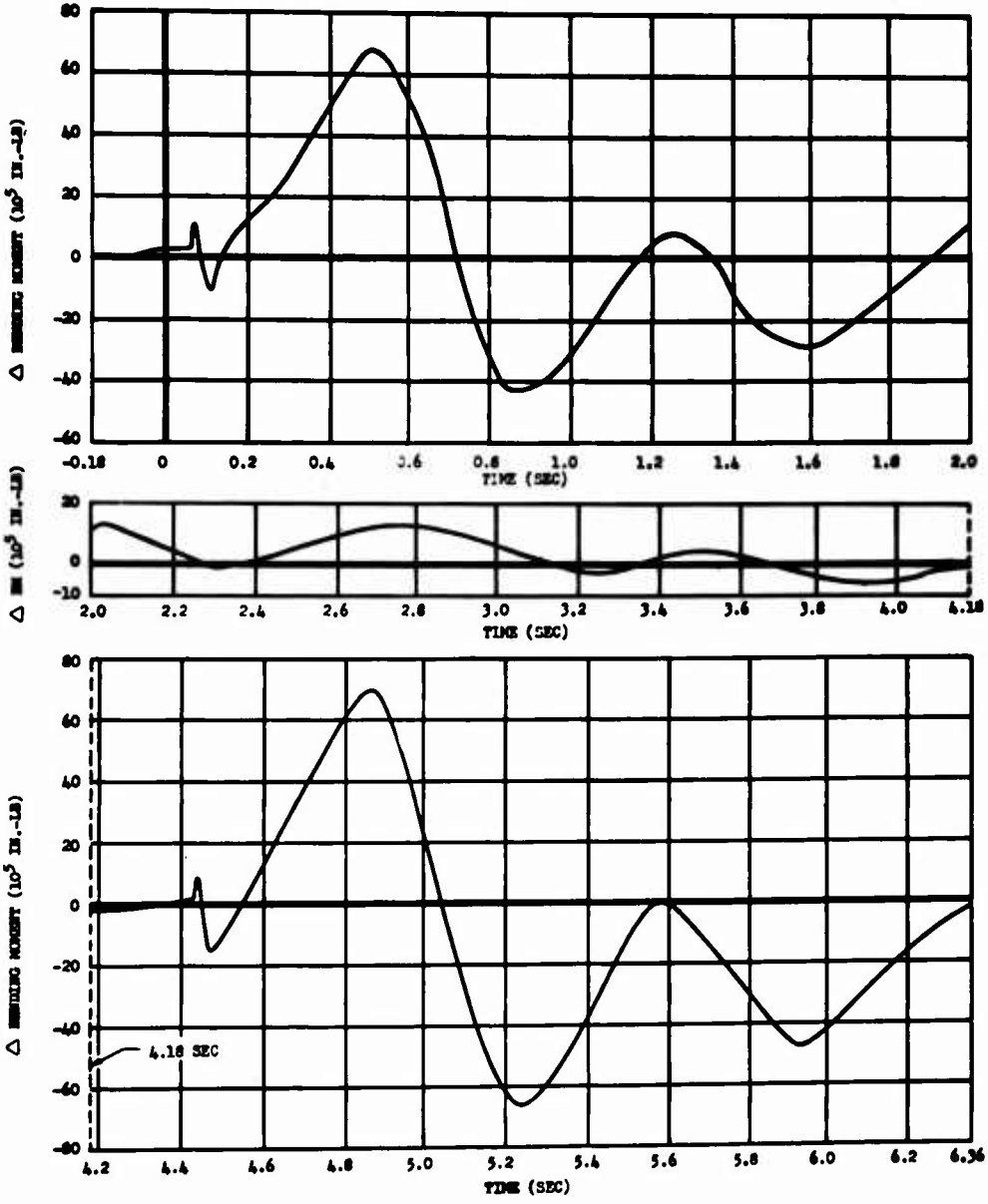

Fig. 5.2 Wing Bending versus Time after Shock Arrival, Right Wing Station 390, B-36D, Shot 9

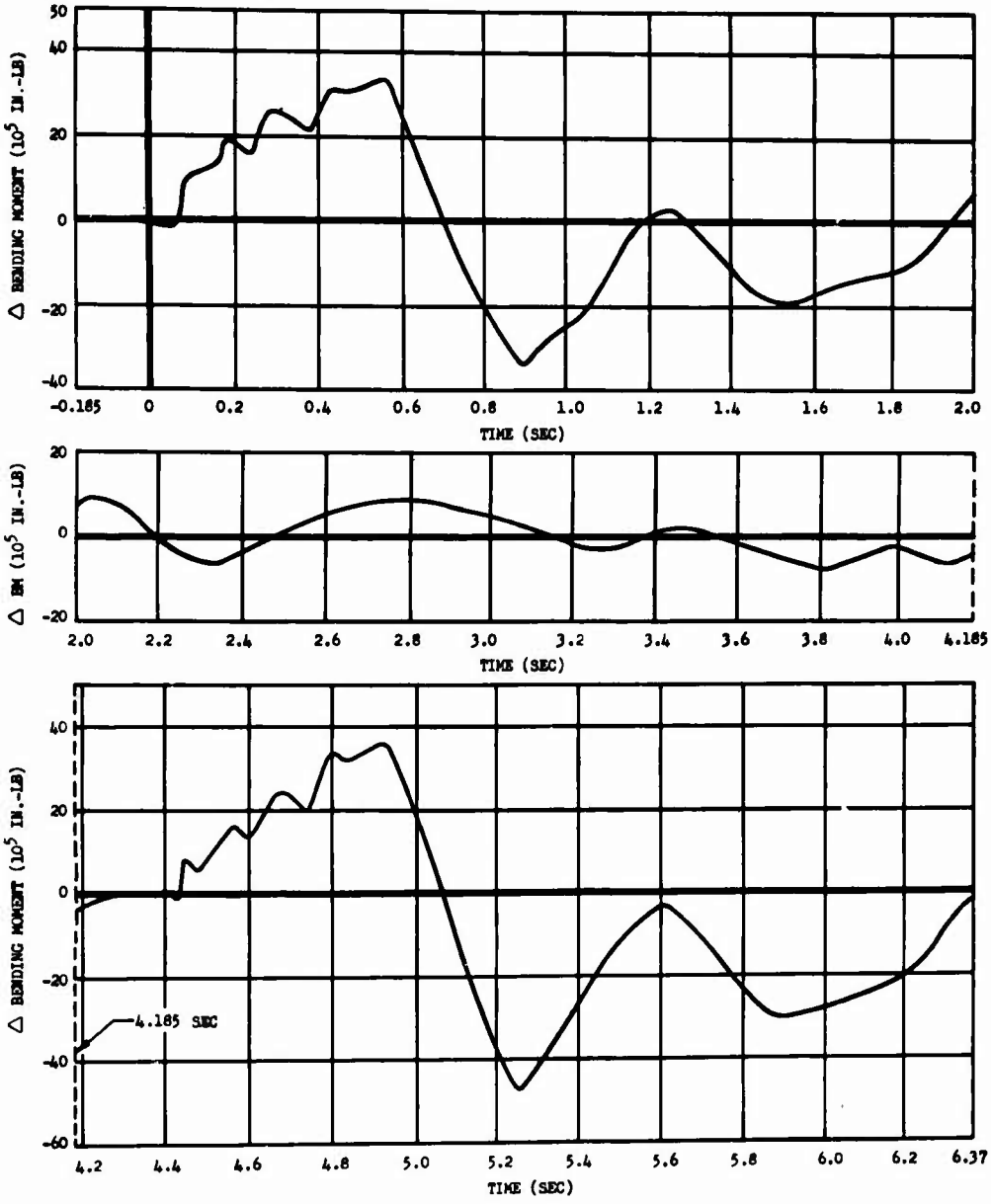

Fig. 5.3 Wing Bending versus Time after Shock Arrival, Left Wing Station 604, B-36D, Shot 9

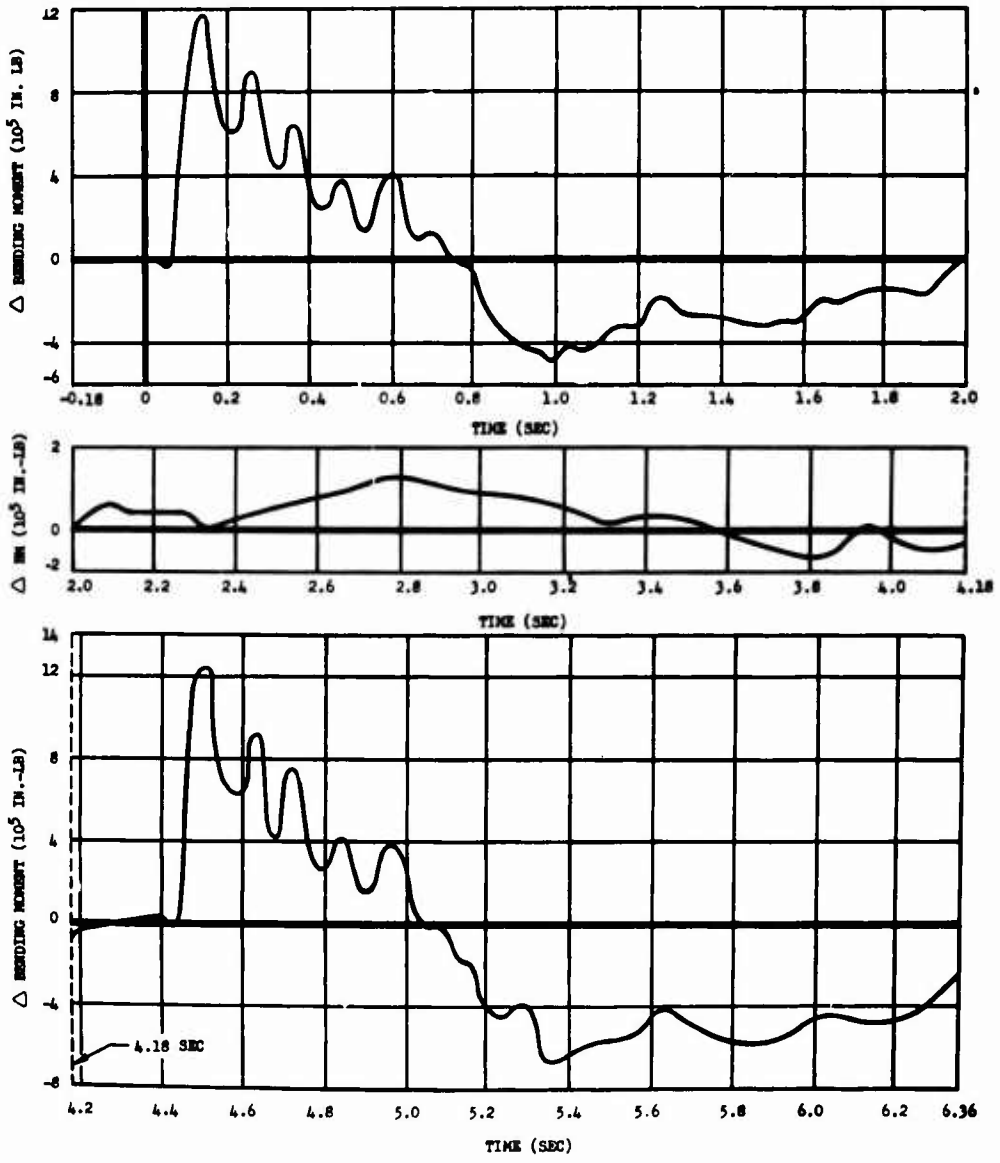

Fig. 5.4 Wing Bending versus Time after Shock Arrival, Left Wing Station 1062, B-36D, Shot 9

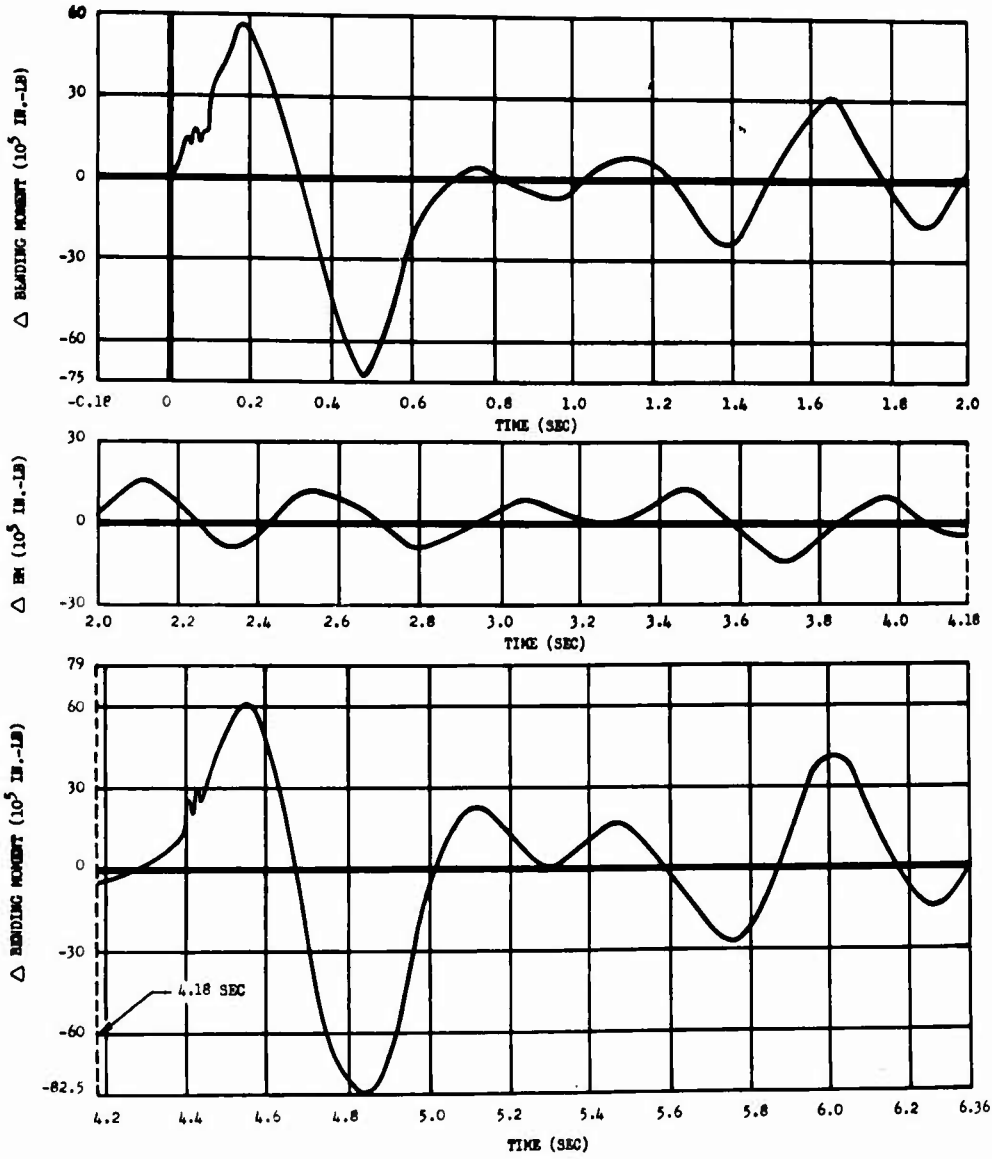

Fig. 5.5 Fuselage Bending versus Time after Shock Arrival, Fuselage Station 1040, B-36D, Shot 9

[redacted]

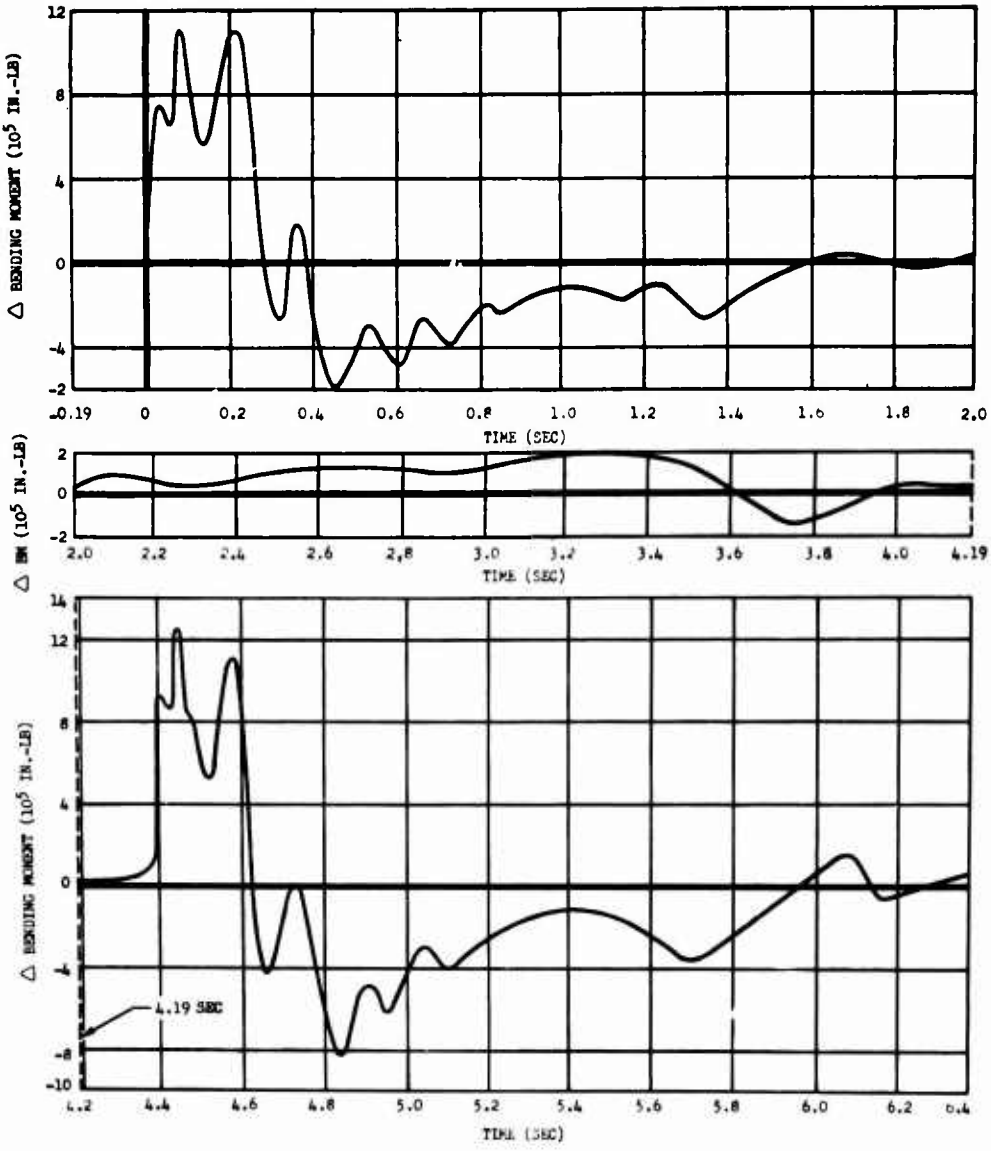

Fig. 5.6 Stabilizer Bending versus Time after Shock Arrival, Left Horizontal Stabilizer Station 62, B-36D, Shot 9

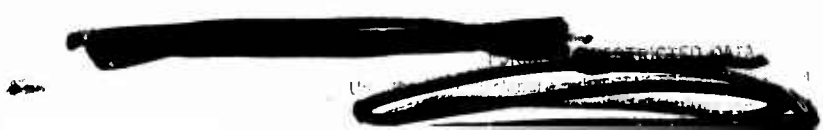

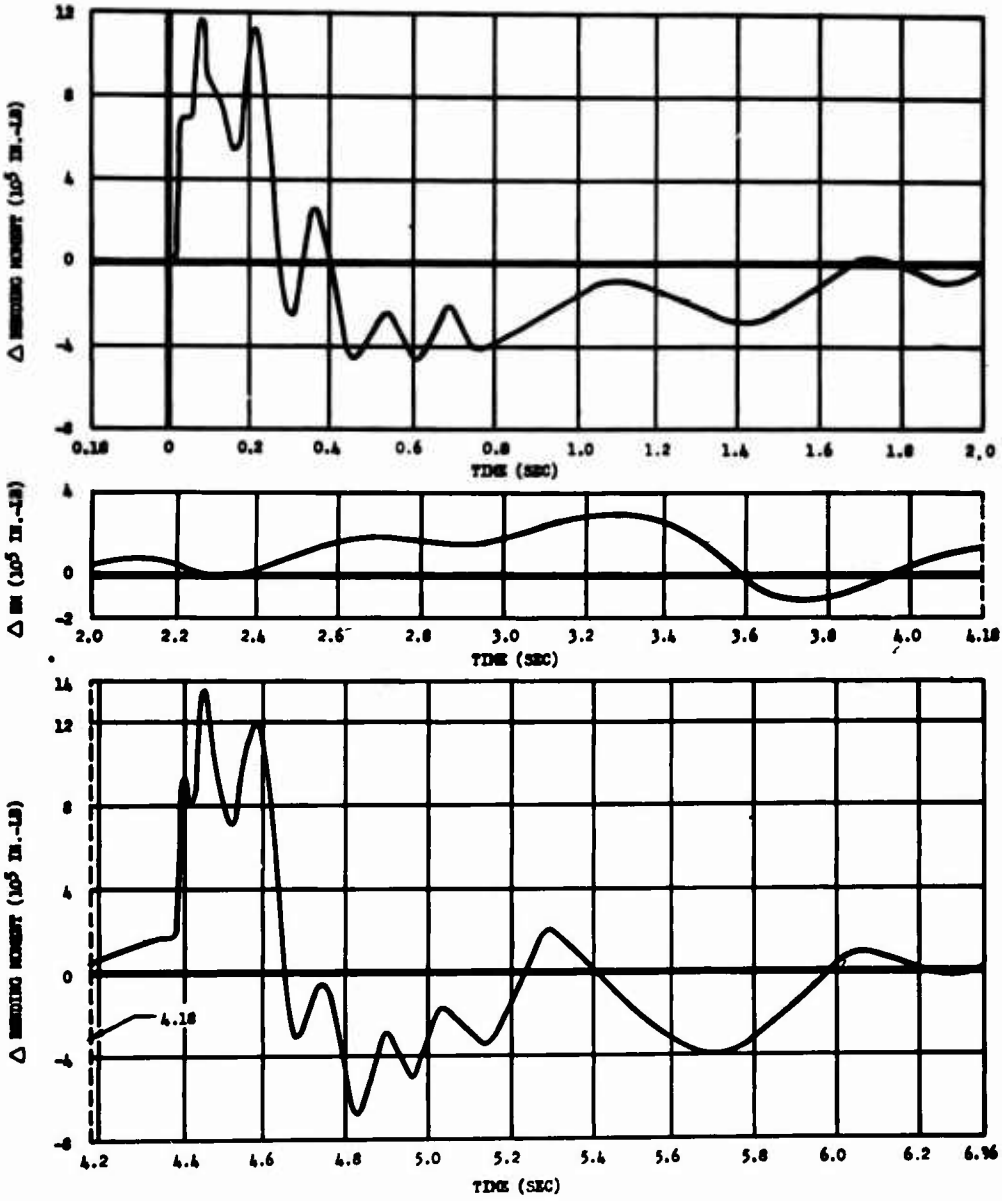

Fig. 5.7 Stabilizer Bending versus Time after Shock Arrival, Right Horizontal Stabilizer Station 62, B-36D, Shot 9

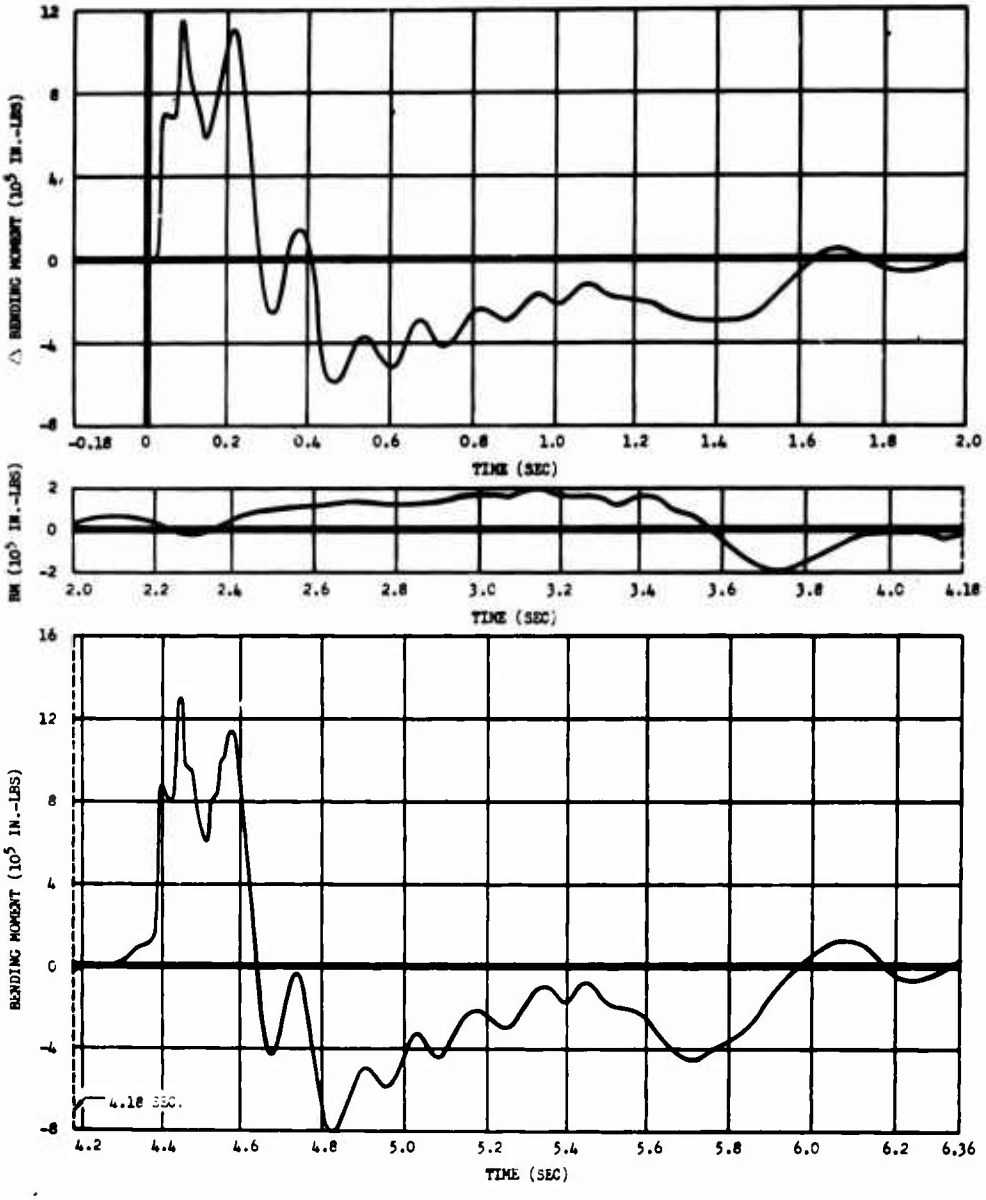

Fig. 5.8 Stabilizer Bending (Point Load Measurement) versus Time after Shock Arrival, Left Horizontal Stabilizer Station 62,B-36D, Shot 9

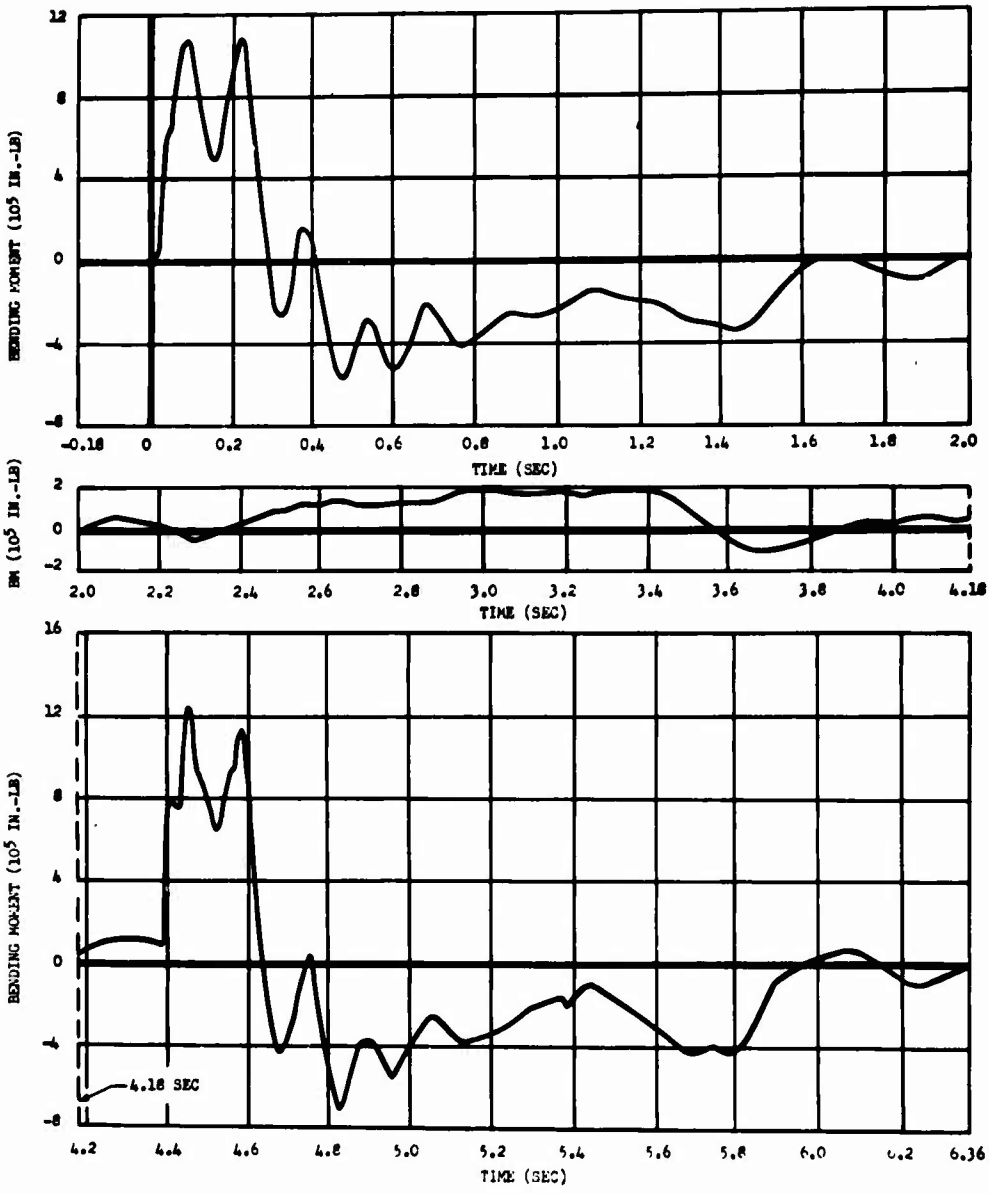

Fig. 5.9 Stabilizer Bending (Point Load Measurement) versus Time after Shock Arrival, Right Horizontal Stabilizer Station 62, B-36D, Shot 9

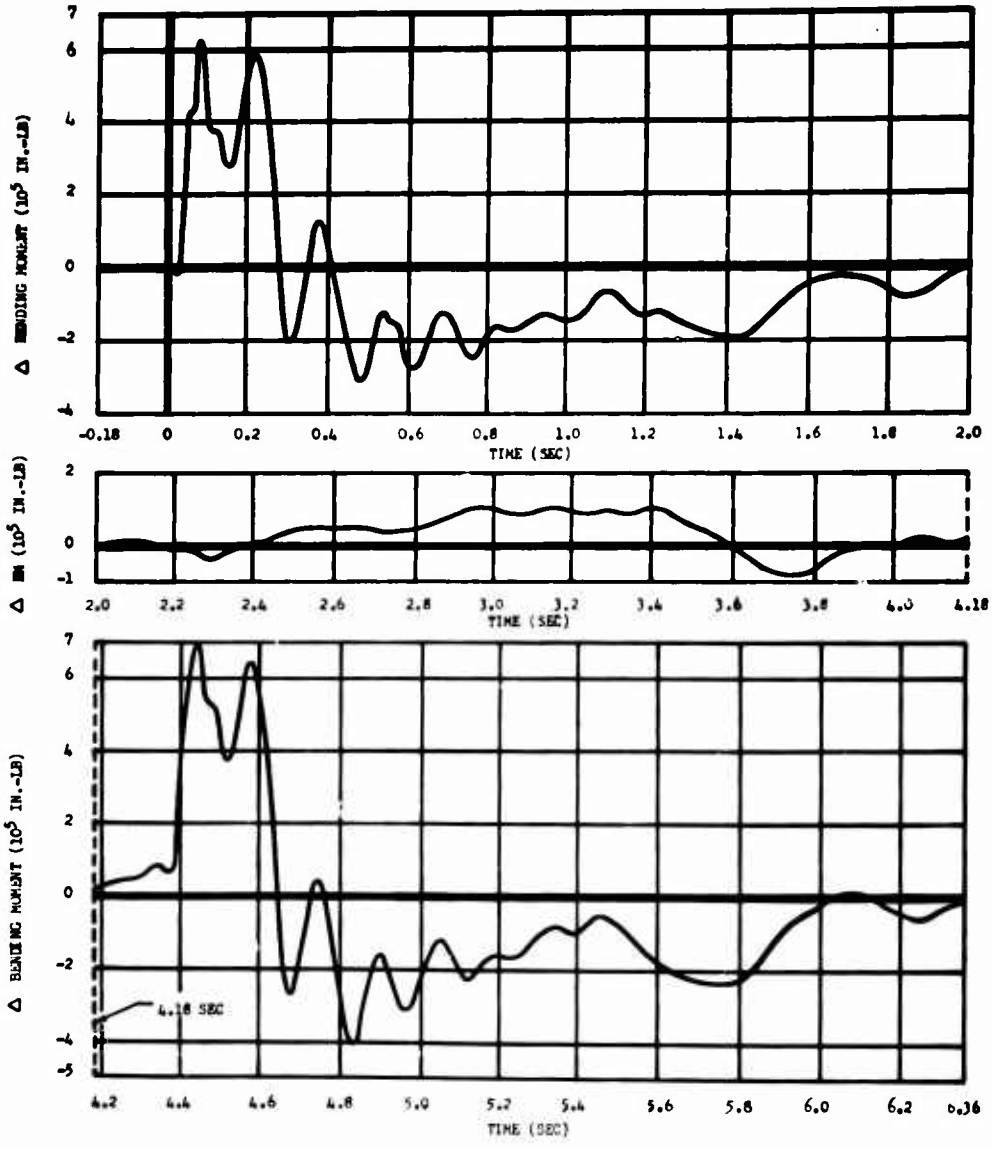

Fig. 5.10 Stabilizer Bending (Point Load Measurement) versus Time after Shock Arrival, Right Horizontal Stabilizer Station 144, B-36D, Shot 9

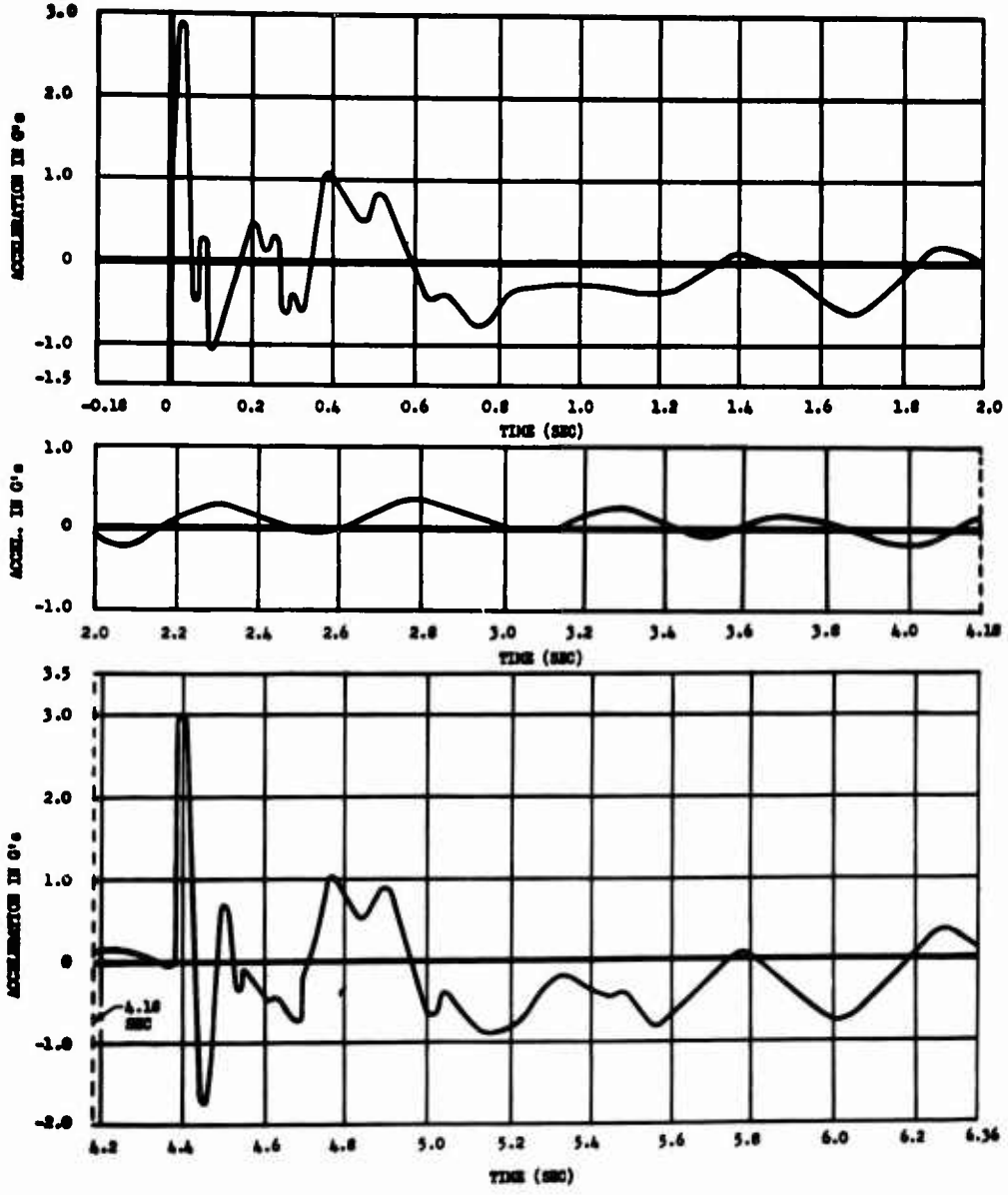

Fig. 5.11 Vertical Acceleration versus Time after Shock Arrival, B-36D Tail, Fuselage Station 1770, Shot 9

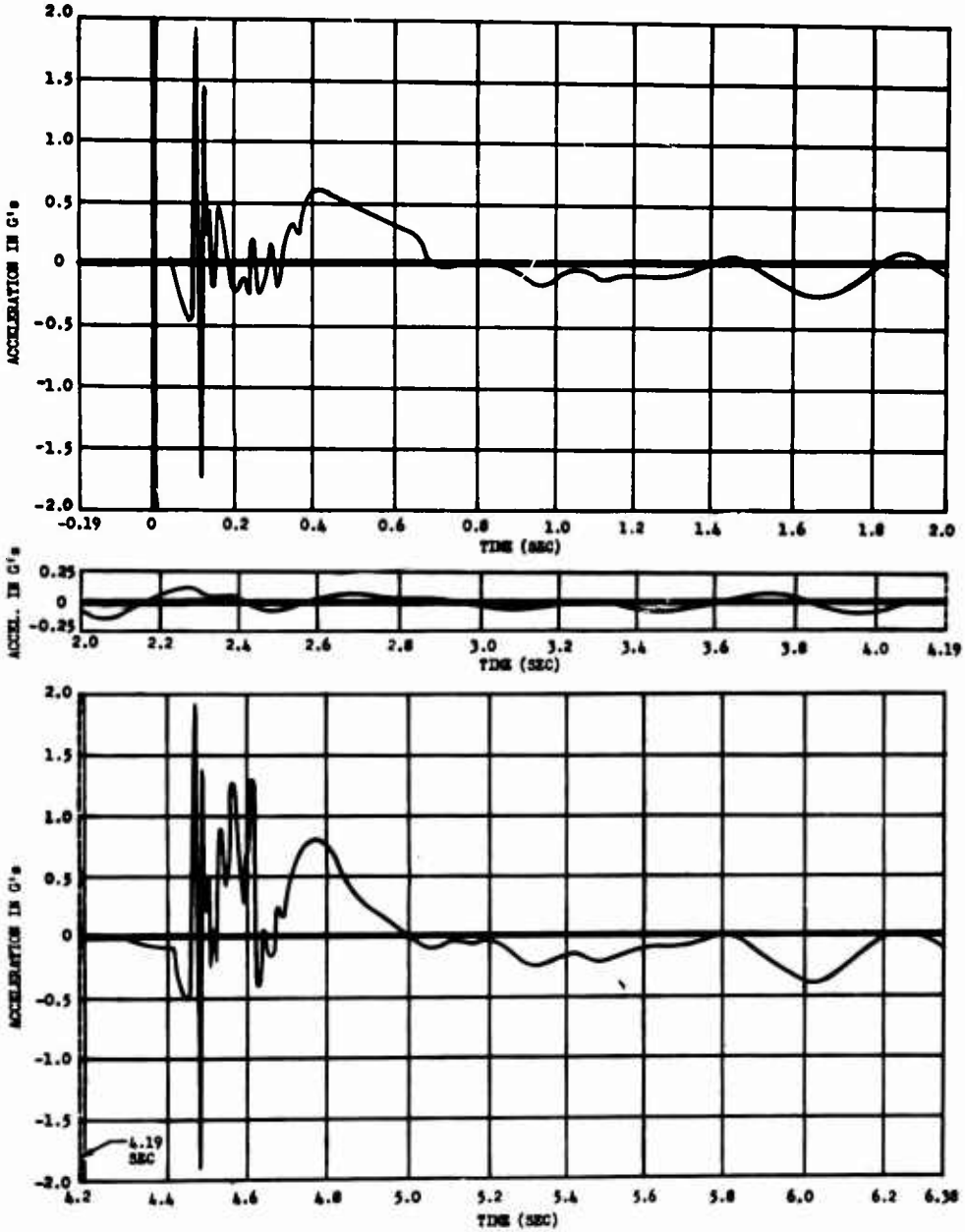

Fig. 5.12 Vertical Acceleration versus Time after Shock Arrival, B-36D Nose, Fuselage Station 212, Shot 9

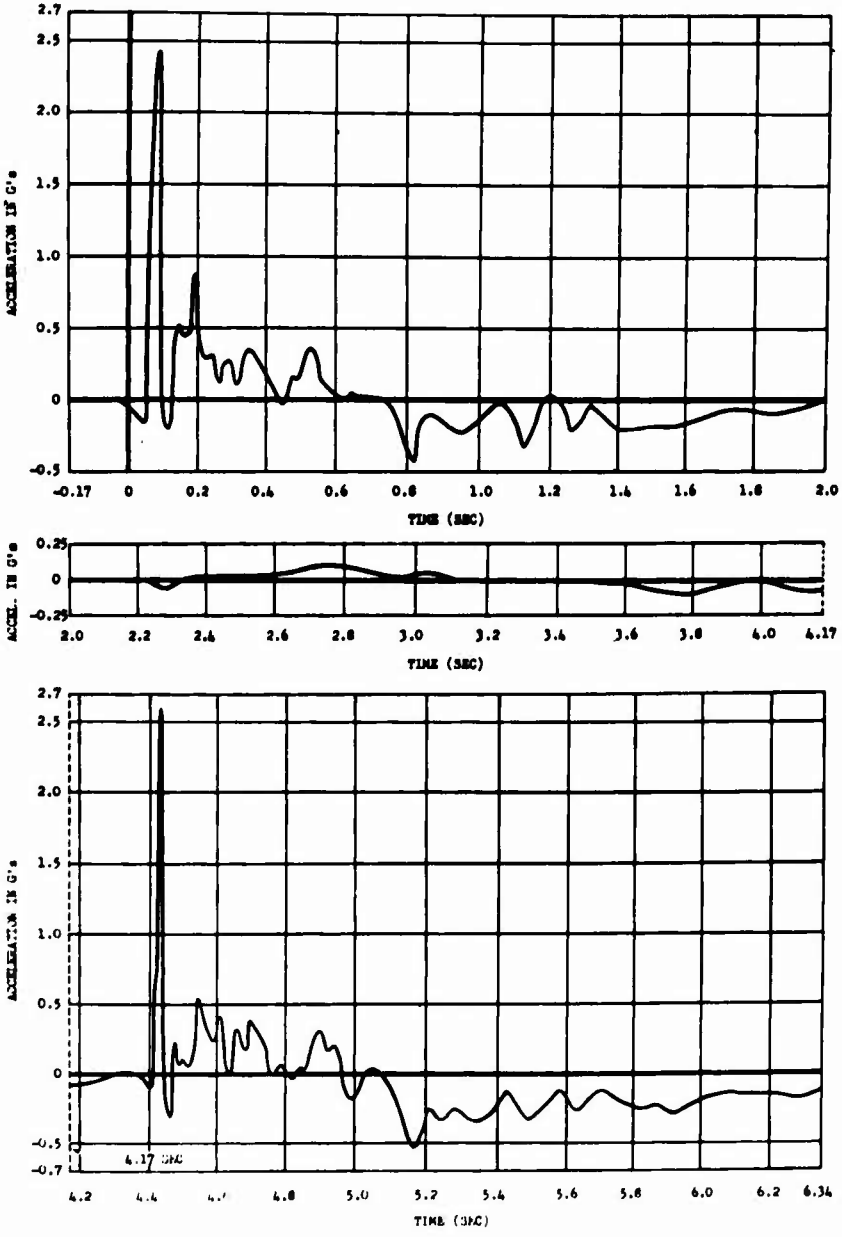

Fig. 5.13 Vertical Acceleration versus Time after Shock Arrival, B-36D Center of Gravity, Fuselage Station 907, Shot 9

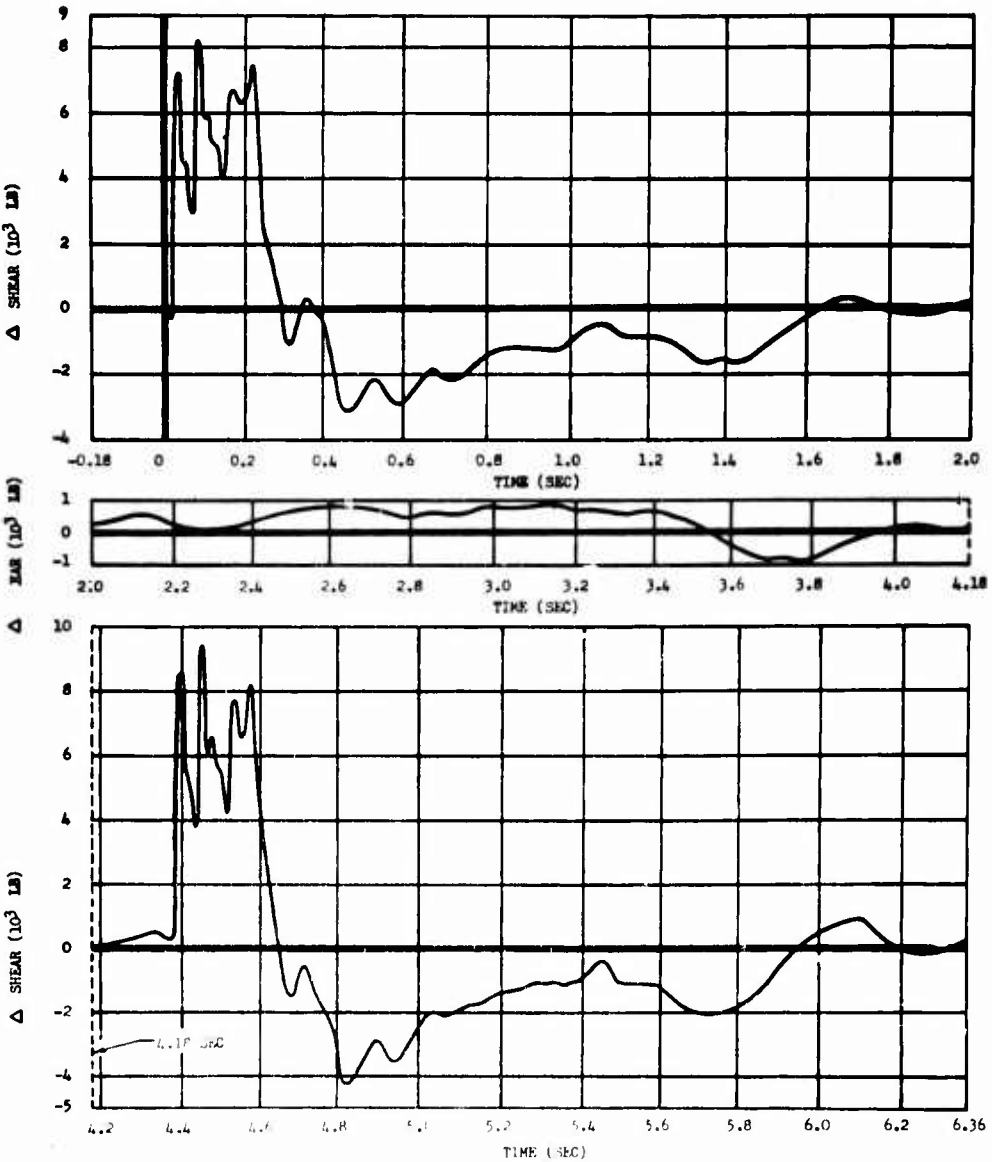

Fig. 5.14 Stabilizer Shear (Point Load Measurement) versus Time after Shock Arrival, Left Horizontal Stabilizer Station 62, B-36D, Shot 9

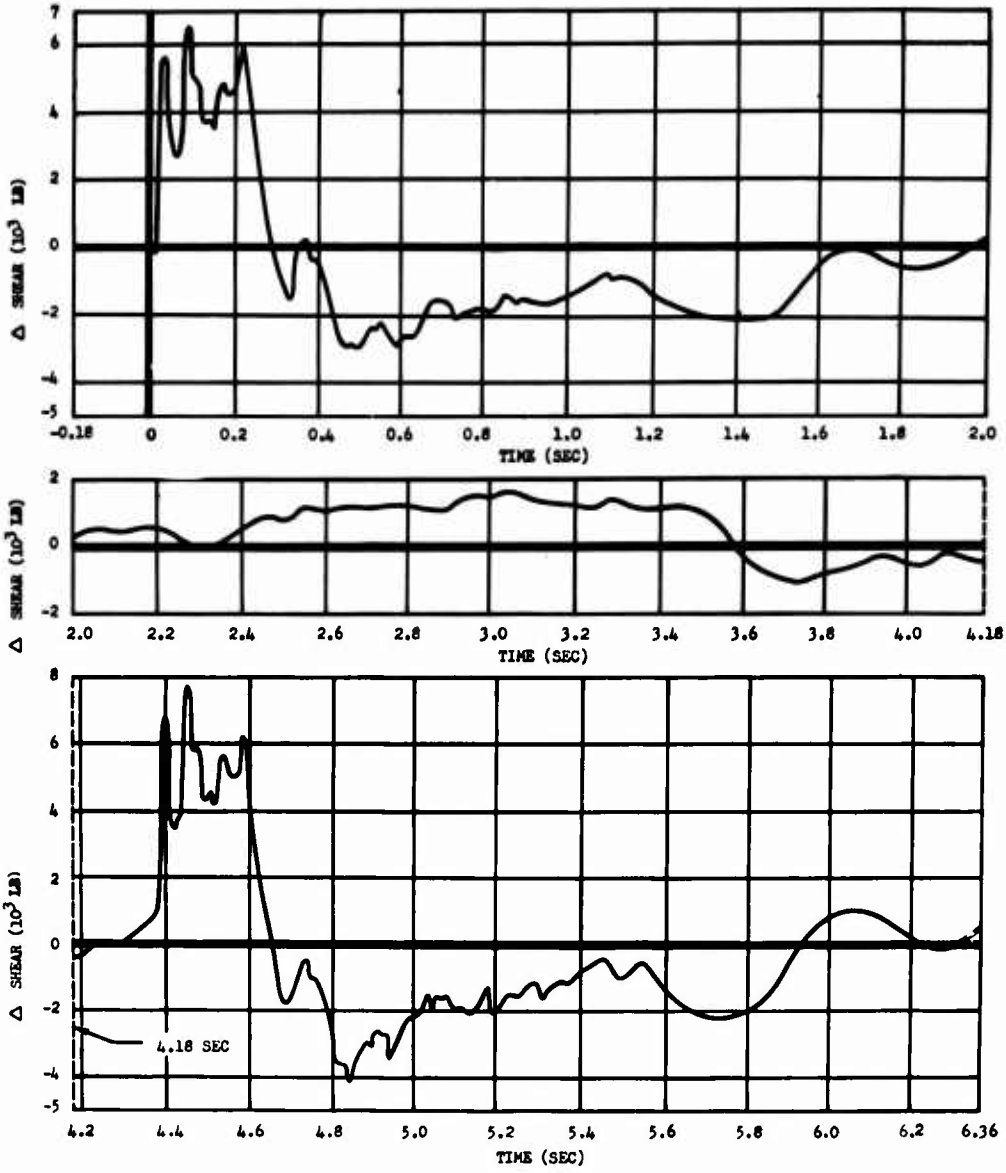

Fig. 5.15 Stabilizer Shear (Point Load Measurement) versus Time after Shock Arrival, Right Horizontal Stabilizer Station 62, B-36D, Shot 9

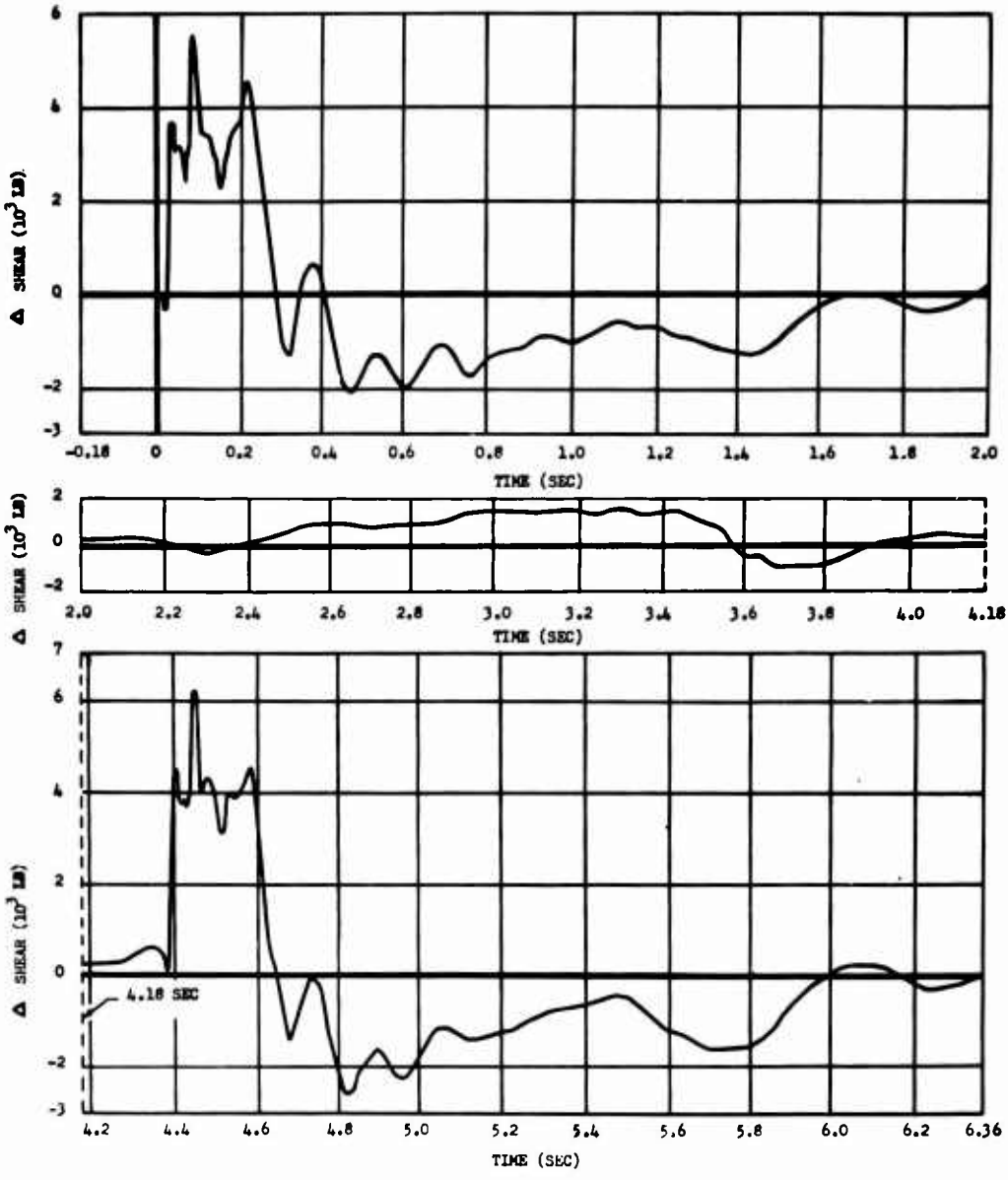

Fig. 5.16 Stabilizer Shear (Point Load Measurement) versus Time after Shock Arrival, Right Horizontal Stabilizer Station 144, B-36D Shot 9

CHAPTER 6

DISCUSSION

6.1 GENERAL

Since it is not economically feasible to obtain sufficient empirical data to permit accurate prediction of structural loads for the variety of parameters that must be considered in the operational planning of a nuclear strike, it is necessary to employ analytic methods, the reliability of which has been adequately demonstrated by actual flight testing. The data presented in this report were obtained primarily for the verification of a technique for calculating gust-induced loads in aircraft flying in the vicinity of a nuclear explosion. Because of the spread between maximum probable and most probable yield for the experimental devices being tested, and the necessity of positioning on the basis of the maximum probable yield, the peak loads realized were generally well below design limit. Further, on two of the three shots, the aircraft were positioned at blast inputs lower than the maximum allowable because thermal criteria were controlling. Nevertheless, reliable blast response data were obtained which should prove adequate for the correlation, verification, and if necessary the revision of the present blast/load theory. The direct application of these data to the blast/load theory is beyond the scope of this report. Therefore, the discussion presented here has been confined to a rather general survey of the results, intended primarily to establish the validity and limitations of the data presented. Since the data presented on the B-47 aircraft are limited to four measurements, the discussion will refer to the measurements made of the B-36 aircraft, unless specifically stated otherwise.

Although the data presented in this report were gathered under adverse environmental conditions, it is believed instrumentation procedures were such that climatic and other effects did not appreciably influence instrumentation accuracy. For the overseas tests, the aircraft was completely calibrated before and after the operation. Comparison of the post-test calibration with the pre-test calibration afforded an excellent check on the stability of the instrumentation. That over-all instrumentation precision was well within the standard accuracy limitations generally attributed to the type of instrumentation employed is adequately demonstrated by the excellent agreement between measurements of the hori-

zontal tail loads made by two different and completely independent methods.

Prior to IVY, the design limit upload on the horizontal tail of the B-36 aircraft was published as 38,200 lb. Further analysis and recalculation by Consolidated Vultee Aircraft Corporation (CVAC) after IVY produced a revised design limit load of 63,000 lb. This higher figure was later confirmed by static tests conducted by CVAC under contract to WADC. The tests were not completed until after Shot 9; therefore, the B-36 aircraft was positioned on the lower allowable tail load for this shot, as well as the two IVY shots. In this report, however, all comparisons of measured loads with design limit load are made with respect to the higher figure of 63,000 lb. On this basis the peak measured load was only 45 per cent of design limit load; however, if calculated on the same basis used to position the aircraft, the peak measured load would have approached more closely the design limit.

In all exposures the aircraft were positioned with the tail toward the explosion; therefore, symmetrical loading on the wing and horizontal tail was expected.

6.2 WING BENDING

Bending measurements on the right and left wing at station 390 were equivalent for Mike and King Shots but differed greatly in Shot 9. Although no direct evidence has been found that would invalidate either of the measurements, for reasons given below it is believed the lower value, which was that measured on the left wing during Shot 9, is incorrect, and asymmetrical loading is not indicated.

To determine whether or not measured values were in approximate agreement relative to each other, the maximum positive bending moments measured at each instrumented station for each shot, except for the station farthest outboard, were plotted as a function of the distance from the aircraft center line. The resulting curves drawn for each shot are shown in Fig. 6.1. The relationship of bending moment versus span calculated for the condition of uniform load shows it is reasonable to expect a plot of peak values to produce a curve of the general shape shown, i.e., higher loads at the inboard stations, decreasing with increasing span. A dynamic analysis would be required to determine the exact curve at any given time. The above method of comparison provides a good check on the validity of the test data. The peak bending moments from station 1062 have not been plotted because the influence of the higher vibration modes caused the peak value to be reached at a much earlier time than for the instrumented stations inboard of station 1062. The response curves of the suspect measurements made at station 390 are practically identical, except that the left wing measurement consistently equals one-half the right wing measurement. This low reading can easily be explained as an instrumentation failure; however, excluding data reduction errors, it is almost impossible for an instrumentation failure to cause a high reading. The peak value of these Shot 9 measurements have both been plotted in Fig. 6.1. The curves presented were drawn on the basis of the composite data, excluding the points in question, and show that the higher value is in the region predicted by the curve, whereas the lower value falls considerably below the curve. If the Shot 9 curve

were redrawn to favor the lower value, the resulting curve would neither follow the trend established by the other two curves nor represent what

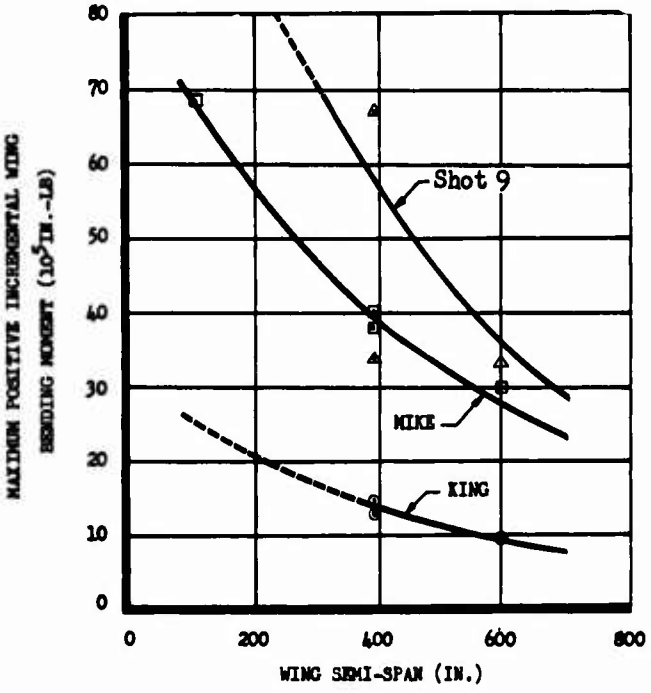

Fig. 6.1 Peak Positive Wing Bending Moments Measure in Mike, King, and Shot 9 Plotted versus Wing Station (Expressed as Distance in Inches from Aircraft Center Line)

would logically be expected. In view of the above, the data from the station 390 installation on the right wing is regarded as the correct measurement for Shot 9.

The curve for Shot 9 rises somewhat more sharply at the inboard stations than what might be expected from the shape of the Mike curve. It should be remembered, however, that in Shot 9 the aircraft was exposed to a bomb of considerably lower yield at a position where the angle of blast incidence was closer to the normal. In addition, the weight configuration was such that more weight was concentrated in or near the fuselage for Shot 9. This was accomplished by loading 25,000 lb of bombs in the forward bomb bay and carrying the majority of the fuel in the inboard tanks. A theoretical evaluation of the effect of the above difference should explain the apparent deviation.

The peak bending moments measured were, in general, quite low with the highest somewhere in the neighborhood of 10 per cent of limit load. The low values did not materially effect the instrumentation accuracy. The over-all sensitivity was sufficient to provide adequate galvanometer deflection, and the resultant data are believed to possess the accuracy generally attributed to the measurement of aircraft structural loads in flight.

6.3 STABILIZER BENDING

The time-history curves for bending measurements made at station 62 of the horizontal stabilizer during Mike and Shot 9 are shown in superposition in Fig. 6.2 to facilitate comparison of the two responses. To obtain a clearer presentation, the curve for King Shot was omitted; however, since the stabilizer response in King Shot was similar to that of Mike except for amplitude, comparisons of Mike and Shot 9 will suffice to show general response differences. As shown in the figure, both curves show the characteristic double peak followed by a lower peak. Furthermore, the peaks occur at approximately the same time in both curves and are displaced from each other at approximately equal intervals, suggesting the peaks correspond with the natural frequency of the stabilizer. Thus, the regularity and similarity of response obtained in the three independent tests lends strong support to the conclusion that the data represent actual bending stresses induced.

Other than magnitude, the only essential difference between the Shot 9 and Mike responses is the relatively high negative bending moment measured in Shot 9 and undetected in Mike. The return to zero after the positive pulse was more gradual in Mike and no appreciable negative bending moment was attained. This difference in stabilizer response is attributed primarily to the difference in positive phase duration of the shock wave on Mike and Shot 9. The longer positive phase in Mike Shot caused the upload on the stabilizer to be maintained for a longer time, thereby inhibiting the natural spring-back of the stabilizer. Because of this effect, the peak negative bending moment was both delayed and of a low amplitude. The maximum bending moment recorded was during Mike Shot of IVY. This value represented 45 per cent of the present design limit load. During UPSHOT-KNOTHOLE, only 34 per cent of design limit load was realized. However, as explained before, these values are based on the new design limit load that was verified after the tests. If the old limit load were used, their values would have been much higher.

The bending moments measured on the horizontal tail of the B-36D aircraft using the conventional method were in good agreement with the point load method. For Shot 9 the bending moment measured at station 62 on the right stabilizer was slightly lower than that measured on the left for both the conventional and point load method. The shear, measured only by the point load system, is also lower at station 62 right than at station 62 left. There are several possible explanations for this difference in measured loads. The most probable explanation is that the test aircraft was not pointed directly away from the explosion, thereby giving a side load on the vertical fin that was transmitted to the horizontal stabilizer. A load on the left side of the vertical tail would tend to increase the bending moment on the left horizontal tail and decrease the bending moment on the right horizontal tail.

Since the loads measured by two completely independent methods agree; i.e., both methods give higher values on the left side, it is believed that the measurements are correct and that there is a definite reason for the difference.

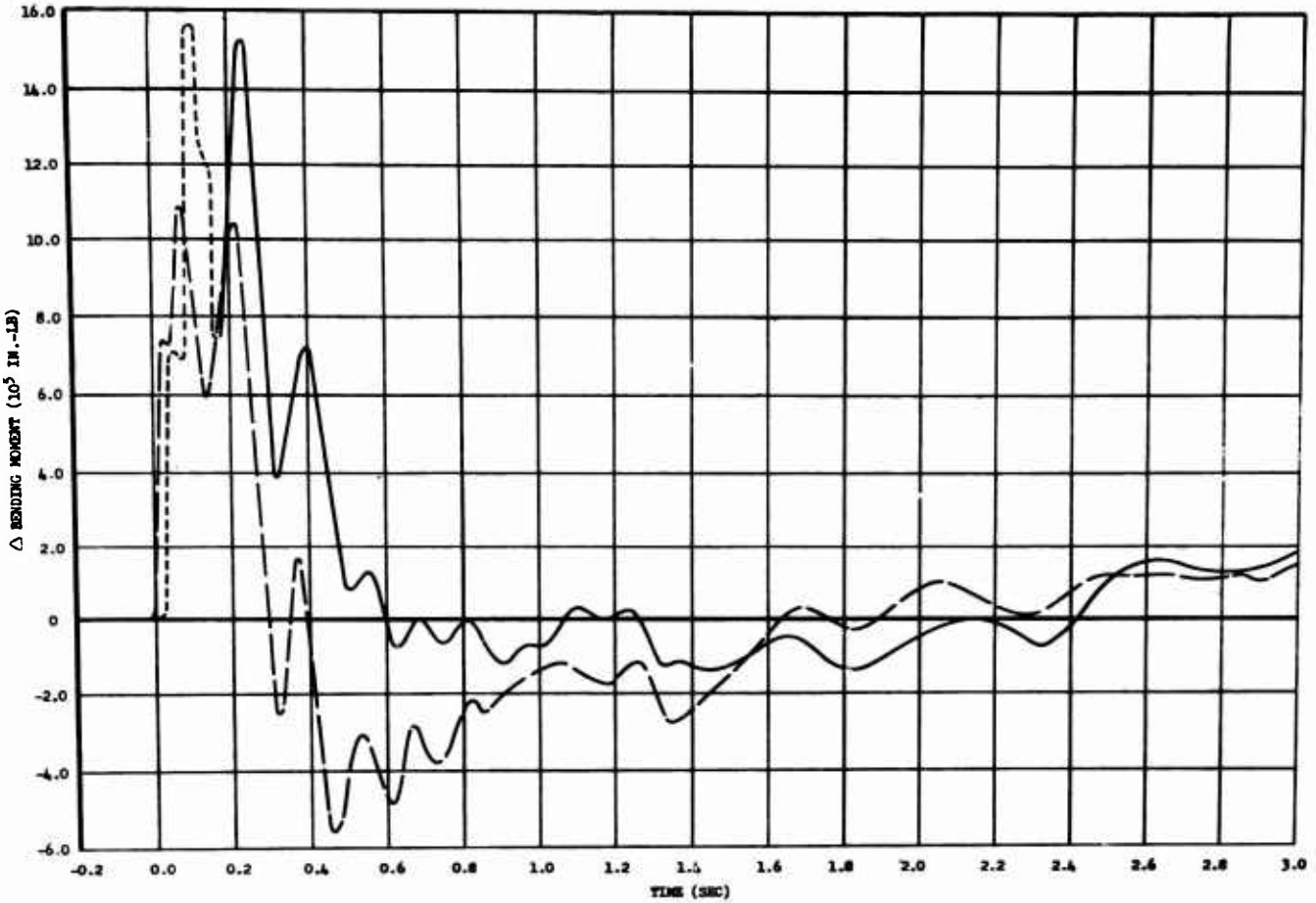

Fig. 6.2 Comparison of Bending Measurements made at Station 62 of the Left Horizontal Stabilizer, B-36D during Mike and Shot 9

6.4 FUSELAGE BENDING

The aft fuselage bending moment measurements obtained at station 1040 on the B-36 aircraft for the three shots are shown as superimposed time-history curves in Fig. 6.3. From the figure it can be seen that the curves for Mike and King are quite similar, especially in the early portion, but differ in this region from the Shot 9 curve. The peak positive value is reached at approximately the same time, 0.18 sec, on all three shots; however, the Shot 9 curve swings negative earlier and reaches a considerably higher negative value. The response curve for Shot 9 is also more regular, having no secondary peaks in the first positive swing.

The differences noted above are not unexpected if it is assumed that the fuselage bending stresses, at least initially, are primarily a function of the loads on the horizontal stabilizers. It was noted in paragraph 6.3 that after the first positive peak the horizontal stabilizer bending moment for Mike and King remained positive for a longer time than it did in Shot 9, and, further, in Shot 9 a considerably higher negative bending moment was obtained. The duration of the first positive swing of the stabilizer in Shot 9 was sufficiently short so that it was approximately in phase with the fuselage, thus helping to produce the large negative fuselage bending moment observed. The longer duration of the upload on the stabilizers during Mike and King shot retarded the downbending of the fuselage causing relatively lower negative bending moments. It is therefore concluded that the observed deviation represents no reason to question the validity of the curves presented.

6.5 ACCELERATION

The acceleration measurements made on the three different shots were not very similar, except for the undesirable high frequency oscillations characteristic of impact loading. These high frequency oscillations are caused by the vibration of the particular structural member to which the accelerometer is attached. The desired measurement is the net acceleration of this member, i.e., the over-all reaction of the aircraft at the accelerometer location. If the reaction of the member is such that the net vertical acceleration is considerable in comparison to the vibrational acceleration, it is possible to obtain the desired acceleration by graphically averaging the original curve. If the relative magnitude of the undesired oscillations is too great, the averaging procedure is impossible or at best questionable. In Mike Shot the oscillations were of such a magnitude and frequency as to render the initial position of the traces unreadable. After the spurious oscillations diminished, the traces became readable and yielded good data. The blast input on King Shot was too low to provide acceleration data of value equivalent to Mike Shot. From an over-all standpoint, Shot 9 provided the best acceleration measurements obtained.

The readable portion of the Mike acceleration data show that the nose, tail, and center of gravity accelerations were roughly in phase 0.4 sec after shock arrival. Since in Mike Shot the blast wave struck the tail before the wings, one could expect a pitching motion to result. If this did occur (acceleration data are unavailable), the motion damped

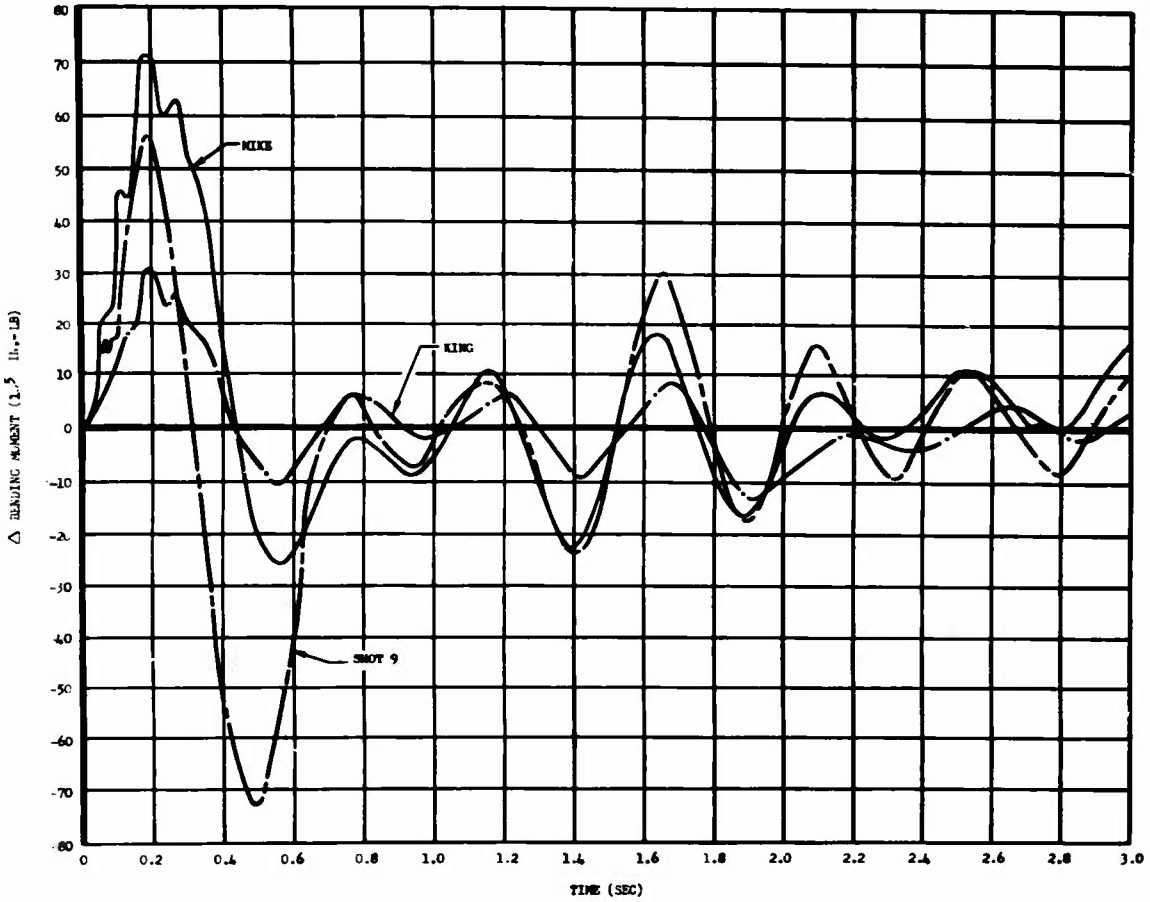

Fig. 6.3 Comparison of Fuselage Bending Measurements made at Station 1040 on the B-36D during Mike, King and Shot 9

out in less than 0.4 sec. Whereas a complete time-history of nose, tail, and center of gravity accelerations were obtained on King Shot, the low response limits the value of the data. The high amplitude fluctuations make determination of an average value for the early portion rather questionable, and the lower values thereafter are of limited utility. It should be possible to draw realistic average curves from Shot 9 acceleration data adequate for data correlation purposes. For instance, a smooth curve very similar to an overpressure time curve for a blast wave can be drawn through the Shot 9 center of gravity acceleration data.

6.6 SUMMARY

Prior to IVY, the measured structural responses of test aircraft and the theoretical analysis indicated that normally the wing is the most critical component if the aircraft is flying directly toward or away from the burst point. However, the loads measured on IVY and UPSHOT-KNOTHOLE definitely established that the most critical component of the B-36 aircraft for a tail-on exposure was not the wing. Based on the initial allowable tail load (38,200 lb), the horizontal tail was the most critical; however, using the new allowable load (63,000 lb), there is considerable doubt as to which component, aft fuselage or horizontal tail, is the most critical.

From the loads measured on these two operations, the most critical component cannot be definitely determined. The horizontal tail loads were approximately 50 per cent of design limit, and the loads measured on the fuselage were approximately 40 per cent of design limit. However, the fuselage loads were measured at a station which may not be critical. Before the most critical component can be determined, the data presented in this report must be used to perform a complete analysis of the aft fuselage section response. These data then should be verified by in-flight measurements at the critical stations. In general the theoretically predicted loads for the wing section of the B-36D aircraft were in agreement with the measured loads. The predicted loads for the aft fuselage and tail section, however, were low for IVY and high for UPSHOT-KNOTHOLE. There has been a dynamic analysis conducted on the wing section of the B-36D aircraft but not on the aft fuselage or tail section. Because gust induced loads cause acceleration and vibration of the elastic airplane structure, the method of dynamic analysis must be employed for analytic determination of structural loads. Therefore, a complete dynamic analysis is required for accurate prediction of aircraft loads encountered in the vicinity of a nuclear explosion.

In Fig. 6.4 the normal center of gravity acceleration and the wing root bending moment are presented for comparison. It can be clearly seen from this figure that the wing bending moment and normal acceleration are of the same frequency and relative magnitude. Theoretical analysis has shown this is an expected correlation.

The loads measured from the ground-reflected shock wave on the horizontal stabilizer and aft fuselage were higher than those from the direct shock wave. This fact can be seen very clearly in the Shot 9 response data presented in Chapter 5. It also can be seen from these time-histories that the vibration from the direct shock wave had not

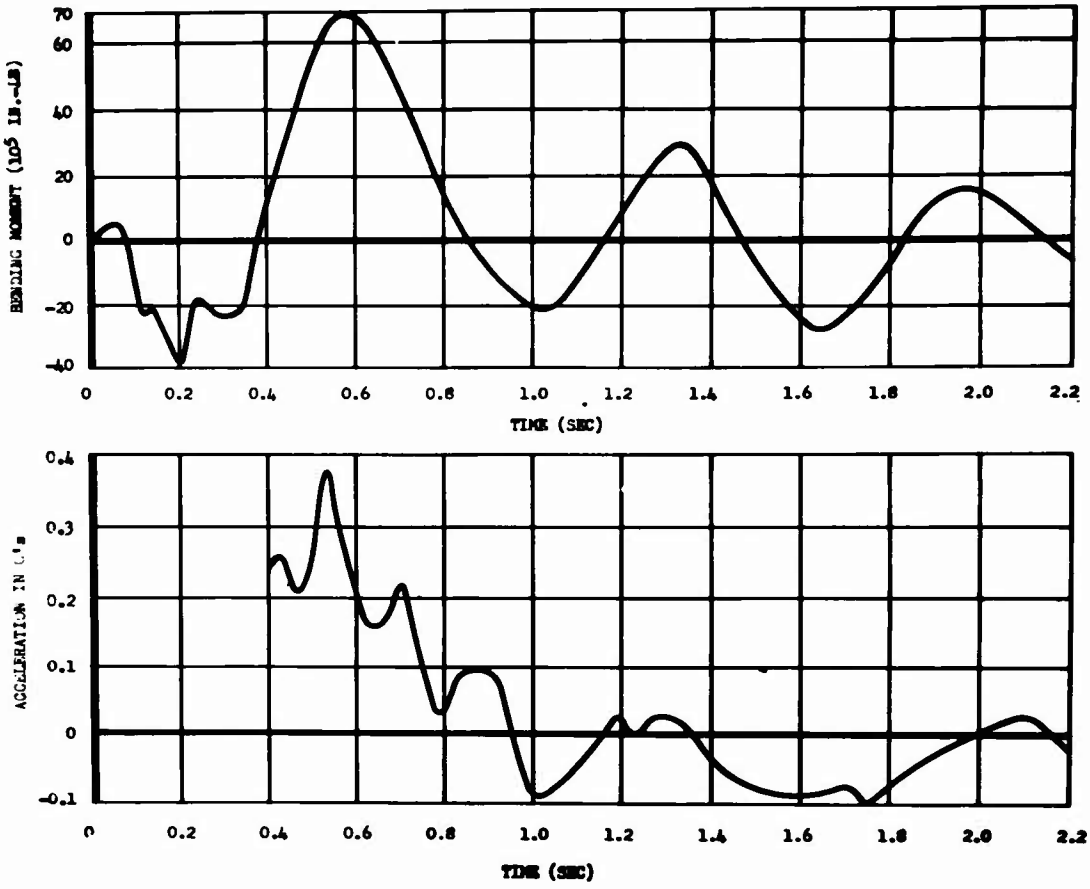

Fig. 6.4 Comparison of Center of Gravity Acceleration Versus Time with Wing Bending (Station 110) Versus Time, B-36D, Mike Shot

completely damped out at the time of the reflected shock arrival, 4.44 seconds later. The timing was such that the response to the reflected shock was in phase with the vibrations produced by the initial shock, thereby producing higher loads for the second shock than the first. Although this coupling effect caused only a small per cent increase in the total load measured, there are conditions where the effect could be considerably greater.

The blast loads measured on the B-47 aircraft and presented in this report substantiate the theoretical prediction that for straight-over weapon delivery, thermal, not blast, criteria are controlling.

[redacted]

CHAPTER 7

CONCLUSIONS AND RECOMMENDATIONS

7.1 CONCLUSIONS

From the data presented in this report it is concluded that:

1. The aircraft loads presented will permit the correlation, verification, and if necessary the revision of the present blast/load theory for loads up to 50 per cent design limit.
2. The aircraft loads presented are valid, accurate, have good repeatability and correlation, and are of sufficient quantity and quality to be used with confidence.
3. The most critical component of the B-36 aircraft for tail-on gust loading is either the horizontal tail or aft fuselage.
4. There is a definite requirement for a complete dynamic analysis on the B-36 aircraft.
5. Phasing of the responses from the direct and reflected shock waves and the total time interval between shocks can be important factors in the gust loading of an aircraft.
6. For straight-over delivery techniques, blast loading will not limit the maximum delivery capabilities of B-47 aircraft.

7.2 RECOMMENDATIONS

It is recommended that:

1. The aircraft loads presented be used to correlate, and if necessary revise the present blast/load theory.
2. A complete dynamic analysis be conducted on the B-36 type aircraft.
3. The most critical component of the B-36 aircraft be defined and if necessary additional loads be measured for verification.
4. A study be initiated by WADC to define the conditions under which the coupling effect between the initial and reflected shock waves become critical. Also, that the probability of this occurrence be explored and if this occurrence is realistic for weapon delivery, that it be added to the "feasibility" diagrams.
5. The information in this report be made available to the Operational Analysis Section of the Strategic Air Command.

[redacted]

DISTRIBUTION

Military Distribution Categories 5-21 and 5-60

ARMY ACTIVITIES

1 Asst. Chief of Staff, G-3, D/A, Washington 25, D.C. ATTN: Dep. CofS, G-3 (RR&SW)
2 Chief of Research and Development, D/A, Washington 25, D.C., ATTN: Special Weapons and Air Defense Div.
3 Chief of Ordnance, D/A, Washington 25, D.C. ATTN: ORDTX-AR
4- 6 Chief Signal Officer, D/A, P&O Division, Washington 25, D.C. ATTN: SIGOP
7 The Surgeon General, D/A, Washington 25, D.C. ATTN: Chief, R&D Division
8- 9 Chief Chemical Officer, D/A, Washington 25, D.C.
10 The Quartermaster General, CBR, Liaison Officer, Research and Development Div., D/A, Washington 25, D.C.
11- 15 Chief of Engineers, D/A, Washington 25, D.C. ATTN: ENGNB
16 Chief of Transportation, Military Planning and Intelligence Div., Washington 25, D.C.
17- 19 Commanding General, Continental Army Command, Ft. Monroe, Va.
20 President, Board #1, Headquarters, Continental Army Command, Ft. Bragg, N.C.
21 President, Board #2, Headquarters, Continental Army Command, Ft. Knox, Ky.
22 President, Board #3, Headquarters, Continental Army Command, Ft. Benning, Ga.
23 President, Board #4, Headquarters, Continental Army Command, Ft. Bliss, Tex.
24 Commanding General, U.S. Army Caribbean, Ft. Amador, C.Z. ATTN: Cml. Off.
25 Commander-in-Chief, European Command, APO 128, c/o PM, New York, N.Y.
26- 27 Commander-in-Chief, Far East Command, APO 500, c/o PM, San Francisco, Calif. ATTN: ACofS, J-3
28- 29 Commanding General, U.S. Army Europe, APO 403, c/o PM, New York, N.Y. ATTN: OPOT Div., Combat Dev. Br.
30- 31 Commandant, Command and General Staff College, Ft. Leavenworth, Kan. ATTN: ALLLS(AS)
32 Commandant, The Artillery School, Ft. Sill, Okla.
33 Secretary, The AA&GM Branch, The Artillery School, Ft. Bliss, Tex. ATTN: Lt. Col. Albert D. Epley, Dept. of Tactics and Combined Arms
34 Commanding General, Medical Field Service School, Brooke Army Medical Center, Ft. Sam Houston, Tex.
35 Director, Special Weapons Development Office, Ft. Bliss, Tex. ATTN: Lt. Arthur Jaskierny
36 Commandant, Army Medical Service Graduate School, Walter Reed Army Medical Center, Washington 25, D.C.
37 Superintendent, U.S. Military Academy, West Point, N.Y. ATTN: Prof. of Ordnance
38 Commandant, Chemical Corps School, Chemical Corps Training Command, Ft. McClellan, Ala.
39 Commanding General, Research and Engineering Command, Army Chemical Center, Md. ATTN: Deputy for RW and Non-Toxic Material
40- 41 Commanding General, Aberdeen Proving Grounds, Md. (inner envelope) ATTN: RD Control Officer (for Director, Ballistics Research Laboratory)
42- 44 Commanding General, The Engineer Center, Ft. Belvoir, Va. ATTN: Asst. Commandant, Engineer School
45 Commanding Officer, Engineer Research and Development Laboratory, Ft. Belvoir, Va. ATTN: Chief, Technical Intelligence Branch
46 Commanding Officer, Picatinny Arsenal, Dover, N.J. ATTN: ORDBB-TK
47 Commanding Officer, Army Medical Research Laboratory, Ft. Knox, Ky.
48- 49 Commanding Officer, Chemical Corps Chemical and Radiological Laboratory, Army Chemical Center, Md. ATTN: Tech. Library
50 Commanding Officer, Transportation R&D Station, Ft. Eustis, Va.
51 Director, Technical Documents Center, Evans Signal Laboratory, Belmar, N.J.
52 Director, Waterways Experiment Station, PO Box 631, Vicksburg, Miss. ATTN: Library
53 Director, Armed Forces Institute of Pathology, 7th and Independence Avenue, S.W., Washington 25, D.C.
54 Director, Operations Research Office, Johns Hopkins University, 7100 Connecticut Ave., Chevy Chase, Md. ATTN: Library
55- 61 Technical Information Service, Oak Ridge, Tenn. (Surplus)

NAVY ACTIVITIES

62 Chief of Naval Operations, D/N, Washington 25, D.C. ATTN: OP-36
63 Chief of Naval Operations, D/N, Washington 25, D.C. ATTN: OP-03EG
64 Director of Naval Intelligence, D/N, Washington 25, D.C. ATTN: OP-922V
65 Chief, Bureau of Medicine and Surgery, D/N, Washington 25, D.C. ATTN: Special Weapons Defense Div.
66 Chief, Bureau of Ordnance, D/N, Washington 25, D.C.
67 Chief, Bureau of Ships, D/N, Washington 25, D.C. ATTN: Code 348
68 Chief, Bureau of Yards and Docks, D/N, Washington 25, D.C. ATTN: D-440
69 Chief, Bureau of Supplies and Accounts, D/N, Washington 25, D.C.
70- 71 Chief, Bureau of Aeronautics, D/N, Washington 25, D.C.
72 Chief of Naval Research, Department of the Navy Washington 25, D.C. ATTN: LT(jg) F. McKee, USN
73 Commander-in-Chief, U.S. Pacific Fleet, Fleet Post Office, San Francisco, Calif.
74 Commander-in-Chief, U.S. Atlantic Fleet, U.S. Naval Base, Norfolk 11, Va.
75- 78 Commandant, U.S. Marine Corps, Washington 25, D.C. ATTN: Code AO3H
79 President, U.S. Naval War College, Newport, R.I.
80 Superintendent, U.S. Naval Postgraduate School, Monterey, Calif.
81 Commanding Officer, U.S. Naval Schools Command, U.S. Naval Station, Treasure Island, San Francisco, Calif.
82 Commanding Officer, U.S. Fleet Training Center, Naval Base, Norfolk 11, Va. ATTN: Special Weapons School
83- 84 Commanding Officer, U.S. Fleet Training Center, Naval Station, San Diego 36, Calif. ATTN: (SPWP School)
85 Commanding Officer, Air Development Squadron 5, VX-5, U.S. Naval Air Station, Moffett Field, Calif.
86 Commanding Officer, U.S. Naval Damage Control Training Center, Naval Base, Philadelphia 12, Pa. ATTN: ABC Defense Course
87 Commanding Officer, U.S. Naval Unit, Chemical Corps School, Army Chemical Training Center, Ft. McClellan, Ala.
88 Commander, U.S. Naval Ordnance Laboratory, Silver Spring 19, Md. ATTN: EE
89 Commander, U.S. Naval Ordnance Laboratory, Silver Spring 19, Md. ATTN: EH
90 Commander, U.S. Naval Ordnance Laboratory, Silver Spring 19, Md. ATTN: R
91 Commander, U.S. Naval Ordnance Test Station, Inyokern, China Lake, Calif.
92 Officer-in-Charge, U.S. Naval Civil Engineering Res. and Evaluation Lab., U.S. Naval Construction Battalion Center, Port Hueneme, Calif. ATTN: Code 753

93 Commanding Officer, U.S. Naval Medical Research Inst., National Naval Medical Center, Bethesda 14, Md.
94 Director, U.S. Naval Research Laboratory, Washington 25, D.C. ATTN: Code 2029
95 Commanding Officer and Director, U.S. Navy Electronics Laboratory, San Diego 52, Calif. ATTN: Code 4223
96- 97 Commanding Officer, U.S. Naval Radiological Defense Laboratory, San Francisco 24, Calif. ATTN: Technical Information Division
98 Director, Naval Air Experimental Station, Air Material Center, U.S. Naval Base, Philadelphia, Penn.
99 Commanding Officer and Director, David W. Taylor Model Basin, Washington 7, D.C. ATTN: Library
100 Commander, U.S. Naval Air Development Center, Johnsville, Pa.
101 Director, Office of Naval Research Branch Office, 1000 Geary St., San Francisco, Calif.
102-108 Technical Information Service, Oak Ridge, Tenn. (Surplus)

AIR FORCE ACTIVITIES

109 Asst. for Atomic Energy, Headquarters, USAF, Washington 25, D.C. ATTN: DCS/O
110 Director of Operations, Headquarters, USAF, Washington 25, D.C. ATTN: Operations Analysis
111 Director of Plans, Headquarters, USAF, Washington 25, D.C. ATTN: War Plans Div.
112 Director of Research and Development, Headquarters, USAF, Washington 25, D.C. ATTN: Combat Components Div.
113-114 Director of Intelligence, Headquarters, USAF, Washington 25, D.C. ATTN: AFOIN-1B2
115 The Surgeon General, Headquarters, USAF, Washington 25, D.C. ATTN: Bio. Def. Br., Pre. Med. Div.
116 Deputy Chief of Staff, Intelligence, Headquarters, U.S. Air Forces Europe, APO 633, c/o PM, New York, N.Y. ATTN: Directorate of Air Targets
117 Commander, 497th Reconnaissance Technical Squadron (Augmented), APO 633, c/o PM, New York, N.Y.
118 Commander, Far East Air Forces, APO 925, c/o PM, San Francisco, Calif.
119 Commander, Strategic Air Command, Offutt Air Force Base, Omaha, Nebraska. ATTN: Special Weapons Branch, Inspection Div., Inspector General
120 Commander, Tactical Air Command, Langley AFB, Va. ATTN: Documents Security Branch
121 Commander, Air Defense Command, Ent AFB, Colo.
122-123 Commander, Wright Air Development Center, Wright-Patterson AFB, Dayton, O. ATTN: WCRRN, Blast Effects Research
124 Commander, Air Training Command, Scott AFB, Belleville, Ill. ATTN: DCS/O GTP
125 Assistant Chief of Staff, Installations, Headquarters, USAF, Washington 25, D.C. ATTN: AFCIE-E
126 Commander, Air Research and Development Command, PO Box 1395, Baltimore, Md. ATTN: RDDN
127 Commander, Air Proving Ground Command, Eglin AFB, Fla. ATTN: AG/TRB
128-129 Director, Air University Library, Maxwell AFB, Ala.
130-137 Commander, Flying Training Air Force, Waco, Tex. ATTN: Director of Observer Training
138 Commander, Crew Training Air Force, Randolph Field, Tex. ATTN: 2GTS, DCS/O
140 Commander, Headquarters, Technical Training Air Force, Gulfport, Miss. ATTN: TA&D
141-142 Commandant, Air Force School of Aviation Medicine, Randolph AFB, Tex.
143-148 Commander, Wright Air Development Center, Wright-Patterson AFB, Dayton, O. ATTN: WCOSI
149-150 Commander, Air Force Cambridge Research Center, 230 Albany Street, Cambridge 39, Mass. ATTN: CRQST-2
151-153 Commander, Air Force Special Weapons Center, Kirtland AFB, N. Mex. ATTN: Library
154 Commandant, USAF Institute of Technology, Wright-Patterson AFB, Dayton, O. ATTN: Resident College
155 Commander, Lowry AFB, Denver, Colo. ATTN: Department of Armament Training
156 Commander, 1009th Special Weapons Squadron, Headquarters, USAF, Washington 25, D.C.
157-158 The RAND Corporation, 1700 Main Street, Santa Monica, Calif. ATTN: Nuclear Energy Division
159-165 Technical Information Service, Oak Ridge, Tenn. (Surplus)

OTHER DEPARTMENT OF DEFENSE ACTIVITIES

166 Asst. Secretary of Defense, Research and Development, D/D, Washington 25, D.C.
167 U.S. National Military Representative, Headquarters, SHAPE, APO 55, c/o PM, New York, N.Y. ATTN: Col. J. P. Healy
168 Director, Weapons Systems Evaluation Group, OSD, Rm 2E1006, Pentagon, Washington 25, D.C.
169 Armed Services Explosives Safety Board, D/D, Building T-7, Gravelly Point, Washington 25, D.C.
170 Commandant, Armed Forces Staff College, Norfolk 11, Va. ATTN: Secretary
171-176 Commanding General, Field Command, Armed Forces Special Weapons Project, PO Box 5100, Albuquerque, N. Mex.
177-178 Commanding General, Field Command, Armed Forces, Special Weapons Project, PO Box 5100, Albuquerque, N. Mex. ATTN: Technical Training Group
179-187 Chief, Armed Forces Special Weapons Project, Washington 25, D.C.
188 Office of the Technical Director, Directorate of Effects Tests, Field Command, AFSWP, PO Box 577, Menlo Park, Calif. ATTN: Dr. E. B. Doll
189-195 Technical Information Service, Oak Ridge, Tenn. (Surplus)

ATOMIC ENERGY COMMISSION ACTIVITIES

196-198 U.S. Atomic Energy Commission, Classified Technical Library, 1901 Constitution Ave., Washington 25, D.C. ATTN: Mrs. J. M. O'Leary (For DMA)
199-201 Los Alamos Scientific Laboratory, Report Library, PO Box 1663, Los Alamos, N. Mex. ATTN: Helen Redman
202-206 Sandia Corporation, Classified Document Division, Sandia Base, Albuquerque, N. Mex. ATTN: Martin Lucero
207-209 University of California Radiation Laboratory, PO Box 808, Livermore, Calif. ATTN: Margaret Edlund
210 Weapon Data Section, Technical Information Service, Oak Ridge, Tenn.
211-220 Technical Information Service, Oak Ridge, Tenn. (Surplus)